universität wien

DISSERTATION / DOCTORAL THESIS

Titel der Dissertation /Title of the Doctoral Thesis

„Characterising Protein-Protein Interactions of the High Osmolarity Glycerol Pathway in *Saccharomyces cerevisiae*“

verfasst von / submitted by

Jillian Augustine-Rubak

angestrebter akademischer Grad / in partial fulfilment of the requirements for the degree of

Doctor of Philosophy (PhD)

Wien 2018 / Vienna 2018

Studienkennzahl lt. Studienblatt / degree programme code as it appears on the student record sheet:	A 794 684 490
Dissertationsgebiet lt. Studienblatt / field of study as it appears on the student record sheet:	Molekulare Biologie
Betreut von / Supervisor:	ao. Univ.-Prof. i.R. Dr. Gustav Ammerer

TABLE OF CONTENTS

ACKNOWLEDGMENTS 6

ABBREVIATIONS 7

ABSTRACT 8

ZUSAMMENFASSUNG 10

1. INTRODUCTION 11

1.1. MAPK SIGNALLING 11

1.2. THE HIGH OSMOLARITY GLYCEROL (HOG) RESPONSE 13

1.2.1. ACTIVATION OF THE SLN1 BRANCH 14

1.2.2. ACTIVATION OF THE SHO1 BRANCH 14

1.2.3. DEACTIVATION OF HOG PATHWAY 16

1.2.4 CURRENT MODEL OF PATHWAY ACTIVATION AND DEACTIVATION 17

1.3. PROTEIN INTERACTION ASSAYS 19

1.3.1. MICROSCOPY METHODS 19

1.3.2. TRANSCRIPTIONAL ASSAYS 21

1.3.3. AFFINITY PURIFICATION METHODS 21

1.3.4. M-TRACK 24

1.4. IMPORTANCE OF THE STUDY AND AIMS 27

2. RESULTS 30

2.1. PBS2 LOCALISATION 30

2.1.1. PBS2 INTERACTS MORE WITH SHO1 DURING OSMOTIC STRESS 30

2.2. INTERACTIONS OF THE TRANSMEMBRANE PROTEINS WITH EACH OTHER 34

2.2.1. SHO1 INTERACTS MORE WITH SHO1 DURING OSMOTIC STRESS 34

2.2.2. SHO1 IS IN CLOSE PROXIMITY TO MSB2 BOTH IN THE ABSENCE AND PRESENCE OF STRESS 36

2.2.3. OPY2 AND MSB2 INTERACT MORE DURING OSMOTIC STRESS 38

2.2.4. THE SHO1-OPY2 INTERACTION INCREASES DURING STRESS IN AN MSB2/HKR1-DEPENDENT MANNER 39

2.2.5. THE ROLE OF MSB2/HKR1 CANNOT BE BYPASSED BY ARTIFICIAL DIMERIZATION OF SHO1 AND OPY2 41
2.2.6. THE STRESS-INDUCED SHO1-SHO1 INTERACTION IS ENHANCED IN AN *MSB2/HKR1* BACKGROUND BUT REDUCED IN AN *OPY2* BACKGROUND 44
2.3. STE11 LOCALISATION 48
2.3.1. THE INTERACTION OF STE11 WITH SHO1 INCREASES DURING STRESS, AND IS INDEPENDENT OF ITS ACTIVATION STATE 49
2.3.2. THE INTERACTION OF STE11 WITH MSB2 AND OPY2 INCREASES DURING STRESS, AND IS INDEPENDENT OF ITS ACTIVATION STATE 50
2.3.3. STRESS-INDUCED STE11/50-OPY2 PROXIMITY IS REDUCED BUT NOT ABOLISHED IN THE ABSENCE OF SHO1 54
2.3.4. STRESS-INDUCED STE11/50-OPY2 PROXIMITY IS REDUCED BUT NOT ABOLISHED IN THE ABSENCE OF MSB2, HKR1 AND SHO1 58
2.3.5. THE STRESS-INDUCED INCREASE OF THE STE11/50-OPY2 INTERACTION OCCURS IN THE ABSENCE OF CALCINEURIN ACTIVITY 62
2.3.6. INHIBITION OF YPK1/2 ACTIVITY DOES NOT CAUSE THE STE11/50-OPY2 INTERACTION 65

3. DISCUSSION AND CONCLUSION 66

3.1. PBS2 LOCALISATION 66
3.2. THE SHO1-SHO1 INTERACTION 67
3.3. THE MSB2-SHO1 INTERACTION 69
3.4. THE MSB2-OPY2 INTERACTION 69
3.5. THE SHO1-OPY2 INTERACTION AND DEPENDENCE ON MSB2/HKR1 70
3.6. STE11/50 LOCALISATION 71
3.7. THE INDUCIBLE M-TRACK METHOD 73
3.8. GENERAL CONCLUSIONS 75

4. MATERIALS AND METHODS 78

4.1. ROUND THE HORN (RTH) MUTAGENESIS 78
4.2. TRANSFORMATION INTO *E. COLI* 78
4.3. PCR FOR TRANSFORMATION INTO YEAST 78
4.4. ANNEALING OLIGONUCLEOTIDES TO CREATE DOUBLE-STRANDED DNA 79
4.5. PREPARATION OF INTEGRATIVE PLASMIDS FOR TRANSFORMATION 79
4.6. TRANSFORMATION PROTOCOL 79

4.7. PCR FOR CHECKING 80
4.8. M-TRACK ASSAY 80
4.8.1. STRAIN PREPARATION 80
4.8.2. GROWING CULTURES 80
4.8.3. INHIBITION OF YPK1-AS 80
4.8.4. RAPAMYCIN INDUCTION 81
4.8.5. SALT STRESS 81
4.8.6. HARVESTING 81
4.8.7. CELL BREAKAGE 81
4.9. WESTERN BLOT ANALYSIS 82
4.9.1. SDS PAGE AND PROTEIN TRANSFER 82
4.9.2. ANTIBODY INCUBATION CONDITIONS 83
4.9.3. DETECTION OF PROTEINS 84
4.9.4. QUANTIFICATION OF BLOTS 84
4.10. DROPLET TESTS 85
4.11. LIST OF YEAST STRAINS USED 86
4.12. LIST OF PLASMIDS USED 90
4.13. LIST OF PRIMERS USED 92

5. REFERENCES 98

Acknowledgments

I would firstly like to thank Gustav for trusting me with this project and allowing me to pursue interesting directions. I would also like to thank him for his scientific discussions and guidance throughout the years.

I would like to thank all the members of the Ammerer lab, past and present. Thank you to Wolfi and Jiri for technical advice and discussions. Thank you to David for being an endless source of useful literature to read. Thank you to Gaby, Jessy and Mary for always lightening the mood of the lab in stressful times. I also cannot forget to thank Aleks and Harald Nierlich (honorary lab member) for being able to provide reagents at short notice on many, many (many) occasions.

I would also like to thank the Kraft, Ogris and Kuchler labs for their resources and advice, as well as my PhD committee, Claudine Kraft, Egon Ogris and Karl Kuchler for their constructive feedback on my project's progress. Thank you also to my reviewers, Sascha Martens and Paula Alepuz, for taking the time to read this thesis.

I would like to thank my friends from the VBC PhD Selection Winter 2013 for coming on this journey with me. Finally, I would like to thank my entire family for encouraging and supporting me, and helping me reach this point in my life, especially my husband Chris, without whom none of this would have been possible.

Abbreviations

APS	Ammonium persulphate
bp	Basepairs
BSA	Bovine serum albumin
dNTPs	Deoxynucleotides
H3	Histone 3
H3K9	Lysine residue at position 9 on histone 3
HA	Epitope derived from haemagglutinin
LiAc	Lithium acetate
MAPK	Mitogen-activated protein kinase
MAPKK	MAPK kinase
MAPKKK	MAPKK kinase
MAPKKKK	MAPKKK kinase
me3	H3K9 trimethylation
myc	Epitope derived from c-Myc
nt	Nucleotide
ORF	Open reading frame
PBST	Phosphate buffered saline with 0.05% Tween-20
pHog1	Hog1 phosphorylated at both T174 and Y176
pSlt2	Slt2 phosphorylated at both T190 and Y192
SDS	Sodium dodecyl sulphate
SDS PAGE	SDS polyacrylamide gel electrophoresis
Ssk2/22	Ssk2 and Ssk22
TBST	Tris-buffered saline with 0.1% Tween-20
TEMED	Tetramethylethylenediamine
V5	Epitope derived from RNA polymerase α subunit of simian parainfluenza virus type 5
YEPD	Yeast extract peptone dextrose
α-(epitope)	Antibody recognising epitope in parentheses

Abstract

The ability of organisms to sense and respond to changes in their environment is one of the key characteristics of life. This is possible due to cell signalling; the inter- and intracellular transmission of messages throughout an organism. In eukaryotic organisms, cells can respond to a range of stimuli such as UV light, heat and hyperosmotic stress through the activation of signalling responses involving the mitogen-activated protein kinase (MAPK) p38 also referred to as a stress-activated protein kinase (SAPK) (Cuadrado & Nebreda 2010; Wagner & Nebreda 2009; Zarubin & Han 2005).

In the yeast *Saccharomyces cerevisiae*, as part of the High Osmolarity Glycerol (HOG) response, a MAPK cascade is activated the upon exposure to hyperosmotic conditions which leads to activation of the MAPK and p38 homologue, Hog1. Although many proteins required for Hog1 activation have been identified, conflicting results regarding the roles of these proteins mean that the exact mechanism of pathway activation is not clearly understood.

In this work, I used the M-Track assay, a protein-proximity assay specially designed to detect short-lived protein-protein interactions in *S. cerevisiae*, to study the interactions of kinases of the MAPK cascade and their associated proteins. I found that, in contrast to current models of pathway activation, the MAPKKK Ste11 and its adaptor protein Ste50 only localise to the plasma membrane upon hyperosmotic stress and are not “primed” at the membrane as was previously thought. Moreover, although Ste11/50 membrane localisation is enhanced by the presence of transmembrane proteins Msb2, Hkr1 and Sho1, it can still localise independently of these factors. In addition, Ste11 is recruited to the membrane independently of its activation state. Through further experiments I could exclude the possibility that activation of Calcineurin signalling or inactivation of Tor1-Ypk1/2 signalling (both HOG pathway-independent hyperosmotic stress responses) were major regulation events in the process of Ste11 membrane localisation.

In addition, I found that MAPKK Pbs2 interacts with Sho1 in the absence of osmotic stress, but this interaction is strongly enhanced during osmotic stress. Finally, the question of how the transmembrane proteins interact with each other was addressed. I found that Opy2 and Sho1, the membrane anchors for Ste11 and Pbs2 respectively, come into closer proximity to each other during osmotic stress and this increase in proximity depends on the osmosensors Msb2 and Hkr1.

Taken together, these results suggest that although Ste11 and Pbs2 are recruited to the plasma membrane independently of each other, stress-induced clustering of proteins around the osmosensors Msb2 and Hkr1 ensures efficient MAPK cascade activation during hyperosmotic stress.

Zusammenfassung

In den Zellen höherer Eukaryoten führen die meisten physikochemischen Stressbedingungen zur Aktivierung der sogenannten mitogen-aktivierten Proteinkinase (MAPK) p38, welche auch als stress-aktivierte Proteinkinase (SAPK) bezeichnet wird (Cuadrado & Rebreda 2010; Wagner & Nebreda 2009; Zarubin & Han 2005). In der Bäckerhefe *Saccharomyces cerevisiae* wird bei erhöhter extrazellulärer Osmolarität die p38-homologe MAPK Hog1 aktiviert. Obwohl bereits viele der Proteine, welche für die Regulation von Hog1 benötigt werden, identifiziert wurden ist der Mechanismus der Aktivierung dieser Signaltransduktionskaskade noch nicht vollständig aufgeklärt. In dieser Arbeit konzentriere ich mich auf das Interaktions- und Lokalisationsverhalten unterschiedlicher "upstream" Faktoren dieser Kaskade. Hierzu verwendete ich einen Interaktions Assay (M-Track (Zuzuarregui, 2015)), der speziell zum Nachweis kurzlebiger Protein-Protein-Wechselwirkungen in *S. cerevisiae* entwickelt wurde.

Ich konnte zeigen, dass die MAPKK Kinase Ste11 und ihr Adapterprotein Ste50 nur unter hyperosmotischen Stressbedingungen an die Plasmamembran rekrutiert werden und dass diese nicht, wie bisher angenommen, permanent membran-assoziiert sind. Obwohl die Membranlokalisierung von Ste11 und Ste50 durch die Transmembranproteine Msb2, Hkr1 und Sho1 unterstützt wird, kann sie auch unabhängig von diesen stattfinden. Außerdem wird Ste11 unabhängig von ihrem Aktivierungszustand an die Plasmamembran rekruitiert. Darüber hinaus findet die Membranrekrutierung von Ste11 unabhängig von Calcineurin- oder Tor1-Ypk1/2-Signalen (beide sind Schlüsselfaktoren in HOG-unabhängigen Stressantworten der Bäckerhefe) statt. Zusätzlich fand ich heraus, dass die MAPK Kinase Pbs2 bereits in Abwesenheit von osmotischem Stress mit dem membran-assoziierten Osmosensor Sho1 interagiert, diese Wechselwirkung unter osmotischen Stress aber wesentlich verstärkt wird. Schließlich konnte ich zeigen, dass die Membrananker für Ste11 und Pbs2, Opy2 und Sho1, bei osmotischem Stress abhängig von den Osmosensoren Msb2 und Hkr1 verstärkt miteinander interagieren.

Zusammengefasst legen meine Resultate folgende zwei Punkte nahe: 1) Ste11 und Pbs2 werden unabhängig voneinander zur Plasmamembran rekrutiert. 2) Die stressinduzierte Clusterbildung um die Osmosensoren Msb2 und Hkr1 sorgt für eine effiziente Aktivierung der Signaltransduktionskaskade während des hyperosmotischen Stresses.

1. Introduction

1.1. MAPK Signalling

Survival is the key driving factor of life. All organisms must be able to survive in their environment. To do this, they must monitor their environment, be able to detect changes in their environment and respond appropriately in a timely manner. The ability to survive in changing environments is made possible through cell signalling. In the case of multicellular organisms, signalling often involves receiving and transmitting signals between cells. In the case of unicellular organisms, signalling occurs within the cell in response to both extra- and intracellular stimuli. One form signalling which is highly conserved from yeasts to mammals is that of mitogen-activated protein kinases (MAPK) cascades. Despite the name, MAPK cascades not only respond to growth signals but also to a range of stimuli such as light, temperature and hyperosmotic stress. They are therefore also referred to as stress-activated protein kinases (SAPKs) or extracellular signal-regulated kinases (ERKs) (Cuadrado & Nebreda 2010; Wagner & Nebreda 2009; Zarubin & Han 2005).

In the yeast *Saccharomyces cerevisiae*, there are five responses which are orchestrated through MAPK cascades resulting in the activation of a MAPK (summarised in figure 1.1): 1) the MAPK Smk1 is activated in response to starvation through an as yet unidentified mechanism and causes spore wall assembly in diploid cells. Formation of spores, which can survive extreme conditions such as desiccation, allows the cell's genetic material to be protected passed down to the daughter cells once conditions are more favourable. 2) the MAPK Slt2 is activated in response to cell wall stress, for example when there is a depletion in the availability of cell wall components. Activate Slt2 triggers the Cell Wall Integrity (CWI) response and results in increased production of cell wall components. 3) Fus3 is activated in haploid cells in response to pheromones from the opposite mating type in the external environment. This triggers the mating response which causes a change in cell morphology and so-called "shmoo" formation. A shmoo is single projection from the cell formed in the direction of source of pheromone. The presence of the shmoo then aids interaction with cells with cells of the opposite mating type and as a result, mating. 4) Kss1 is activated in response to glucose deprivation in haploid cells and nitrogen deprivation in diploid cells. These conditions trigger the filamentous growth (FG) response in which daughter cells remain attached to the mother cell rather than budding off completely. This allows the connected cells to search for nutrients more efficiently in the extracellular space. 5) the MAPK Hog1 is activated in response to hyperosmotic stress such as high external NaCl or

sorbitol concentrations, and triggers the high osmolarity glycerol (HOG) response (Chen & Thorner 2007; F Posas et al. 1998). The HOG response is the focus of my thesis and is described in greater detail below.

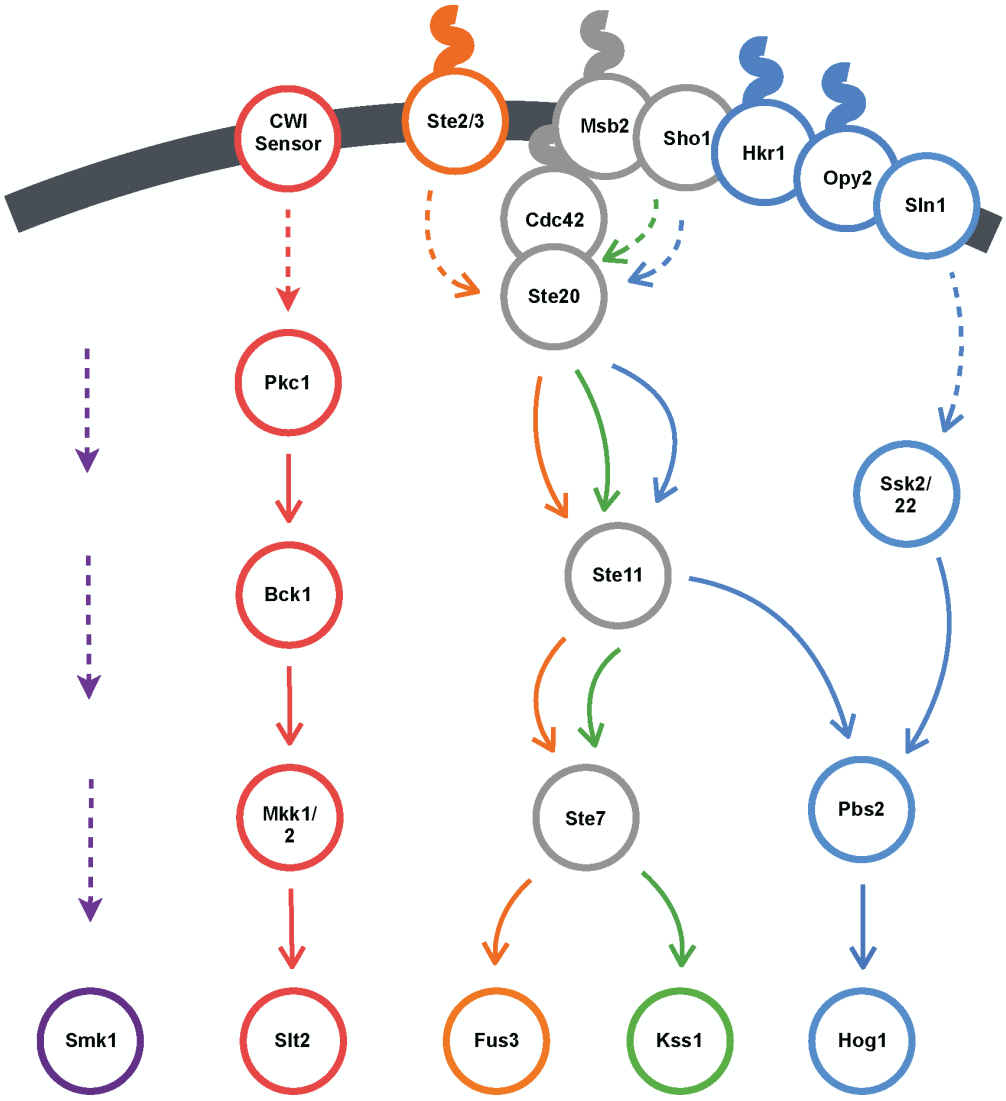

Figure 1.1

The five MAPK cascades of *Saccharomyces cerevisiae*

Pathways from left to right correspond to numbers 1 to 5 in the main text. Solid arrows indicate direct interactions. Dashed arrows indicate indirect interaction through proteins not shown for clarity. (See section 1.1 for details).

Although the five MAPK cascades have specific stimuli, they are interlinked in many ways. Temporary nutrient deprivation triggers the FG response whereas prolonged deprivation induces spore formation. The later stages of HOG response cause cell wall stress and

therefore trigger the CWI response. The FG, mating and HOG pathways share the same MAPKKK, Ste11, as well upstream components Cdc42, Cdc24, and Ste20. The FG and mating pathways share the same MAPKK, Ste7, and the FG and HOG pathways share the same transmembrane sensors, Msb2 and Sho1 (Fig. 1.1). The highly connected nature of MAPK pathways is not a feature exclusive to *S. cerevisiae* but rather a general characteristic of signalling responses (Wagner & Nebreda 2009).

1.2. The High Osmolarity Glycerol (HOG) Response

Another characteristic of signalling responses is their rapid activation upon exposure to stimuli. For example, the MAPK Hog1, a homologue of p38, is phosphorylated and activated within minutes of exposure to a hyperosmotic environmental stressor (Fig 1.2). Upon hyperosmotic stress, cells rapidly lose water through osmosis and shrink in volume. This triggers activation of the HOG response which results in an increased internal glycerol concentration. As glycerol acts as an osmolyte, an increased internal glycerol concentration re-establishes the osmotic balance between the extra- and intracellular environments, thereby removing the hyperosmotic stress (Albertyn et al. 1994; de Nadal et al. 2011; F Posas et al. 1998). The ability to activate Hog1 is essential because cells lacking functional Hog1 die on exposure to high osmolarity conditions (Brewster et al. 1993).

A third characteristic of signalling responses is that they involve multiple protein-protein interactions and often also multiprotein complexes. The very nature of a signalling cascade involves one protein interacting with another and changing its activation state so that the second protein can then interact with a third and alter its activation state and so on. The HOG pathway, responsible for the HOG response, involves many proteins upstream of Hog1 which are required for its activation (Fig. 1.3). The pathway consists of two redundant upstream branches, the SLN1 branch and so-called SHO1 branch, which converge on the MAPKK Pbs2. The SLN1 branch is activated and deactivated more rapidly than the SHO1 branch. Moreover, it is able to phosphorylate more Hog1, and therefore activate the HOG response more strongly (Hersen et al. 2008; Macia et al. 2009). It is therefore responsible for the initial dynamic activation of the HOG pathway, whereas the SHO1 branch is responsible for the duration of the response.

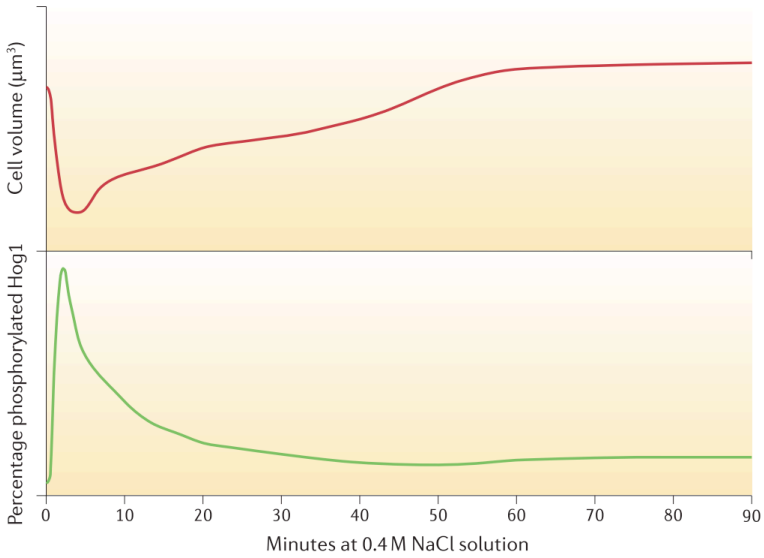

Figure 1.2

The Effect of Hyperosmotic Stress on Cell Volume and Hog1 Phosphorylation (de Nadal et al. 2011)

Within minutes of exposure to hyperosmotic stress, a rapid reduction in cell volume triggers the HOG response which causes a rapid increase in Hog1 phosphorylation.

1.2.1. Activation of the SLN1 Branch

The SLN1 branch is activated through a bacterial-like phosphorelay system (Maeda et al. 1994; Posas et al. 1996). This branch has a high basal level of activation and deactivation. As a result, it is more sensitive to less severe osmotic stressors (Macia et al. 2009). In the absence of osmotic stress, the transmembrane osmosensor and histidine kinase Sln1 autophosphorylates and then transfers this phosphate group to cytoplasmic protein Ypd1. Ypd1 then transfers the phosphate group onto Ssk1 and in doing so, inhibits Ssk1 activity. Upon osmotic stress, Ssk1 inhibition is relieved and active Ssk1 binds and activates the redundant MAPKKKs Ssk2 and Ssk22 (henceforth referred to as Ssk2/22). Ssk2/22 then bind and activate Pbs2 by phosphorylating it at residues Ser514 and Thr518 (Maeda et al. 1995; Tatebayashi et al. 2003). Active Pbs2 then activates the Hog1 by phosphorylating it at residues Thr174 and Tyr176 (Brewster et al. 1993).

1.2.2. Activation of the SHO1 Branch

Although the SHO1 branch was first identified through its dependency on the protein Sho1 (Maeda et al. 1995), it also consists of many other essential proteins, several of which have homologs in multicellular organisms (de Nadal et al. 2002). Moreover, many of the proteins in

the SHO1 branch of the HOG pathway are also needed for to activate the MAPKs of the filamentous growth and pheromone response pathways Kss1 and Fus3 (F Posas et al. 1998). Kss1 and Fus3 homologues in higher eukaryotes are responsible for essential cellular processes such as cell differentiation and development (Zhang et al. 2002). Therefore signalling events in *S. cerevisiae* involving proteins common to all three pathways are also highly relevant.

Ste20 and Cla4 are the two partially redundant MAPKKKKs of the SHO1 branch and are members of the p21-activated protein kinase (PAK) family. Ste20 is activated by the small rho-like GTPase Cdc42 through binding of its autoinhibitory domain (Raitt et al. 2000; Lamson et al. 2002). Since Cdc42 is localised at the plasma membrane, active Ste20 is also localised at the plasma membrane.

The target protein of Ste20 is the cytoplasmic MAPKKK Ste11 (Wu et al. 1995). Membrane localisation of Ste11 is essential for HOG pathway activation and is achieved through binding the adaptor protein Ste50, which binds the transmembrane anchor protein Opy2 (Wu et al. 2006; Francesc Posas et al. 1998). Ste11 and Ste50 bind each other through their N-terminal SAM domains in an osmotic stress-independent manner (Wu et al. 1999; Francesc Posas et al. 1998). Through its C-terminal RA domain, Ste50 binds the cytoplasmic tail of Opy2 (Ekiel et al. 2009; Wu et al. 2006; Yamamoto et al. 2010). As a result of these interactions, Ste11 is localised at the plasma membrane where it is phosphorylated and activated by Ste20 (van Drogen et al. 2000; Lamson et al. 2006).

The target protein of Ste11 is the MAPKK Pbs2 (Posas & Saito 1997). Whereas signalling through the SLN1-branch involves direct binding of the MAPKKKs Ssk2/22 to Pbs2, in the SHO1 branch, Pbs2 binds the transmembrane protein Sho1 (Tatebayashi et al. 2003). In this role, Sho1 functions as an membrane anchor protein and thus, through binding Sho1, Pbs2 can also localise to the plasma membrane. (Maeda et al. 1995; Tatebayashi et al. 2006).

Similarly to how the osmosensor of the SLN1-branch is the transmembrane protein Sln1, the osmosensors of the SHO1-branch, Msb2, Hkr1 and Sho1 itself are also transmembrane proteins (Maeda et al. 1995; Tatebayashi et al. 2007). Therefore, a second function of Sho1 is as an osmosensor. Msb2 and Hkr1 are highly similar transmembrane mucins which act in the HOG pathway in a redundant manner and are also essential for HOG pathway activation (Tatebayashi et al. 2007; Tanaka et al. 2014). In combination with Msb2 and/or Hkr1, Sho1 can sense changes in external osmolarity and activate the HOG pathway (Tatebayashi et al. 2015).

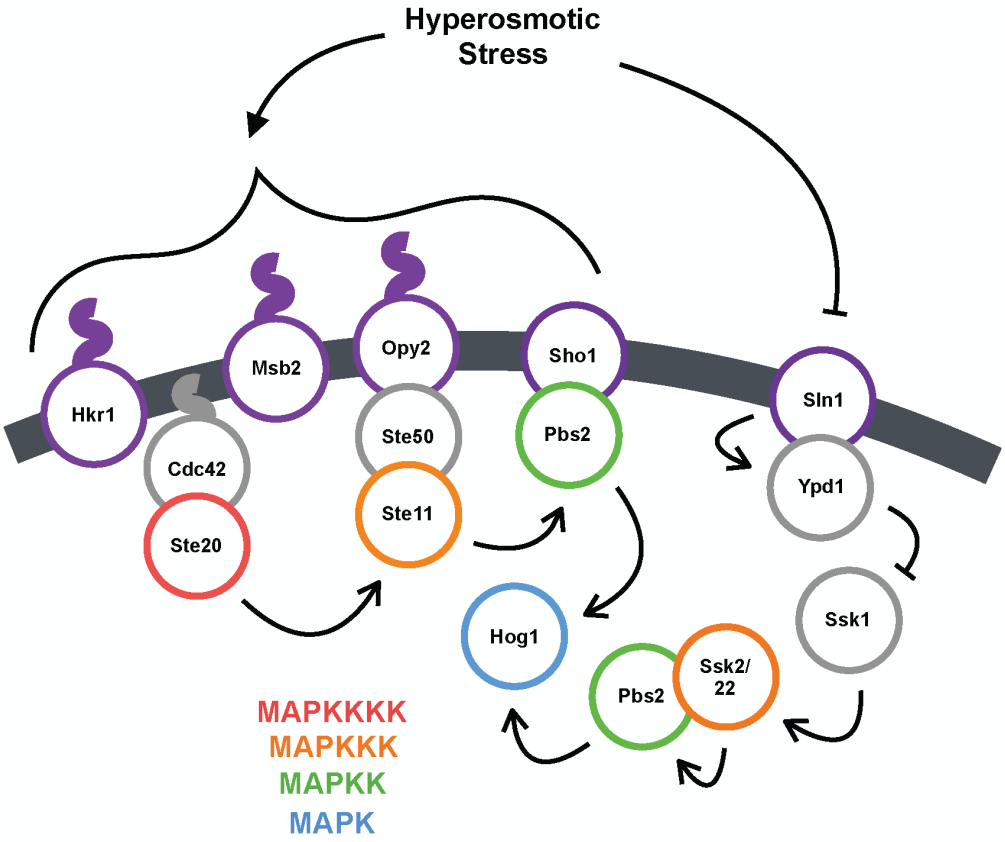

Figure 1.3

HOG Pathway Activation

The SHO1 branch (left) and the SLN1 branch (right) are both activated by the transmembrane osmosensors and result in the activation of Pbs2, which then activates Hog1. The arrows indicate the activation steps.

1.2.3. Deactivation of HOG Pathway

In addition to increasing the intracellular glycerol concentration, active Hog1 also causes cell cycle arrest and a reduction in the expression of housekeeping genes (Martínez-Montañés et al. 2010; Saito & Posas 2012). It is therefore essential that the HOG response is transient rather than sustained and can be downregulated. In wildtype cells, Hog1 is rapidly dephosphorylated after activation and almost returns to basal levels less than 40 minutes after the initial osmotic shock (de Nadal et al. 2011; Macia et al. 2009). This is due in part to negative feedback events. For example, active Hog1 phosphorylates Ste50 which causes it to dissociate from Opy2. This dissociation delocalises Ste11 from the plasma membrane and therefore the SHO1-branch of the pathway can no longer be activated (Yamamoto et al. 2010). Mutants of Ste50 which cannot be phosphorylated cause prolonged pathway activation (Hao

et al. 2007; Yamamoto et al. 2010). In addition, active Hog1 phosphorylates Sho1 monomers, thereby preventing Sho1 oligomerisation which is necessary for signalling (Hao et al. 2007).

Hog1 is also actively dephosphorylated at Thr174 by phosphatases Ptc1, Ptc2 and Ptc3, and at Tyr176 by Ptp2 and Ptp3 (Warmka et al. 2001; Wurgler-Murphy et al. 1997). As a result, deletion of both Ptc1 and Ptp2 is lethal because Hog1 cannot be dephosphorylated sufficiently and thus is hyperactive (Maeda et al. 1993). In addition, deletion of Sln1 is also lethal due to the resulting uncontrolled activation of Ssk1 and its downstream effectors including Hog1 (Maeda et al. 1995).

1.2.4 Current Model of Pathway Activation and Deactivation

In order for Hog1 to be activated, several essential key events must occur: Colocalisation of Ste20 and Ste11, of Ste11 and Pbs2, and of Pbs2 and Hog1. The current model of activation of the SHO1-branch of the HOG pathway, summarised in figure 1.4, is as follows: In the absence of hyperosmotic stress, Ste20 and Ste11 are localised at the plasma membrane (Leberer et al. 1997; Wu et al. 2006). Ste20 binds to Cdc42 which is anchored at the membrane through a geranylgeranyl modification. Ste20 also binds to Bem1 which binds to Cdc42 and to the cytoplasmic domain of the osmosensor Msb2 (Bose et al. 2001; Tanaka et al. 2014). Ste20 binds Hkr1 through an unknown mechanism. Ste11 binds to Ste50 which binds to transmembrane proteins Opy2 and Sho1, and membrane localised Cdc42 (Tatebayashi et al. 2015; Truckses et al. 2006; Yamamoto et al. 2010; Wu et al. 2006). Through their extracellular domains, Msb2 and Hkr1 bind Opy2 (Tatebayashi et al. 2015; Yamamoto et al. 2015). Through their transmembrane domains, they bind Sho1 (Tatebayashi et al. 2007). Sho1 binds to itself to form oligomers and also to Opy2 (Hao et al. 2007; Tatebayashi et al. 2015). It is not known precisely when Pbs2 interacts with Sho1 and Ste11 but these interactions are essential for pathway activation (Maeda et al. 1995; Posas & Saito 1997).

Osmotic stress is sensed by the heavily glycosylated extracellular domains of Msb2 and Hkr1 (Brewster & Gustin 2014). Since Msb2 and Hkr1 interact directly or indirectly with Ste20, Ste11 and Pbs2, structural changes in Msb2 and Hkr1 upon stress cause Ste20, Ste11 and Pbs2 to come together, allowing sequential activation of Ste11 and Pbs2. Once activated by Pbs2, Hog1 phosphorylates Ste50 to cause dissociation of Ste50 and Ste11 from the plasma membrane (Yamamoto et al. 2010). Hog1 also phosphorylates Sho1 which reduces oligomerisation and, as a result, signalling through the pathway (Hao et al. 2007).

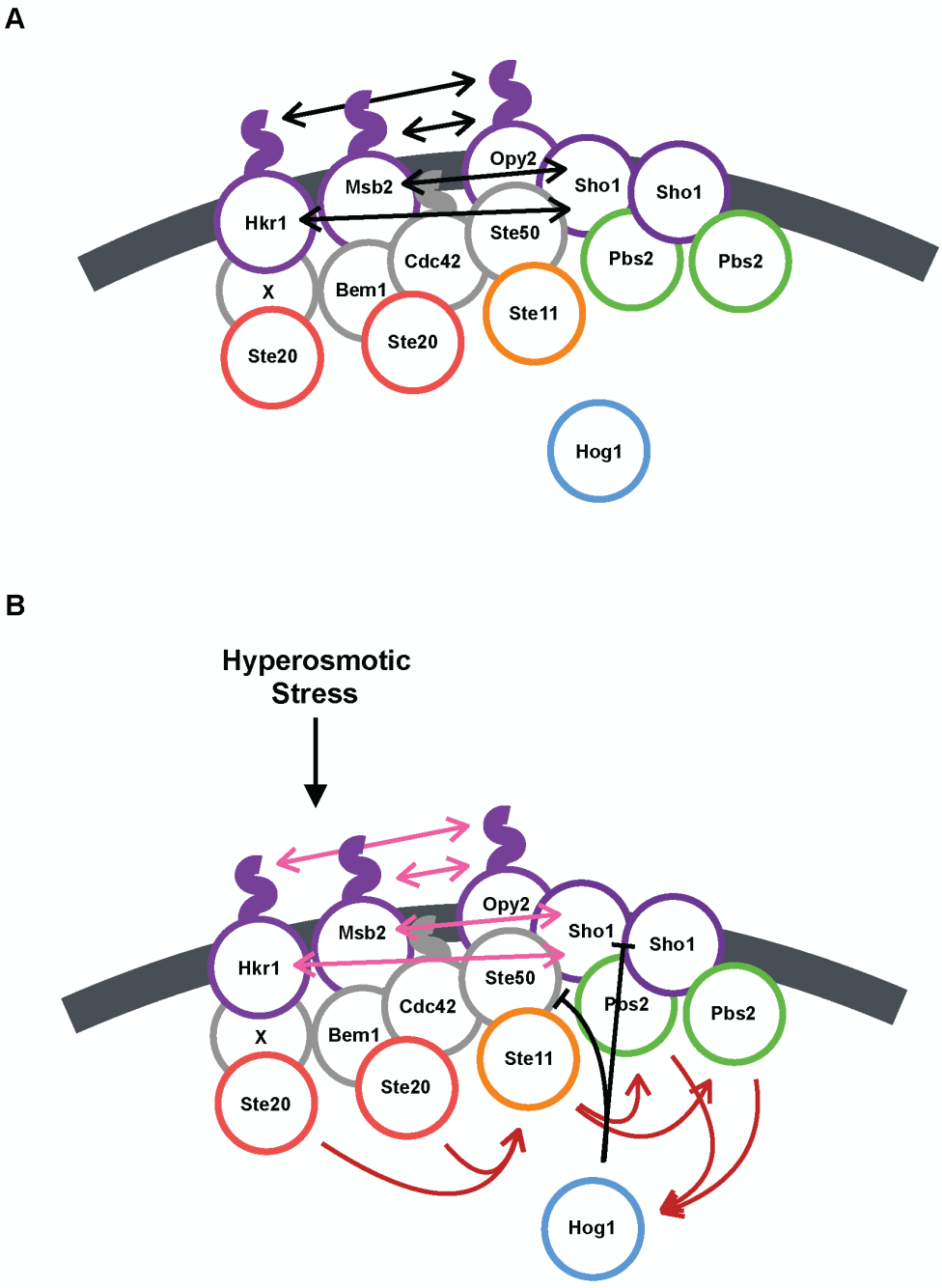

Figure 1.4

Current model of activation of the SHO1 branch of the HOG pathway

(A) In the absence of osmotic stress, proteins are grouped at the plasma membrane, but no signalling occurs. (B) Osmotic stress is sensed by Msb2 and Hkr1 which undergo structural changes and transmit this signal to Opy2 and Sho1 (pink arrows). This causes activation of the kinase cascade. Active Hog1 then inhibits the Ste50-Opy2 interaction and the Sho1-Sho1 interaction. (See section 1.2.4 for further details).

1.3. Protein Interaction Assays

Both a failure to activate the HOG pathway when needed, and activation of the pathway when not needed result in cell death. It is therefore essential that the HOG response is tightly regulated. In order to understand how the pathway is regulated, the mechanisms of pathway activation and inactivation must be elucidated. This involves not only identifying the required genes and describing their mutant phenotypes, but also understanding how the proteins of the HOG pathway interact in physical space before, during and after osmotic stress. Many protein interaction assays exist, all of which have their own advantages and disadvantages making them suitable or unsuitable for specific biological questions. I will now describe some of these methods in more detail.

1.3.1. Microscopy Methods

1.3.1.1. Fluorescence Autocorrelation Spectroscopy (FCS) and Fluorescence Cross-Correlation Spectroscopy (FCCS)

FCS is a technique involving confocal microscopy and a fluorescently tagged protein of interest. The protein of interest can either be in solution or *in vivo*. As the protein diffuses around, it passes in and out of the field of view. This causes peaks and troughs in the amount of fluorescence detected resulting in so-called fluorescence fluctuations over time. These fluorescence fluctuations can be mathematically transformed into a correlation curve. The correlation curve provides information as to the diffusion rate and the concentration of the fluorescently tagged protein. FCS can therefore be used to study membrane localisation because membrane localised proteins diffuse less than free proteins (Bacia et al. 2006).

FCCS is a development of FCS involving the measurement of two fluorescently tagged proteins simultaneously. If two proteins interact or colocalise, they are more likely to move in and out of the field of view together. They would therefore have very similar fluorescence fluctuation patterns. The fluorescence fluctuations of both proteins can be combined and mathematically transformed to generate a cross-correlation curve. The cross-correlation curve provides information as to the colocalisation or binding of the two proteins (Bacia et al. 2006).

FCCS has previously been used in yeast to study the colocalisation of MAPK cascade proteins in the pheromone response pathway (Maeder et al. 2007; Slaughter et al. 2007). An advantage of FCS and FCCS is the small detection volume of less than one femtolitre. Since such small

volumes are required for measurements, measurements can be calculated for different regions of the cell such as cell membrane, cytoplasm and nucleus. A disadvantage of this technique is the fluorescent signals emitted must be bright enough to be detected by the microscope. For highly abundant proteins, this is often not a problem. However, for less abundant proteins, longer exposure times are required which can often lead to photobleaching of the fluorophores. Alternatively, proteins can be deliberately overexpressed to increase signals.

1.3.1.2. Bimolecular Fluorescence Complementation (BiFC)

BiFC is a type of protein-fragment complementation assay. In BiFC, the sequence of a fluorescent protein is split into two parts. One part is fused to a first protein of interest, and the other part is fused to a second protein of interest. Individually, neither part of the fluorescent protein fluoresces, however when the proteins of interest interact, the two parts of the fluorescent protein come together and assemble to create the complete fluorescent protein. In this way, fluorescence can be used to determine if the proteins of interest interact.

When this method was initially developed, it was limited to visualising one interaction at a time. However, thanks to further developments of this method, it is now possible to visualise the interaction of a protein of interest with many interaction partners. This is possible because fluorescent protein parts can assemble in many different combinations, each combination resulting in the formation of a protein with different spectral properties (Hu & Kerppola 2003).

One caveat of this method is the long assembly and maturation times of the fluorescent proteins. Different fluorescent proteins have maturation times which range between a scale of minutes to hours (Balleza et al. 2018). Because the HOG pathway reaches a peak level of activation after approximately 10 minutes (Macia et al. 2009), when used to study the HOG pathway, most fluorescent proteins would not be able assemble and fluoresce before the interaction of the proteins of interest was reduced due to pathway activation.
A second caveat of this method is the stability of the assembled fluorescent protein. It has been shown that, once formed, the interaction of interest which led to the assembly of two parts can be abolished whilst the fluorescent protein remains assembled (Magliery et al. 2005). This would be disadvantageous in the case of proteins that interact before osmotic stress and then dissociate because the reduction in interaction could not be visualised. Moreover, the reduction in interaction might even be prevented as the two proteins would be anchored together via the fluorescent protein parts.

1.3.2. Transcriptional Assays

1.3.2.1. Membrane Yeast Two-Hybrid (MYTH)

Like BiFC, MYTH is also a protein-fragment complementation assay. In MYTH, the sequence of ubiquitin (ub) is split into two parts. The N-terminal part (NubI) contains the mutation I13G and is fused to the first protein of interest. The C-terminal part (Cub) along with transcription factor LexA is fused to a second protein of interest. Normally, due to the I13G mutation, NubI and Cub cannot interact and thus assemble. However when fused to two proteins of interest which interact, they can assemble to form the complete ubiquitin protein. Once formed, this complex is recognised by ubiquitin-specific proteases and cleaved, and LexA is released. LexA can then translocate to the nucleus where it can activate reporter genes such a LacZ of HIS3. Therefore, interaction of two membrane proteins can be measured by the accumulation of blue pigment in cells, or the ability of cells to grow in media lacking histidine (Johnsson & Varshavsky 1994; Stagljar et al. 1998). Although this assay was developed for use with membrane proteins, it can theoretically also be used for the interaction of membrane proteins with cytoplasmic proteins.

A benefit of this method, when compared to microscopy methods, is that it is less dependent on the expression level of the proteins of interest. Although, lower levels of protein expression would, for example, result in slower growth, when compared to an appropriate control, growth should still be measurable. A caveat of this method is that it relies on transcriptional activation which is relatively slow when compared to the dynamic nature of the HOG response. Moreover, as with BiFC, the assembly time of NubG and Cub further increases the time required for reporter gene activation after the proteins of interest interact.

1.3.3. Affinity Purification Methods

1.3.3.1. Co-immunoprecipitation (Co-IP)

Another type of protein interaction assay is co-immunoprecipitation (co-IP). Co-IP involves purifying a protein of interest from a cell lysate using highly specific antibodies attached to a solid surface such as agarose beads. Incubating the cell lysate with the antibody-linked beads allows the protein of interest to bind non-covalently to the beads, i.e. allows the protein of interest to immunoprecipitate. The beads then undergo several washing steps to remove non-specifically bound proteins before the protein of interest and its interacting partners are eluted from the beads. Co-IP is named as such because the protein of interest and its

interacting partners immunoprecipitate together. If the identities of the interacting partners are known, the eluate can be analysed by Western blotting and the presence of interacting partners can be detected using specific antibodies against them (Phizicky & Fields 1995). Alternatively, if the identities of the interacting partners are not known, the eluate can be analysed by mass spectrometry (MS) to find new interacting proteins.

An advantage of co-IP is that the immunoprecipitation step also functions as an enrichment step, meaning that proteins expressed at too low a level to be detected in a cell lysate can be concentrated before being visualised through Western blotting. A caveat of this method however is that in order for proteins to co-immunoprecipitate, they must bind each other strongly enough to remain associated throughout cell lysis, immunoprecipitation and several washing steps. Proteins which bind the protein of interest weakly or transiently will be lost during the washing steps. In addition, the buffer conditions used for immunoprecipitation can also result in the loss of some interactions. Therefore, co-IP is best suited for strong/stable interactions.

As the HOG pathway is rapidly switched on and off, it is thought that many of the interactions involved are dynamic and of low affinity. Thus, these interactions would not be maintained throughout the co-immunoprecipitation process and the proteins investigated would appear not to interact.

1.3.3.2. Crosslinked Co-IP

To circumvent the requirement for stable interactions, the method of co-IP has been combined with the use of crosslinkers (Yakovlev 2009). Crosslinkers are small reactive molecules which can form covalent bonds with at least two functional groups commonly found in proteins. If two proteins are in close proximity to each other either through direct or indirect binding, a single crosslinker molecule can react with both proteins forming a covalent link between the two. This covalent link allows the protein of interest to be immunoprecipitated under much more stringent conditions whilst maintaining its interaction with its binding partners. This method thus allows weaker interactions to be visualised. Moreover, as some crosslinkers can be cleaved, proteins can be visualised through Western blotting or identified through MS in a similar way to traditional co-IP. Furthermore, as cell permeable crosslinkers exist, crosslinking can also be performed *in vivo* before cells are lysed thus preventing the loss of more weakly interacting partners during this step.

One disadvantage of this method however is the incubation time of the crosslinkers. Although incubation times of five minutes have been used successfully to study the HOG pathway (Tatebayashi et al. 2015; Yamamoto et al. 2015), optimal incubation times are 20 minutes or longer. As the HOG pathway is activated less than two minutes after osmotic stress, it is thought that crosslinked co-IP would not be able to capture the initial interactions of the HOG response. Furthermore, the crosslinking of proteins might affect their epitopes recognised by antibodies. For example, if a protein of interest is recognised by an antibody in its C-terminal region, it is possible that certain interactions taking place near the C-terminus (and therefore causing crosslinking near the C-terminus) might prevent antibody binding. The protein of interest would then not be immunoprecipitated and the interacting partner which bound the C-terminal region would not be identified. Whereas interactions taking place near N-terminus would not prevent antibody binding and thus would be identified. This is a potential problem that also applies to traditional co-IP, in which interactions with binding partners prevent antibody binding.

1.3.3.3. BioID

Another type of protein-proximity assay is BioID. The BioID method involves tagging a protein of interest with a mutant form of BirA, a biotin ligase taken from E. coli. The mutant enzyme, called BirA*, catalyses a reaction between biotin and AMP to form biotinyl-AMP which it then releases from its active site. As biotinyl-AMP is a highly unstable species, it readily reacts with lysine residues of nearby proteins, forming a covalent bond resulting in the biotinylation of the protein. In the BioID method, proteins which are in close proximity to the BirA*-tagged protein are therefore biotinylated. The biotinylated proteins can then be affinity purified under denaturing conditions using streptavidin beads. The pulled-down proteins can then be identified through MS analysis (Kim et al. 2016; Roux et al. 2013).

As this method involves purification of proteins through the biotin-streptavidin interaction, extremely stringent washing conditions can be applied without the biotinylated proteins being washed away. This is advantageous when it is suspected that the protein of interacts with transmembrane or membrane-associated proteins because strong detergents are often required to extract and solubilise these proteins. An argument against the use of BioID in yeast, however, is that several proteins in *S. cerevisiae* are biotinylated which would lead to a high background biotinylation level and make MS identification of BirA*-biotinylated proteins more difficult. Furthermore, current protocols for mammalian cells suggest an incubation time of at least 16 hours to allow for maximal biotinylation of substrates. As the HOG response

takes place on a scale of minutes, the timescale of the BioID assay also makes it unsuitable for studying the HOG response in *S. cerevisiae* (Roux et al. 2013).

1.3.4. M-Track

The final method I will describe is the M-Track assay, a protein-proximity assay developed in our group in collaboration with the Ogris group (Zuzuarregui et al. 2012). In the traditional form of this assay, one protein of interest (protein Y) is tagged with an H320R mutant version of human lysine methyltransferase (HKMT) with over 20 times the activity of the wildtype HKMT, and a second protein of interest (protein X) is tagged with several haemagglutinin (HA) epitopes and multiple repeats of a peptide encoding residues 1-21 of Histone 3. When proteins X and Y come into close proximity in the cell, the HKMT of protein Y methylates K9 of the H3HA tag of protein X up to a maximum of three methyl groups per H3 repeat (Fig 1.5). The level of H3K9 methylation on protein X can be then measured by Western blotting using trimethylation specific antibodies.

One advantage of this system is that, unlike biotinylation in the case of BioID, there is no natural H3K9 methylation in *S. cerevisiae* meaning that any methylation observed is due to the close proximity of proteins X and Y. A second advantage of this system is that there is no H3K9 demethylase in *S. cerevisiae* meaning that the methylation mark remains on the H3 tag, even when proteins X and Y are no longer in close proximity (Fig 1.5A right). This allows even transient interactions to be measured. In addition, the HA epitope can be used in Western blotting to measure the total amount of protein X. From these measurements, a me3:HA ratio can be calculated. Moreover, protein X can be immunoprecipitated via the HA epitope to enrich the methylation signal if needed. In an experimental setup using the HOG response, cells can be hyperosmotically stressed and their methylation levels compared to levels from unstressed cells. A higher level of methylation in the stressed samples would be indicative of an increased interaction between proteins X and Y during hyperosmotic stress.

Since the H3K9 methylation is irreversible, it is possible for the H3HA tag to become fully trimethylated, i.e. saturated, if the two proteins interact at all before the assay begins. In this case, if two proteins came together again during osmotic stress, this increase in interaction would not be able to be observed because a further increase in methylation would not be possible. To avoid this problem, the assay was further developed into a rapamycin-inducible form and an FK506-inducible form in collaboration with the Kraft lab (Brezovich et al. 2015). As the FK506-inducible system requires the deletion of *CNB1* and *Δcnb1* cells are known to

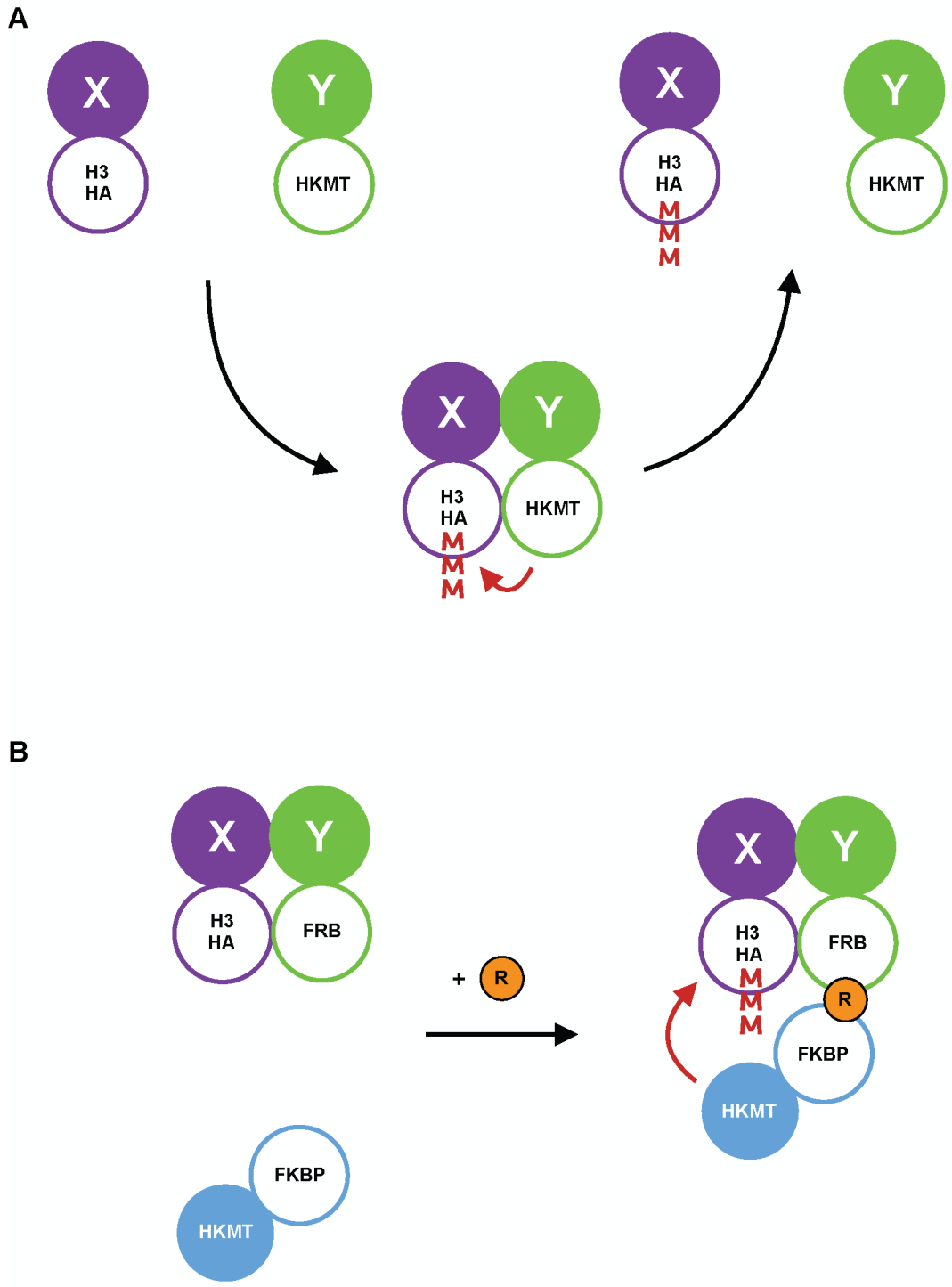

Figure 1.5

The M-Track Protein Proximity Assay

(A) The traditional (non-inducible) system: When proteins X and Y come into close proximity, the H3HA tag of protein X is methylated. Only one H3 repeat is shown for clarity. Even after proteins are no longer in close proximity, the H3HA tag remains methylated. (B) The rapamycin-inducible assay: Even when proteins X and Y are in close proximity before rapamycin (R) addition, no methylation of the H3HA tag occurs.

have increased sensitivity to hyperosmotic stress (Mendoza et al. 1994), the rapamycin-inducible system is more appropriate when studying the HOG response.

In the rapamycin-inducible M-Track assay, protein X is tagged in the same way as in the non-inducible assay. Protein Y, however, is tagged with the **F**KBP12-**r**apamyin **b**inding (FRB) domain of human FRAP (Choi et al. 1996). The HKMT is fused to FKBP12 (FKBP) and expressed separately under the control of the *ADH1* promoter. Upon addition of rapamycin to cells, FKBP and the FRB domain dimerise, bringing the HKMT to protein Y. Then, as in the non-inducible assay, if proteins X and Y are in close proximity, the H3HA tag of protein X can be methylated (Fig. 1.5B).

The inducible systems have several advantages when compared to the non-inducible system. Firstly, in the non-inducible system, if protein X is involved in three different interactions, A, B and C, with three different proximities, but which all result in a saturated signal before the beginning of the assay, these differences in proximities cannot be measured (Fig 1.6A left). However, using an inducible system to study the same three interactions would result in different rates of methylation accumulation after the addition of rapamycin. The interaction pair which came into close proximity most often would have the fastest rate of accumulation and the interaction pair which came into close proximity least often would have the slowest rate of accumulation (Fig. 1.6A right). Therefore, the inducible systems allow differences in proximity to be distinguished which were indistinguishable using the non-inducible system. Secondly, even though the methylation mark is irreversible, the inducible system is able to measure decreases in proximity during osmotic stress. In this case, the hyperosmotically stressed samples would contain lower levels of methylation than the unstressed samples (Fig. 1.6B right).

It should be emphasised that the M-Track assay is a protein-proximity assay and therefore cannot distinguish between direct and indirect interactions. Moreover, the level of methylation on the H3 tag is only a measurement of amount of time it spends interacting with the HKMT. It is therefore an indication of how long the two tagged proteins interact with each other, but it is not necessarily an indication of binding affinity. For example, an interaction with low on and off rates (k_{on} and k_{off}) can have the same dissociation constant (K_d) as an interaction with high on and off rates. However, in the former case, the proteins interact with each other for longer and therefore the H3 tag can be more methylated.

Given the benefits detailed above, I decided to use the rapamycin-inducible assay to measure protein proximities with an aim to provide insight into the regulation of HOG pathway activation.

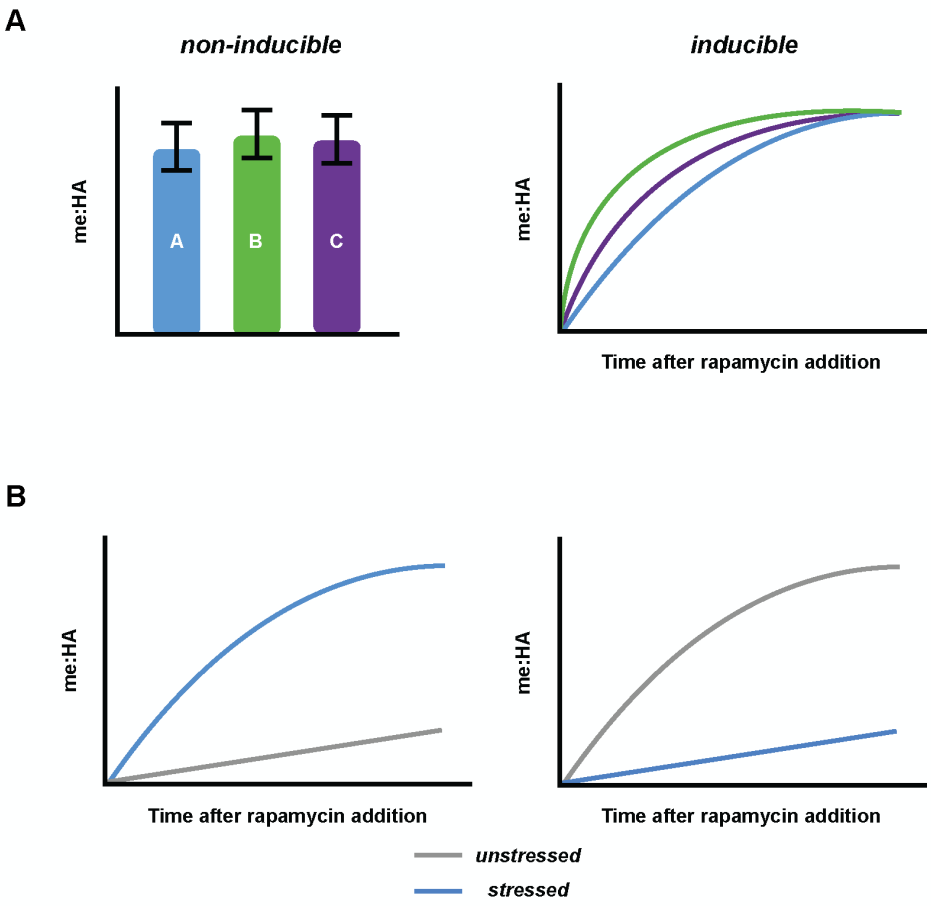

Figure 1.6

Advantages of the Inducible M-Track System

(A) Three interactions whose proximities which are indistinguishable using the non-inducible system (left) result in three different rates of methylation accumulation when using the inducible system (right). Here interaction B has the highest proximity and interaction A has the least. (B) Methylation accumulation in a stress-induced increase in proximity (left) or decrease in proximity (right).

1.4. Importance of the Study and Aims

Although many genes required for HOG pathway activation have been identified the exact mechanism of activation remains unclear. This includes how the proteins of the HOG pathway interact before and during the hyperosmotic stress response, as well as the dependencies of certain interactions on others. Many studies, particularly those from the Saito group, have advanced the knowledge in this field tremendously (Saito & Posas 2012). However, previous work has relied heavily on the use of co-immunoprecipitation, overexpression systems and partially-characterised hyperactive or inactive mutants. Although these methods and tools can enable us to answer key biological questions, it is thought that, in the context of HOG pathway

activation, these methodological approaches have led to some key features of pathway activation being overlooked.

In addition to the caveats of co-immunoprecipitation described above, it is known that the pathway is sensitive to overexpression of proteins, as overexpression of a hyperactive Ste11 allele causes activation of the pathway in the absence of both osmotic stress and membrane-localisation adaptors Ste50 and Sho1 (van Drogen et al. 2000; Posas & Saito 1997; Tatebayashi et al. 2006). Furthermore, hyperactive and inactive alleles are not always able to mimic the wildtype response in the absence or presence of osmotic stress. Although this is a desirable characteristic of mutant alleles, one must interpret the results from such experiments carefully. For example, ΔSTR mutants of Msb2 and Hkr1 are constitutively active and activate the HOG pathway in the absence of stress. They have therefore been used as a proxy for the response of the pathway to exposure to hyperosmotic stress. However, these mutants activate the pathway in the absence of stress only at 10-25% of the level activated by the wildtype alleles in the presence of stress. Furthermore, in the presence of stress, these alleles can only activate the pathway at 20-45% of the wildtype level (Tatebayashi et al. 2007). Therefore, care must be taken when drawing conclusions from experiments using mutants which do not mimic the wildtype response to hyperosmotic stress.

Given the possibility that key pathway features have been overlooked, the aims of my thesis were as follows:
1) use the inducible M-Track system to describe the interactions between proteins of the SHO1-branch of the HOG pathway in the absence and presence of osmotic stress to create a model of the dynamic changes that occur during pathway activation
2) characterise the interdependency these interactions.
Throughout my thesis, unless explicitly stated, “pathway activation” and similar terms refer to activation exclusively via the SHO1-branch of the HOG pathway.

To avoid artefacts due to overexpression of proteins, all proteins were endogenously tagged at their native loci, and expressed under the control of their native promoters unless specified. In addition, all fusion proteins were tested for functionality before use. Although I initially started using the me3:HA ratio as a normalisation method, this normalisation method required me to run two identical SDS-PAGE gels probing one for methylation and the other for HA. As inevitable loading variations between the two gels existed, I then started to normalise the methylation levels on the same gel by probing against levels of Cdc28, a protein whose levels expression levels are not affected by osmotic stress.

The results of my thesis consists of three main parts which will be described in the next chapter:

1) characterisation of Pbs2 membrane localisation (section 2.1)

2) characterisation of the interactions of the transmembrane proteins with each other (section 2.2)

3) characterisation of Ste11 membrane localisation (section 2.3).

2. Results

2.1. Pbs2 Localisation

Studies of Pbs2 localisation during osmotic stress have given conflicting results. In both the absence and presence of osmotic stress, the MAPKK is located in the cytoplasm (Ferrigno et al. 1998; Reiser et al. 2000; Tatebayashi et al. 2003). However, in order for it to be activated by Ste11 it must bind its membrane anchor Sho1 at the plasma membrane (Maeda et al. 1995; Tatebayashi et al. 2003). Furthermore, results from our group have also suggested that Pbs2 and Sho1 interact both in the absence and presence of stress (Friedmann 2010).

Pbs2 contains a polyproline motif which interacts with the C-terminal SH3 domain of Sho1. Mutations in either the polyproline motif or SH3 domain abolish both the Pbs2-Sho1 interaction and HOG pathway activation upon osmotic stress (Maeda et al. 1995; Tatebayashi et al. 2003; Tatebayashi et al. 2006). Moreover, SH3 domain mutants with reduced affinity to Pbs2 also show reduced levels of pathway activation (Marles et al. 2004; Zuzuarregui et al. 2012). Therefore, the Pbs2-Sho1 interaction is an essential step in HOG pathway activation. Given that osmotic stress-related localisation of Pbs2 is still unclear, I used the M-Track system to study the Pbs2-Sho1 interaction as proxy for Pbs2 membrane localisation.

2.1.1. Pbs2 interacts more with Sho1 during osmotic stress

Higher levels of methylation were found in osmotically stressed samples than in unstressed samples (Fig 2.1A). Quantification of signals showed that methylation accumulated at a faster rate in stressed samples and also the average level of methylation was higher for stressed samples than unstressed samples at all three timepoints (Fig 2.1B and C). This indicates that, during osmotic stress, Pbs2 interacts more with Sho1 and, in doing so, relocalises to plasma membrane.

Sho1 localises to the bud and bud neck, and has previously been reported to form oligomers, suggesting that Pbs2 might also localise to these oligomeric structures (Hao et al. 2007; Marles et al. 2004; Reiser et al. 2000; Tatebayashi et al. 2015). Thus, I next aimed to investigate Sho1 oligomerisation and the interactions of Pbs2 with the oligomeric complex.

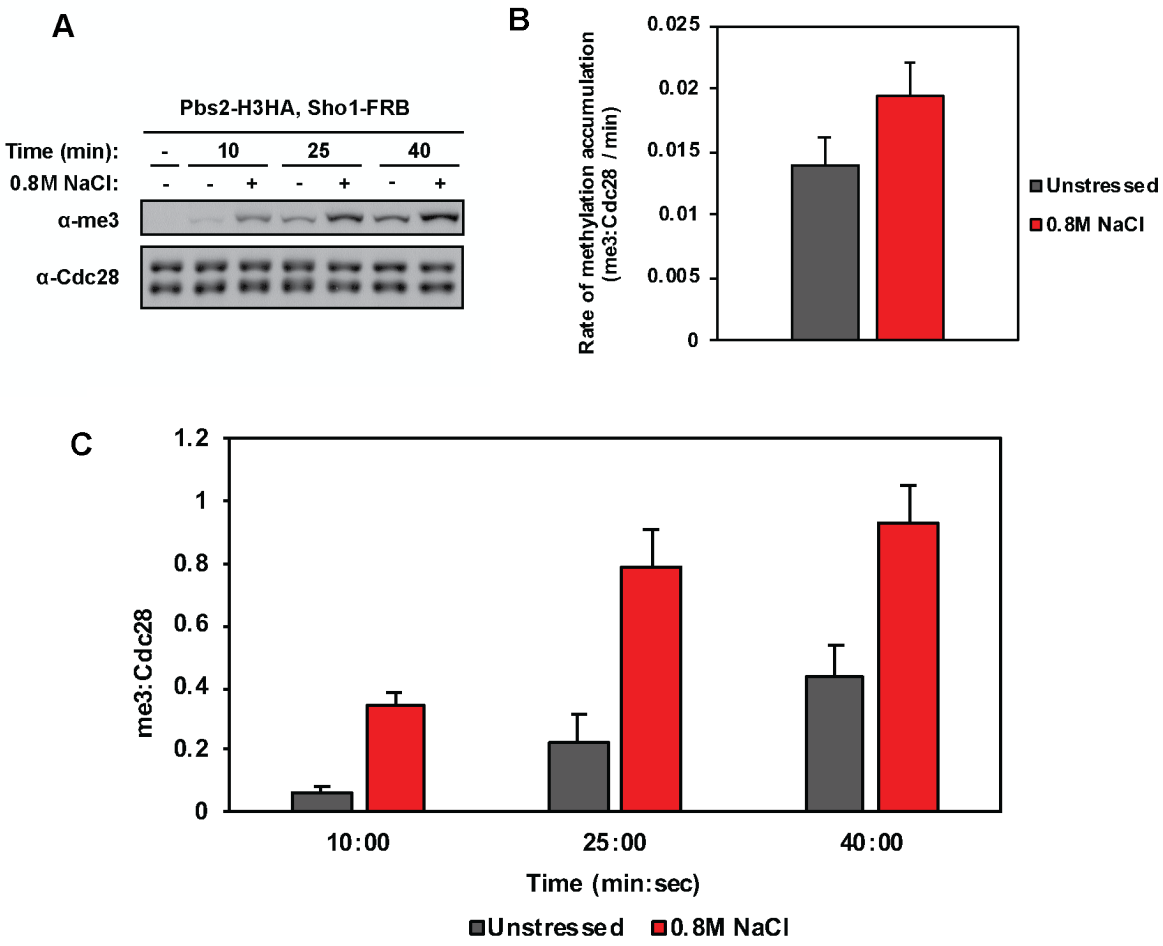

Figure 2.1

M-Track analysis of the Pbs2-Sho1 interaction

(A) Immunoblot of the M-Track assay using strains yJA390 as described in the Materials and Methods section. (B) Rate of methylation accumulation. Error bars represent SD (n=3). (C) Mean of calculated me3:Cdc28 ratios. Error bars represent SD (n=3).

Sho1 oligomers have been reported to undergo structural changes upon exposure to hyperosmotic stress (Tatebayashi et al. 2015). I used the M-Track assay to measure the interaction of two differently-tagged forms of Sho1 in the same strain. Upon addition of rapamycin, methylation accumulated in both the osmotically stressed and unstressed samples at the same rate (Fig 2.2A and B). In addition, the average levels of methylation were the same in both stressed and unstressed samples at all three timepoints (Fig. 2.2C). This indicates that Sho1 is in close proximity to itself. It is not surprising that one form of Sho1 localises to where the other form of Sho1 localises because they are the same protein. This experiment, however, could not distinguish between non-specific colocalisation and a purposeful interaction.

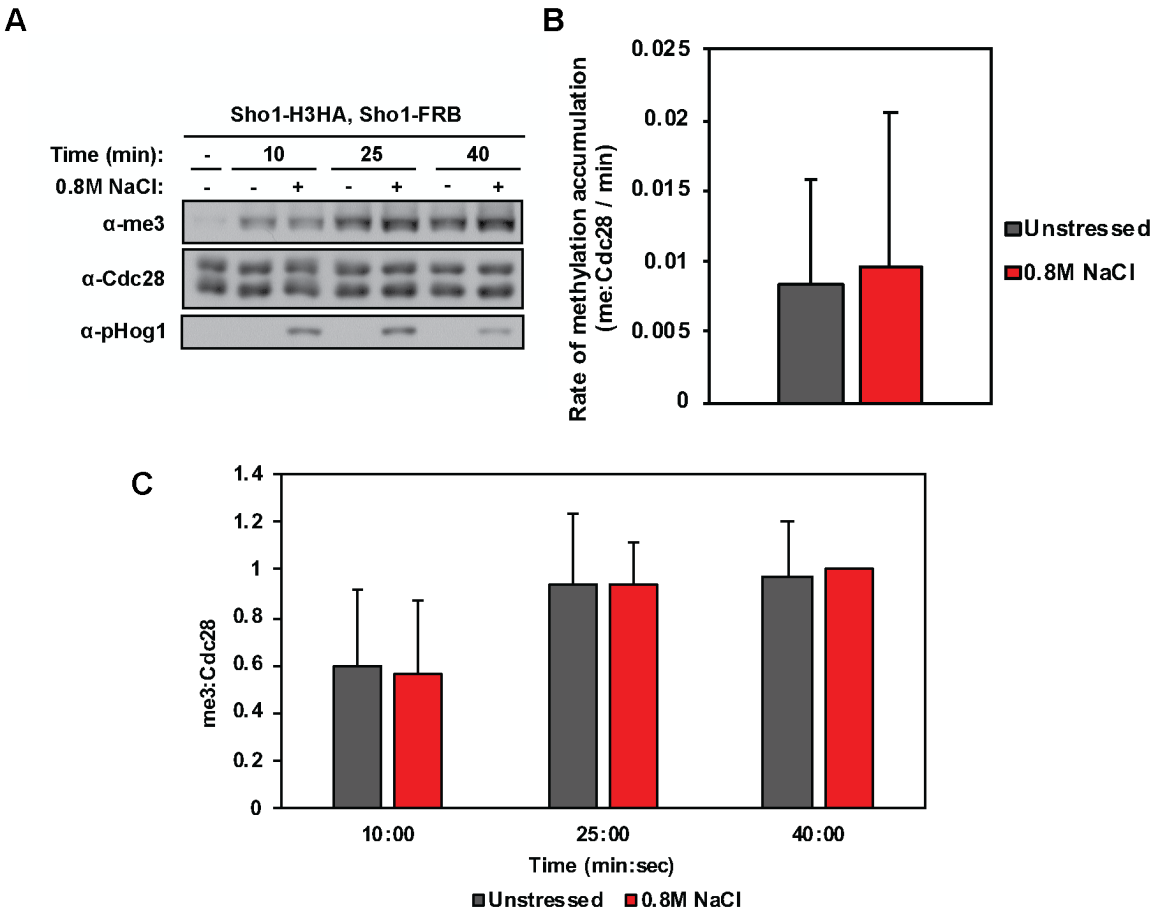

Figure 2.2

M-Track analysis of the Sho1-Sho1 interaction during 40 minutes of osmotic stress

(A) Immunoblot of the M-Track assay using strain yJA372 as described in the Materials and Methods section. (B) Rate of methylation accumulation. Error bars represent SD (n=3). (C) Mean of calculated me3:Cdc28 ratios. Error bars represent SD (n=3).

If Sho1-Sho1 proximity were indicative of a purposeful interaction, i.e. proximity was required for a certain event to occur, then if this proximity were abolished, the dependent event would not occur. Following this logic, a previous study from our group showed that if Sho1ΔSH3 (which is unable to bind Pbs2) could interact with wildtype Sho1, then it could interact indirectly with Pbs2. However, when wildtype Sho1 was not present, Sho1ΔSH3 could not interact with Pbs2 (Zuzuarregui et al. 2012). One drawback of this study is that it did not compare the interaction in osmotically stressed cells to that in and unstressed cells and also used a non-inducible version of the M-Track assay. I therefore repeated the experiment using both stressed and unstressed cells and the rapamycin-inducible assay. In this experiment I aimed to confirm the results from the previous study and identify any osmotic stress-related changes in interaction.

I tagged Pbs2 with H3HA and expressed either wildtype Sho1-FRB or Sho1ΔSH3-FRB. In addition, I created strains with or without the wildtype copy of Sho1 expressed in the background. I found an increase in methylation upon osmotic stress in cells expressing wildtype Sho1-FRB in both the presence and absence of wildtype Sho1 expressed in the background (Fig 2.3A, lanes 1-6). This increase was also found in cells expressing Sho1ΔSH3-FRB with wildtype Sho1 in the background (lanes 7-9). However, no methylation could be see when wildtype Sho1 was not expressed in the background in Sho1ΔSH3-FRB-expressing cells (lanes 10-12). This confirms the results of the previous study that the interaction of wildtype Sho1 and Sho1ΔSH3 is needed for Pbs2 to interact with Sho1ΔSH3. These results support the idea that Sho1-Sho1 proximity is the result of a purposeful interaction and not due to non-specific colocalisation.

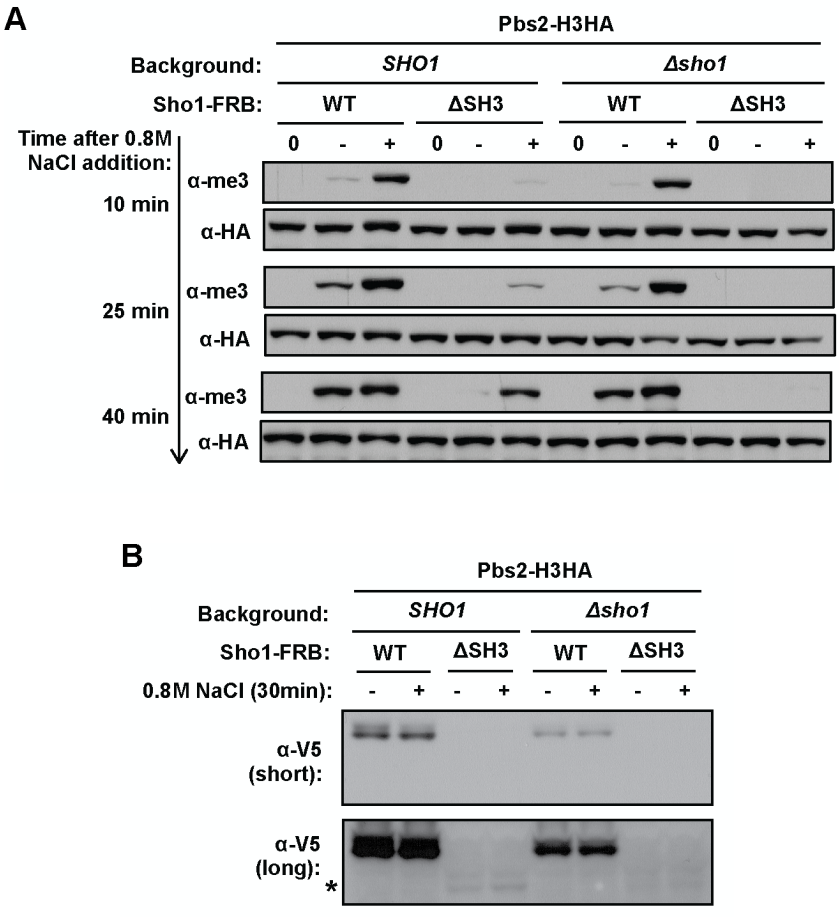

Figure 2.3

M-Track analysis of the Pbs2 interaction with wildtype Sho1 and Sho1ΔSH3 in *SHO1*$^{+}$ and sho1 backgrounds

(A) Immunoblot of the M-Track assay using strains yJA370, yJA362, yJA390 and yJA388 as described in the Materials and Methods section. (B) Immunoblot of Sho1FRB-V5 expression levels during the M-Track assay. * indicates the height of the band showing weak levels of Sho1ΔSH3 expression.

When measuring the amount of methylation in cells expressing wildtype Sho1-FRB, the osmotic stress-induced increase in methylation could be seen most clearly at the 10-minute timepoint. The methylation signals in the stressed cells were already saturated by the 25-minute timepoint and by the 40-minute timepoint, methylation signals in the unstressed samples were also reaching saturation levels. As a result, at the 40-minute timepoint, the osmotic stress-induced increase in the Pbs2-Sho1 interaction could not be seen.

2.2. Interactions of the transmembrane proteins with each other

2.2.1. Sho1 interacts more with Sho1 during osmotic stress

As previous experiment involved measuring the interaction of two proteins that were bridged by a third, the interaction observed was sum of two interactions: the untagged Sho1-Pbs2 interaction, and the untagged Sho1-Sho1ΔSH3. Although I had already measured Pbs2-Sho1 and Sho1-Sho1 interaction individually, given the signal saturation observed Fig. 2.3A, I suspected I might have overlooked osmotic stress-induced changes in the Sho1-Sho1 interaction. Moreover, at the 40-minute timepoint, the HOG pathway is already being switched off (as indicated by the reducing levels of Hog1 phosphorylation in Fig 2.2A). I therefore repeated the Sho1-Sho1 M-Track assay using shorter timepoints (at which Hog1 phosphorylation was not yet reducing, see Fig 2.12D).

Higher levels of methylation were found in osmotically stressed samples than in unstressed samples at the first two timepoints, however by the 10-minute timepoint, the methylation signal appear to be saturated thereby preventing further signal increase (Fig 2.4A). As a result, the calculated rate of increase (which was calculated across all three timepoints) was lower for osmotically-stressed cells than for unstressed cells (Fig 2.4B). This can be seen in Fig. 2.4C since, between the second and final timepoint, the average methylation level of the unstressed samples increased by 35% (from 0.69 to 0.93) whereas the corresponding increase for the stressed samples was only 12% (from 0.89 to 1.00). These results indicate that the Sho1-Sho1

interaction increases during osmotic stress. As the Sho1-Sho1 interaction increase is an example of a dynamic interaction between transmembrane proteins, this raised the question of whether the other transmembrane proteins, Msb2, Hkr1 and Opy2 also undergo osmotic stress-induced changes in proximity.

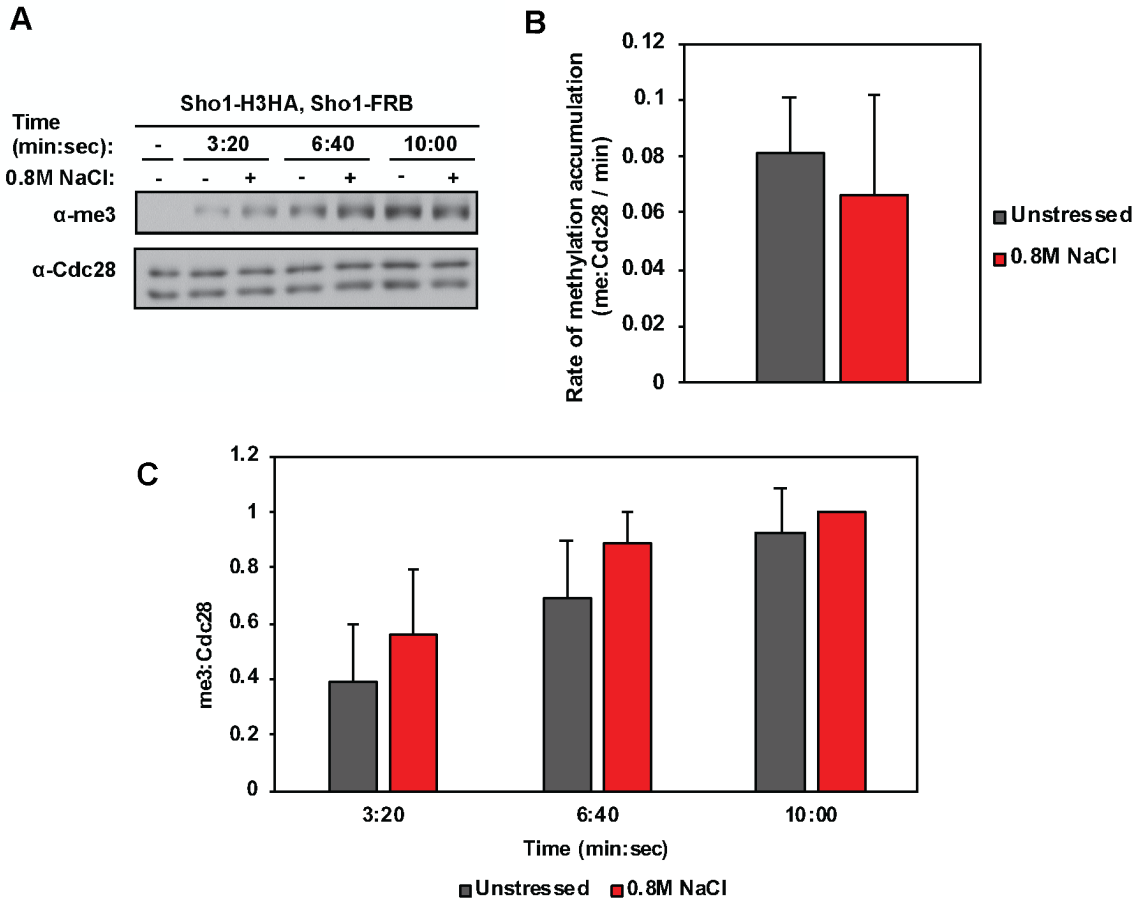

Figure 2.4

M-Track analysis of the Sho1-Sho1 interaction during 10 minutes of osmotic stress

(A) Immunoblot of the M-Track assay using strain yJA372 as described in the Materials and Methods section. (B) Rate of methylation accumulation. Error bars represent SD (n=3). (C) Mean of calculated me3:Cdc28 ratios. Error bars represent SD (n=3).

Sho1, Msb2 and Hkr1 function as osmosensors in the SHO1-branch of the HOG pathway (Tanaka et al. 2014; Tatebayashi et al. 2007; Tatebayashi et al. 2015). Unlike Sho1 which is has no distinct extracellular domain (Maeda et al. 1995), Msb2 and Hkr1 have large extracellular domains which are heavily glycosylated (Cullen et al. 2004; Tatebayashi et al. 2007). It is speculated that these large glycosylated domains interact with the cell wall and, upon hyperosmotic stress-induced cell shrinkage, might trigger pathway activation (Brewster & Gustin 2014; de Nadal et al. 2007). Furthermore, deletion of the STR domains of Msb2 and Hkr1 leads to hyperactivation of the pathway in the absence of osmotic stress (Tatebayashi

et al. 2007). Msb2 and Hkr1 are thus considered to be the main osmosensors of the SHO1-branch.

Msb2 and Hkr1 have been reported to interact with Opy2; the extracellular HMH domains of Msb2 and Hkr1 were found to bind the extracellular CR domain of Opy2 and this interaction was essential for pathway activation (Tatebayashi et al. 2015; Yamamoto et al. 2015). Furthermore, the Msb2-Opy2 interaction is thought to undergo structural changes upon exposure to hyperosmotic stress (Yamamoto et al. 2015). Both Msb2 and Hkr1 also interact with Sho1, and Sho1 mutants with reduced binding to Msb2 and Hkr1, also have reduced pathway activation (Tatebayashi et al. 2007; Tatebayashi et al. 2015). Taken together, these observations indicate that the interactions of Msb2 and Hkr1 with other transmembrane proteins are important for pathway activation.

2.2.2. Sho1 is in close proximity to Msb2 both in the absence and presence of stress

As the above studies demonstrated interactions using overexpression systems and co-immunoprecipitation, the finer dynamics of these interactions might have been overlooked. Therefore, I used the M-Track system to study these interactions and their role in pathway activation with the aim of creating a more detailed description of these dynamics. Because Msb2 and Hkr1 show such similar behaviour, I decided not to study the interactions of both, but rather to focus on those of Msb2.

I first measured the interaction of Msb2 with Sho1. Upon addition of rapamycin, methylation accumulated in both the osmotically stressed and unstressed samples at the same rate (Fig 2.5A and B). In addition, the average levels of methylation were the same in both stressed and unstressed samples at all three timepoints (Fig. 2.5C). This indicates that Msb2 and Sho1 interact in an osmotic stress-independent manner.

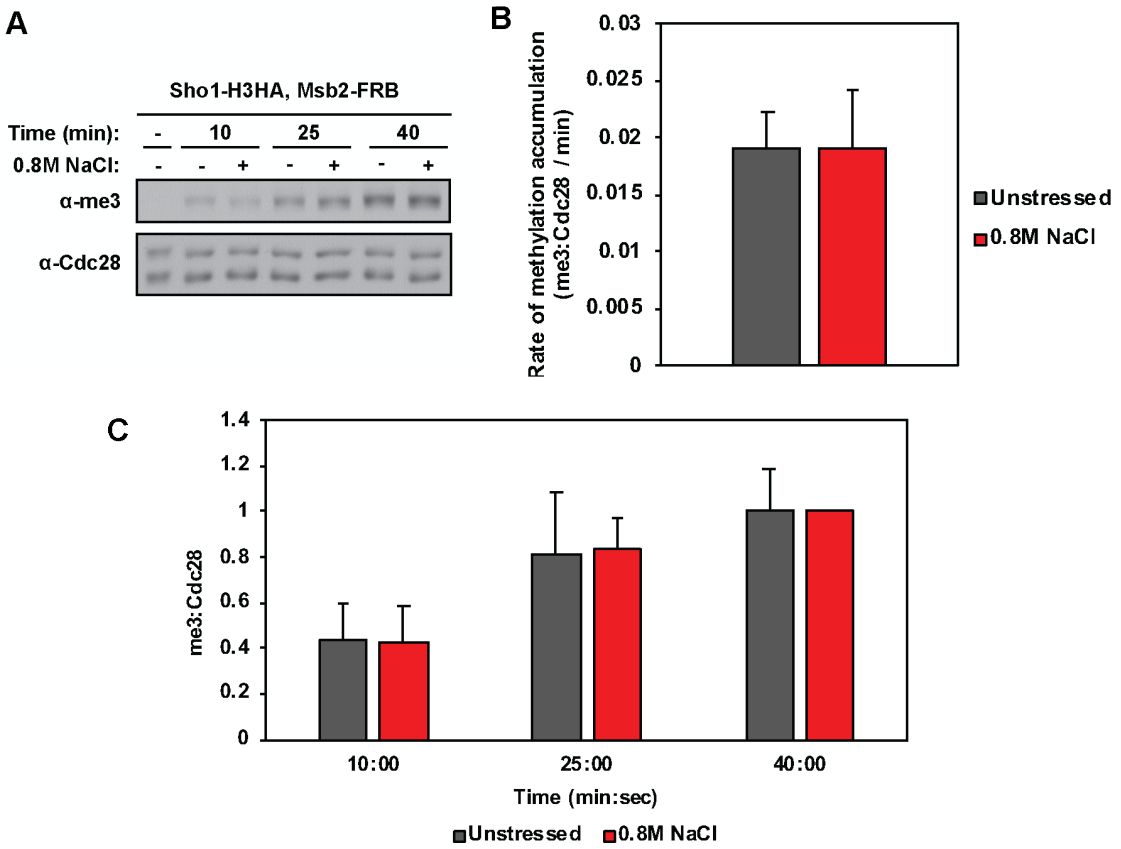

Figure 2.5

M-Track analysis of the Msb2-Sho1 interaction

(A) Immunoblot of the M-Track assay using strain yJA355 as described in the Materials and Methods section. (B) Rate of methylation accumulation. Error bars represent SD (n=3). (C) Mean of calculated me3:Cdc28 ratios. Error bars represent SD (n=3).

2.2.3. Opy2 and Msb2 interact more during osmotic stress

I then measured the Msb2-Opy2 interaction. Slightly higher levels of methylation were found in osmotically stressed samples than in unstressed samples (Fig 2.6). Although the rates of methylation accumulation were similar in both conditions, the average methylation level of stressed samples was higher than that of unstressed samples at all three timepoints. These results suggest that Msb2 increases in proximity to Opy2 upon osmotic stress.

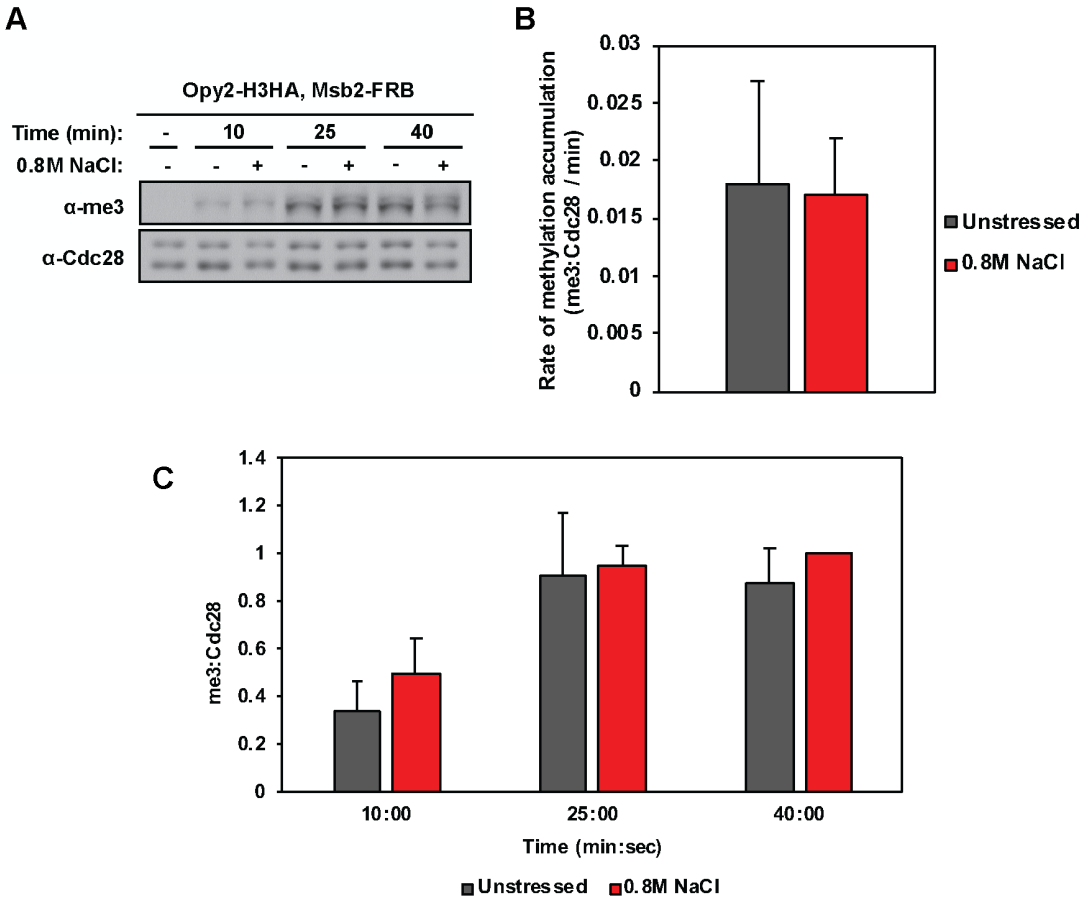

Figure 2.6

M-Track analysis of the Msb2-Opy2 interaction

(A) Immunoblot of the M-Track assay using strain yJA467 as described in the Materials and Methods section. (B) Rate of methylation accumulation. Error bars represent SD (n=3). (C) Mean of calculated me3:Cdc28 ratios. Error bars represent SD (n=3).

2.2.4. The Sho1-Opy2 interaction increases during stress in an Msb2/Hkr1-dependent manner

Msb2 appears to interact with both Sho1 and Opy2 during osmotic stress, however whether these interactions sequential or simultaneous is not clear. That is to say, it is not known if Msb2 interacts first with Sho1, then Opy2, or if it interacts with both at the same time. If the second scenario were true, I would expect Sho1 and Opy2 to be in close proximity.

Sho1 has previously been suggested to interact with Opy2 (Tatebayashi et al. 2015). In addition, Opy2 mutants which interacted with Sho1 to a greater and lesser extent were able to activate the HOG pathway to a greater and lesser extent respectively. These results highlight the importance of the Sho1-Opy2 interaction for HOG pathway activation.

To find out if Sho1 and Opy2 interact, I performed the M-Track assay. Upon addition of rapamycin, methylation accumulated in both the stressed and unstressed conditions. However, higher levels of methylation were found in osmotically stressed samples than in unstressed samples (Fig 2.7A, lanes 1-7). Quantification of signals showed that methylation accumulated at a faster rate in stressed samples and the average level of methylation was higher for stressed samples than unstressed samples at all three timepoints (Fig 2.7B and C). This indicates that, in the absence of osmotic stress, Sho1 and Opy2 interact but that during osmotic stress, the interaction increases. This also supports the idea that Msb2 interacts with Sho1 and Opy2 at the same time.

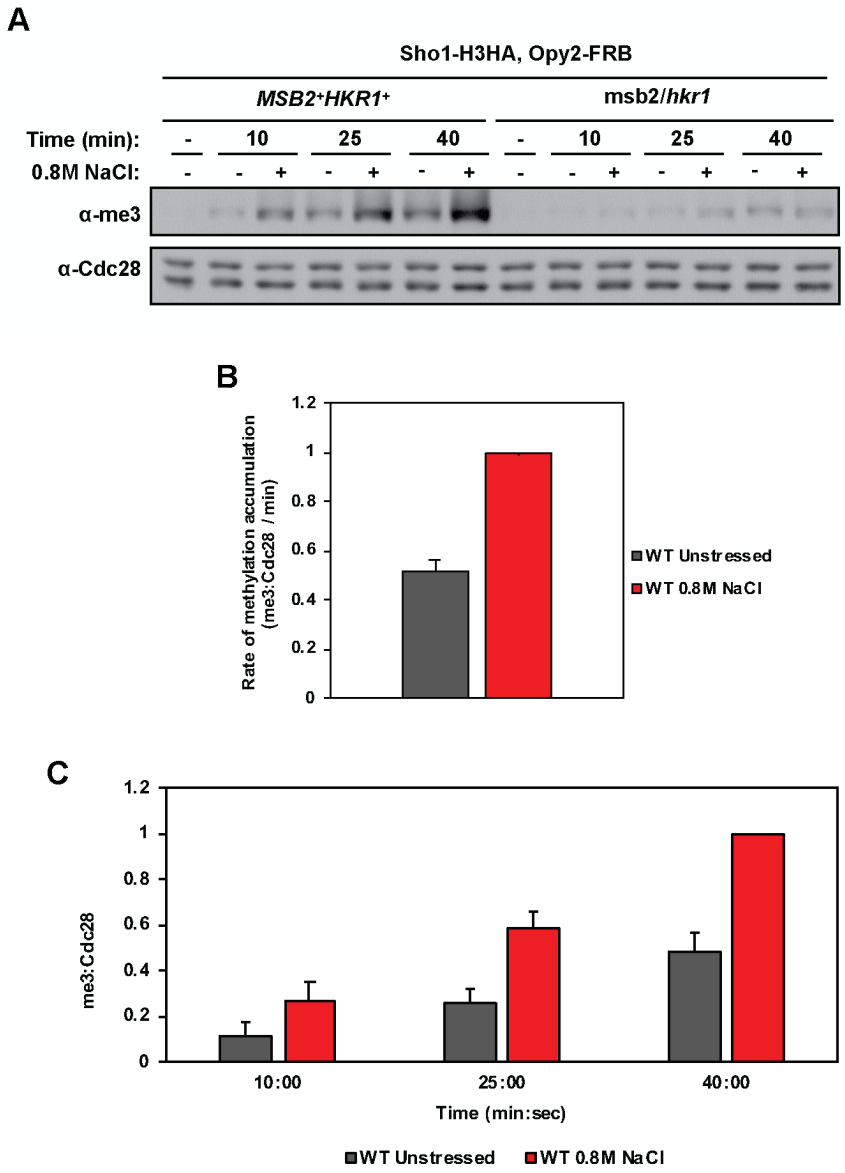

Figure 2.7

M-Track analysis of the Sho1-Opy2 interaction in *MSB2*$^{+}$/*HKR1*$^{+}$ and *msb2/hkr1* backgrounds

(A) Immunoblot of the M-Track assay using strains yJA359 and yJA408 as described in the Materials and Methods section. (B) Rate of methylation accumulation for strain yJA359 only. Error bars represent SD (n=3). (C) Mean of calculated me3:Cdc28 ratios for strain yJA359 only. Error bars represent SD (n=3).

Given that the strength of the Sho1-Opy2 interaction positively correlates with the extent of pathway activation, the presence of Msb2 (or Hkr1) is essential for HOG pathway activation, and Msb2 interacts with both Sho1 and Opy2, I hypothesised that Msb2 acts as an adaptor protein, bringing Sho1 and Opy2 together. Thus, I used the M-Track assay to investigate the role of Msb2 in the Sho1-Opy2 interaction. I found that in the absence of both Msb2 and Hkr1, Sho1 and Opy2 barely interact (Fig 2.7A, comparing lanes 1-7 with lanes 8-14). Furthermore,

in the absence of only one of Msb2 or Hkr1, the Sho1-Opy2 interaction was maintained (Fig. 2.8). Taken together, these results indicate that Msb2 and Hkr1 act as adaptor proteins for Sho1 and Opy2.

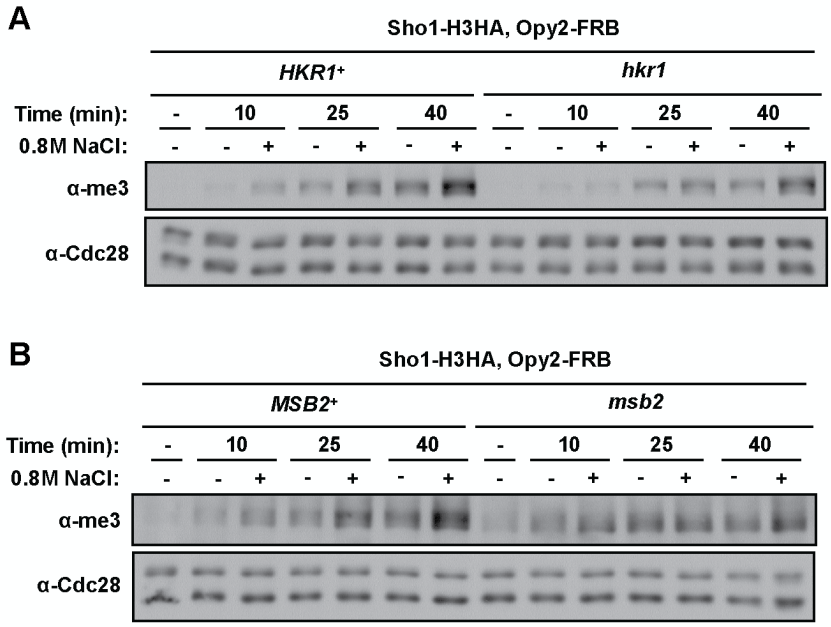

Figure 2.8

M-Track analysis of the Sho1-Opy2 interaction in *HKR1*$^+$ and *hkr1* backgrounds, and in *MSB2*$^+$ and *msb2* backgrounds

(A) Immunoblot of the M-Track assay using strains yJA359 and yJA414 as described in the Materials and Methods section. (B) Immunoblot of the M-Track assay using strains yJA359 and yJA396 as described in the Materials and Methods section.

As Sho1 and Opy2 are adaptor proteins for Pbs2 and Ste11 respectively, and activation of Pbs2 by Ste11 is an essential step in the HOG MAPK kinase cascade, this result, at least partially, explains the requirement of Msb2 and Hkr1 for HOG pathway activation.

2.2.5. The role of Msb2/Hkr1 cannot be bypassed by artificial dimerization of Sho1 and Opy2

A feature of adaptor proteins is that their function can be bypassed by tethering the two proteins they bridge together. For example, if the only function of Msb2 were as an adaptor protein for Sho1 and Opy2, then directly tethering Sho1 to Opy2 would allow for pathway activation in the absence of Msb2 and Hkr1. Following this logic, and using the Induced Bypass (iPass) system of inducible direct tethering established by the Kraft group (Torggler et al. 2016), I directly tethered Opy2 to Sho1 in a rapamycin-inducible manner and measured

pathway activation (Figs. 2.9 and 2.10). Strains in which Sho1 and Opy2 were tagged, were functional, as indicated by their osmotic resistance and ability to phosphorylate Hog1 in the presence of Msb2 and upon exposure to osmotic stress (Fig 2.10). However, upon direct tethering of Sho1 and Opy2 in the absence of both Msb2 and Hkr1, cells did not show osmotic resistance and were unable to phosphorylate Hog1 upon exposure to osmotic stress. Therefore, although Msb2 acts as an adaptor for Sho1 and Opy2, this is not its only role in HOG pathway activation.

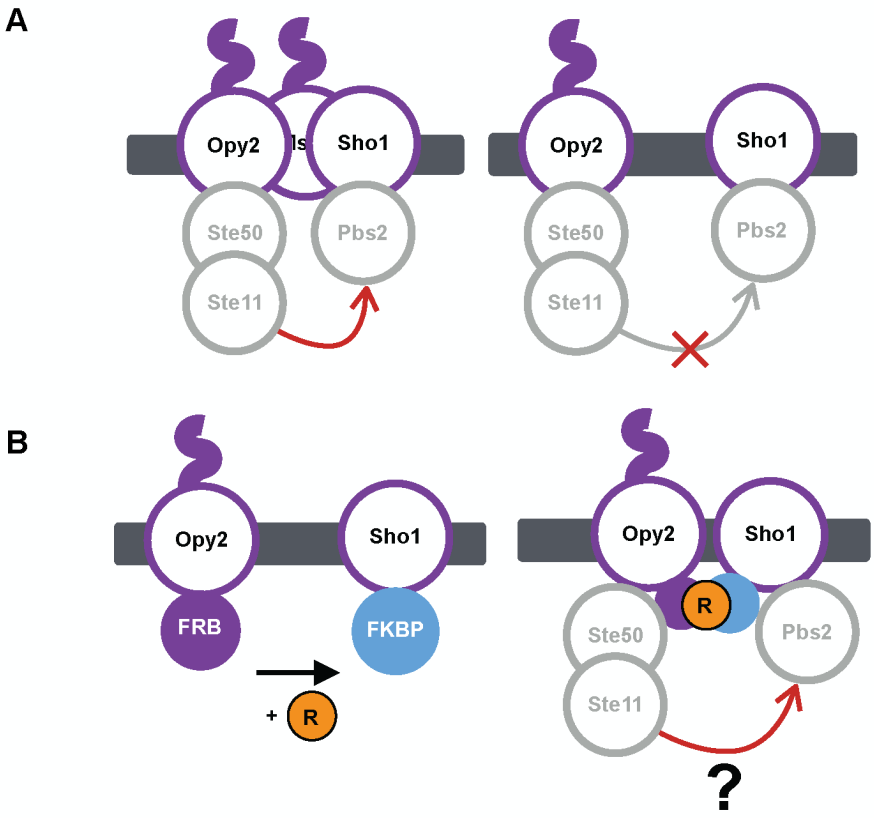

Figure 2.9

Proposed model of artificial dimerization of Sho1 and Opy2 using the Induced Bypass (iPass) system

(A) Proposed role of Msb2(/Hkr1) in Sho1-Opy2 association and thus Pbs2 activation and phosphorylation by Ste11.

(B) Schematic of the experimental iPass setup. Rapamycin-induced dimerization of Sho1 and Opy2 might allow Ste11 to phosphorylate and activate Pbs2 in *msb2/hkr1* cells.

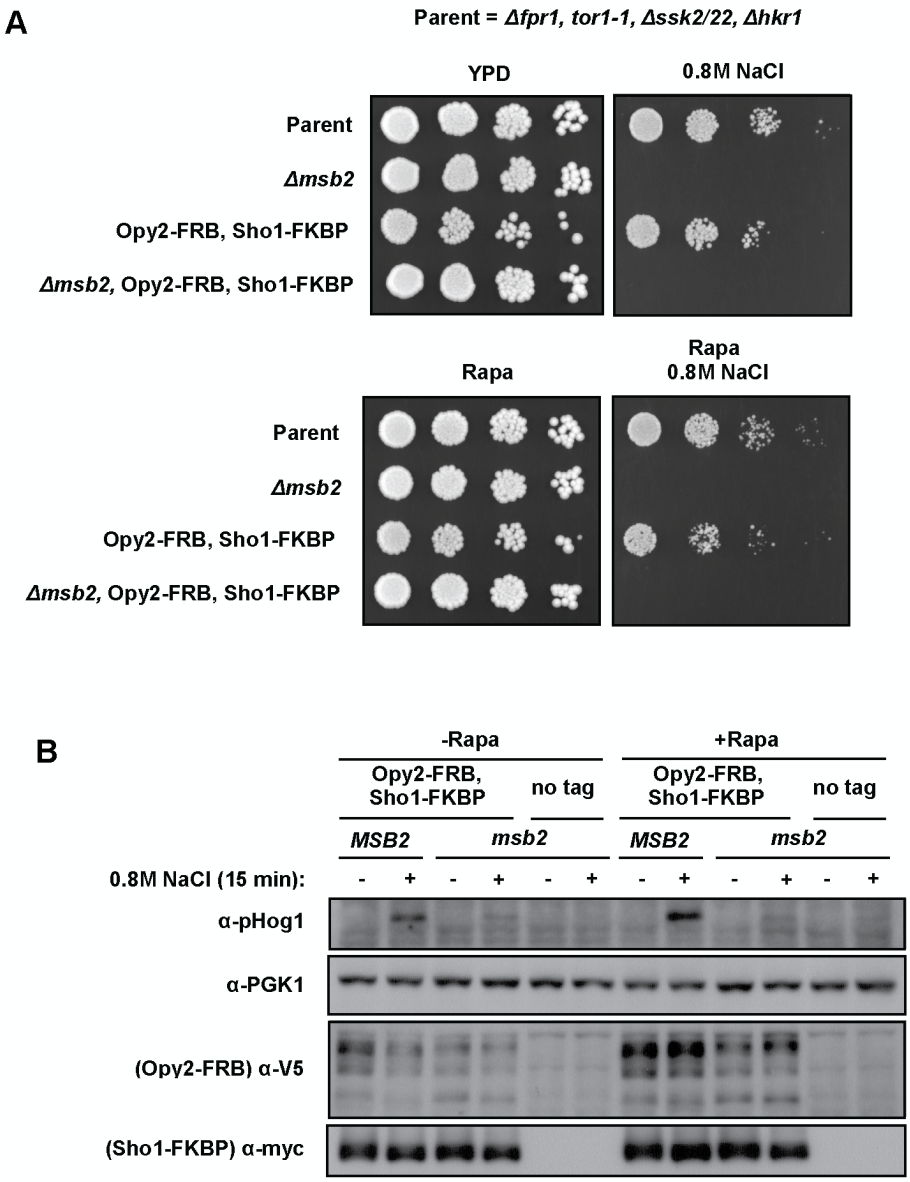

Figure 2.10

iPass analysis of the role of Msb2 in pathway activation by using artificial dimerization of Sho1 and Opy2

(A) Droplet test of strains yJA516, yJA543, yJA532 and yJA582 on plates with or without 0.M NaCl and with or without 1µg/mL Rapamycin.

(B) Strains yJA532, yJA582 and yJA543 were pre-treated either with rapamycin (final conc. 1µg/mL) or equivalent volumes of mock (90% Ethanol, 10% Tween-20) for 15 minutes. At time = 0 min, unstressed samples harvested and NaCl (final conc. 0.8M NaCl) was added. At time = 15 min, the stressed samples were harvested. Harvesting, cell breakage and Western Blot analysis were performed as described in the Materials and Methods section.

2.2.6. The stress-induced Sho1-Sho1 interaction is enhanced in an *msb2/hkr1* background but reduced in an *opy2* background

As Msb2 was found to be an adaptor for the dynamic Sho1-Opy2 interaction, I next hypothesised that Msb2 could also be an adaptor for the dynamic Sho1-Sho1 interaction. I therefore used the M-Track assay to measure the Sho1-Sho1 interaction in the absence of Msb2 and Hkr1. As figure 2.11 shows, methylation was still able to accumulate in cells in which MSB2 and HKR1 were deleted, suggesting that they do not act as adaptors for the Sho1-Sho1 interaction. Interestingly, the methylation accumulated faster in *msb2/hkr1* cells suggesting that Msb2 and Hkr1 prevent maximal proximity of Sho1 to itself.

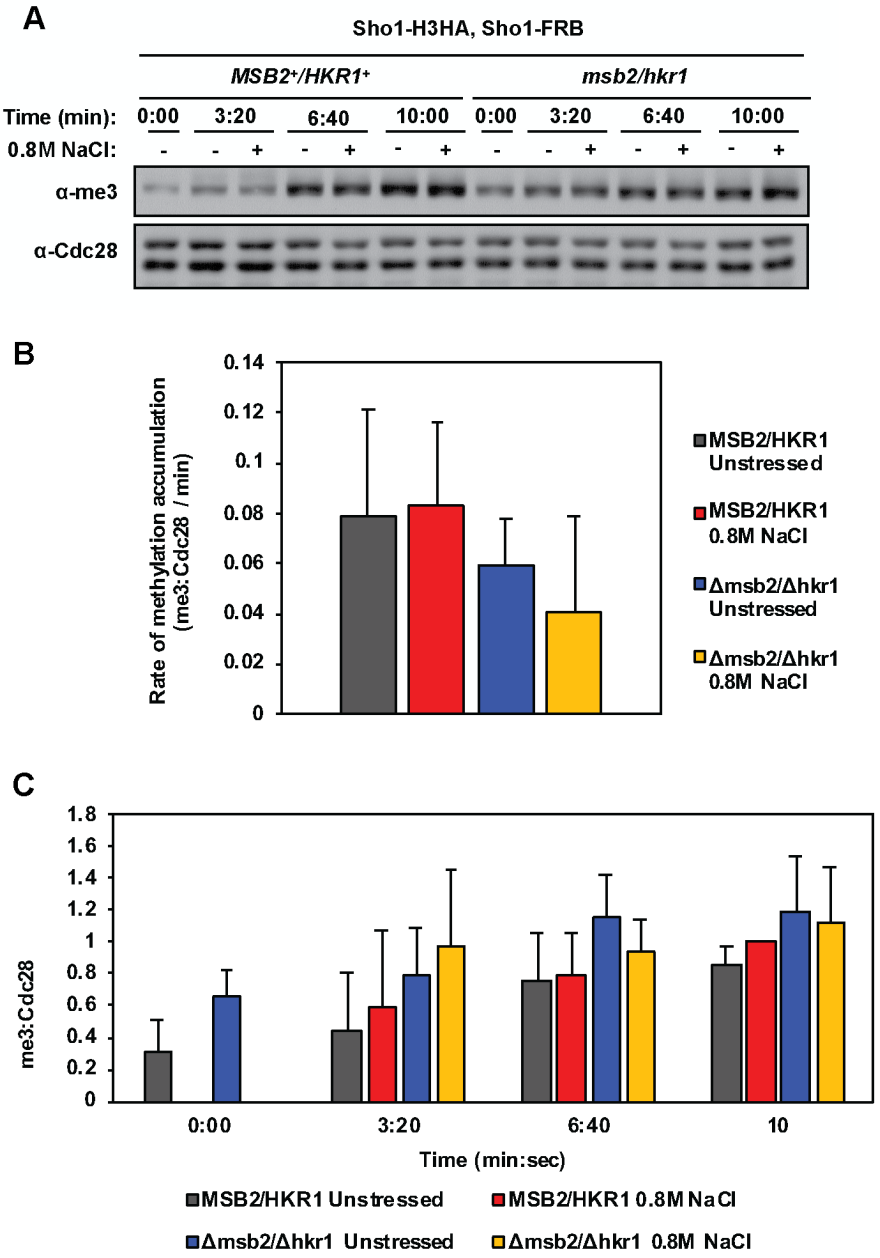

Figure 2.11

M-Track analysis of Sho1-Sho1 proximity during 10 minutes of osmotic stress in *MSB2⁺/HKR1⁺* and *msb2/hkr1* backgrounds

(A) Immunoblot of the M-Track assay using strains yJA372 and yJA411 as described in the Materials and Methods section. (B) Rate of methylation accumulation. Error bars represent SD (n=3). (C) Mean of calculated me3:Cdc28 ratios. Error bars represent SD (n=3).

Since Opy2 also interacts with Sho1, it could also be considered a potential adaptor for the Sho1-Sho1 interaction. However, I previously showed that, in the absence of Msb2 and Hkr1, Opy2 cannot interact with Sho1, and that the Sho1-Sho1 interaction is maintained. This suggests that Opy2 is not responsible for maintaining the Sho1-Sho1 interaction. I, therefore,

hypothesised that, deletion of Opy2 would not result in loss of the Sho1-Sho1 interaction and performed the M-Track assay to test this.

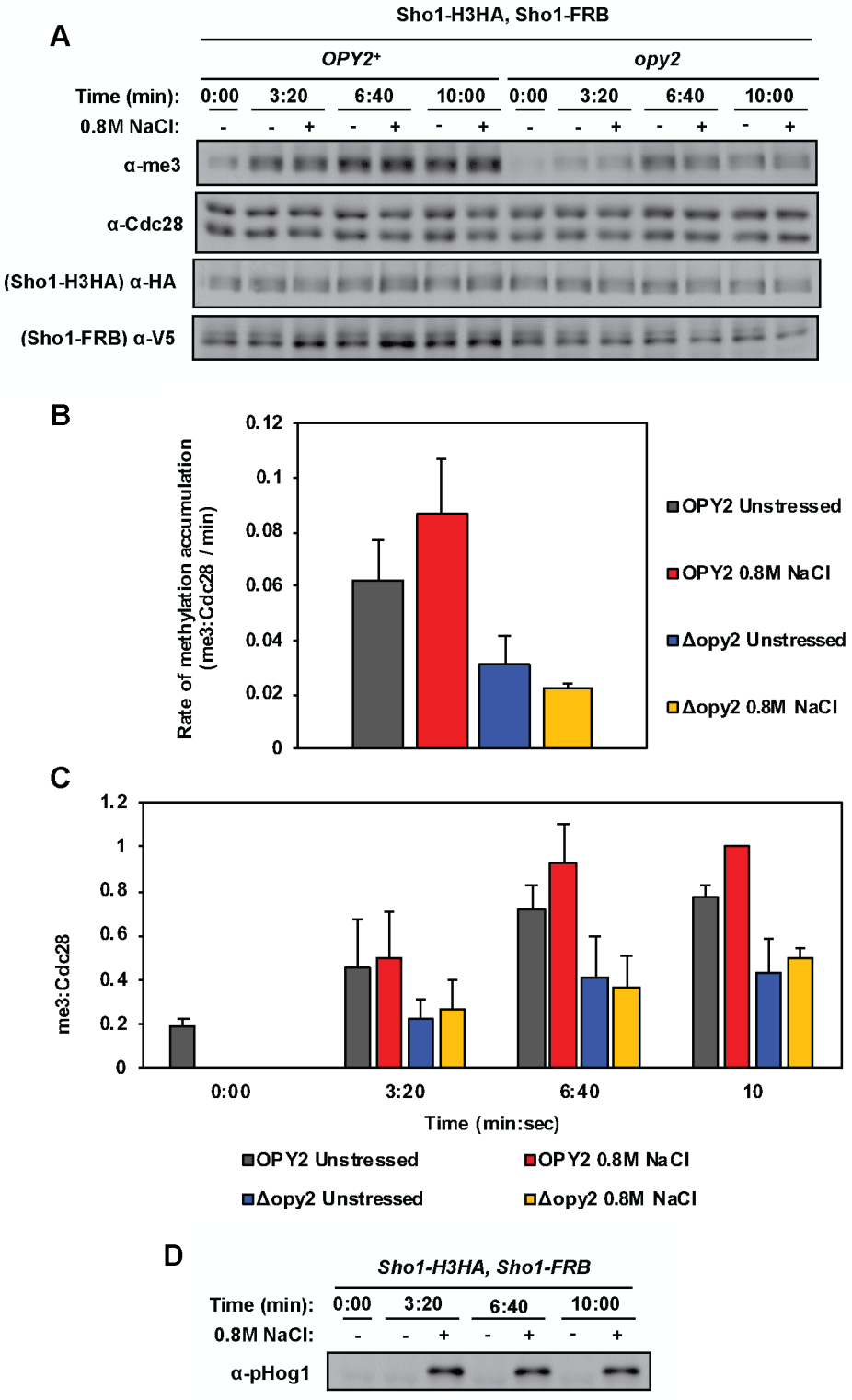

Figure 2.12

M-Track analysis of the Sho1-Sho1 interaction during 10 minutes of osmotic stress in *OPY2*$^{+}$ and *opy2* backgrounds

(A) Immunoblot of the M-Track assay using strains yJA372 and yJA613 as described in the Materials and Methods section. (B) Rate of methylation accumulation. Error bars represent SD (n=3). (C) Mean of calculated me3:Cdc28 ratios. Error bars represent SD (n=3). (D) Immunoblot of Hog1 phosphorylation during the M-Track assay.

Surprisingly, I found that methylation was reduced in *Δopy2* cells (Fig. 2.12A). The rate of accumulation was lower, and the average amount of methylation was also reduced in absence of Opy2 (Fig 2.12B and C). However, when checking the expression levels of both forms of Sho1 in the mutant background, I found that although Sho1-H3HA was expressed at levels similar to those in the wildtype cells, the expression of Sho1-FRB was reduced (Fig. 2.12A). Therefore, in this case, the reduced levels of Sho1-FRB expression might be responsible for the reduced levels of methylation.

2.3. Ste11 Localisation

So far, I have described the localisation of Pbs2 to the plasma membrane, and the grouping of the transmembrane proteins. These two events alone, however, would not be sufficient for HOG pathway activation because Ste11 must also localise to the plasma membrane.

Similarly to Pbs2, it has been shown that in both the absence and presence of osmotic stress, Ste11 is located in the cytoplasm (Francesc Posas et al. 1998). However, in order for it to be activated by Ste20, and to activate Pbs2, it must localise to the plasma membrane (Francesc Posas et al. 1998; Tatebayashi et al. 2007; Wu et al. 2006). Furthermore, artificial membrane targeting of Ste11 confers osmotic resistance in the absence of Ste50 and artificial membrane targeting of Ste50 confers osmotic resistance in the absence of Opy2. Moreover, results from our group have also suggested that Ste11 is localised at the plasma membrane both before and during osmotic stress (Zuzuarregui et al. 2015). Not only is it essential that Ste11 can localise to the plasma membrane during osmotic stress, it is equally important that this localisation can be regulated because permanent localisation of hyperactive Ste11 results in activation of the HOG pathway in the absence of stress, which results in cell death (Tatebayashi et al. 2006).

In addition to its N-terminal SAM domain, through which it binds Ste50, Ste11 also contains a central negative regulatory domain and a C-terminal kinase domain (van Drogen et al. 2000; Tatebayashi et al. 2006), Fig. 2.13A). Upon phosphorylation by Ste20 at Ser281, Ser285 and Thr286, Ste11 has been reported to undergo a conformational change, resulting in the release of the kinase domain from the negative regulatory domain (van Drogen et al. 2000). Point mutations in the regulatory domain of residues 281, 285 and 286 to (non-phosphorylatable) alanine, showed stronger binding to the kinase domain than the wildtype regulatory domain. Conversely, point mutations of the same residues to (phospho-mimicking) aspartate, showed weaker binding to the kinase domain than the wildtype regulatory domain. In addition, the 3A mutant was inactive and the 3D mutant was hyperactive; Ste20 was not required for its activity. Similarly, activating point mutations in the kinase domain also resulted in weaker binding than in wildtype Ste11. Taken together, these observations resulted in a model in which Ste11-3A mimics the closed and inactive state of Ste11, whilst Ste11-3D mimics the open an active state of Ste11 (as shown in Fig. 2.13B).

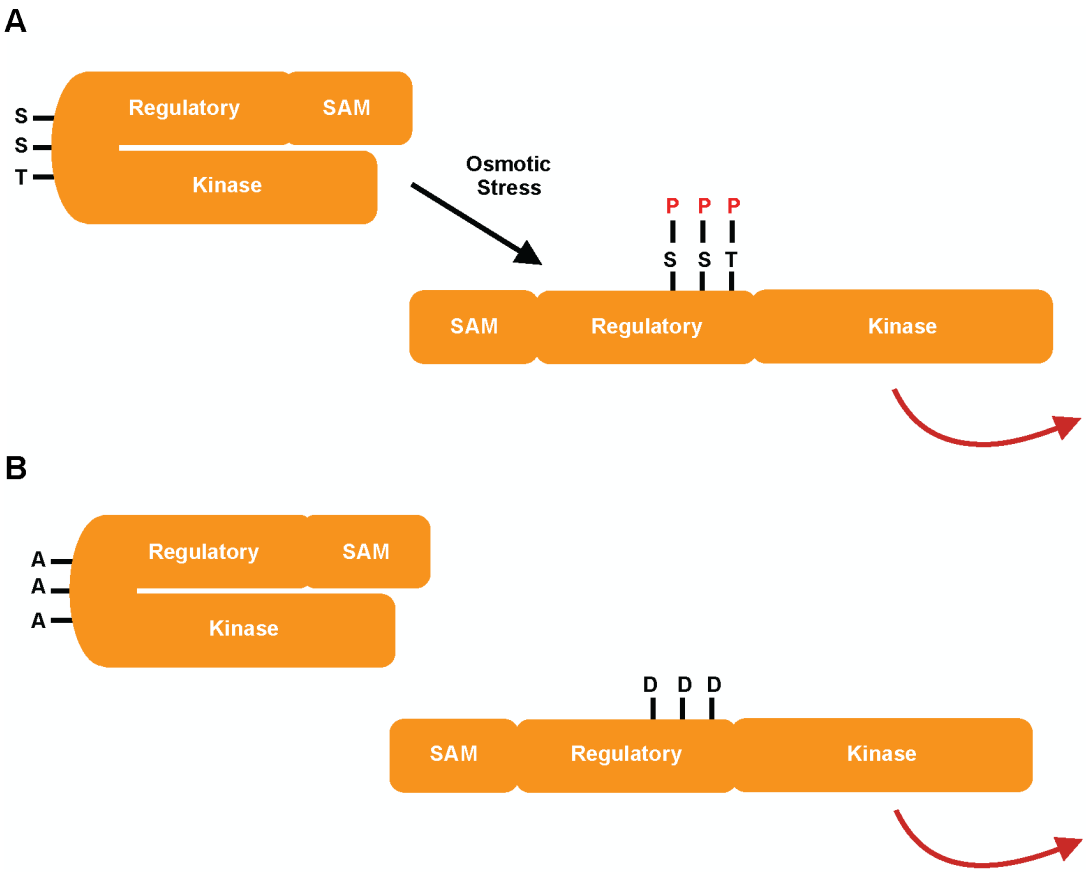

Figure 2.13

Schematic of Ste11 activation states and conformations

(A) Proposed conformation change of Ste11 upon phosphorylation. Prior to phosphorylation, Ste11 is in a closed conformation. Phosphorylation of S281, S285 and T286, which are located in the (negative) regulatory domain, causes release and activation of the kinase domain. The activated protein is now in an open conformation. (B) Proposed conformation of Ste11-3A mimicking the closed and inactive state (left). Proposed conformation of Ste11-3D mimicking the open and active state (left).

2.3.1. The interaction of Ste11 with Sho1 increases during stress, and is independent of its activation state

Given that osmotic stress-related localisation of Ste11 is still unclear, I used the M-Track system to study the proximity of Ste11 to the transmembrane proteins as proxy for Ste11 membrane localisation. A previous study from our group found that Ste11 was in close proximity to Sho1 and Msb2 both before and during osmotic stress (Zuzuarregui et al. 2015). This led to the creation of the following Progression Model of Ste11 plasma membrane localisation: in the absence of osmotic stress, Ste11 is localised at the plasma membrane via Ste50 and Opy2. Before hyperosmotic stress, Ste11 is in close proximity to Msb2. Because

Msb2 binds Ste20 indirectly via Bem1 (Tanaka et al. 2014), upon exposure to hyperosmotic stress, Ste11 is phosphorylated by Ste20 and activated. After activation, Ste11 *progresses* towards Sho1 where it can phosphorylate and activate Pbs2. Based on the Progression Model I made four hypotheses: 1) inactive Ste11 would remain in close proximity to Msb2 upon osmotic stress, 2) active Ste11 would not be in close proximity to Msb2, 3) inactive Ste11 would not be in close proximity to Sho1 and 4) active Ste11 would be in close proximity to Sho1 both before and during osmotic stress.

In order to test these hypotheses, I created H3HA-tagged versions of the 3D and 3A mutants described above expressed from integrative plasmids under the control of their native promoter at the *URA3* locus and measured their interaction with Sho1. I measured the Ste11-Sho1 interaction in strains in which *HOG1* had been deleted, to prevent Hog1-dependent negative feedback mechanisms, prolong pathway activation and therefore potentially allow higher levels of methylation to accumulate (Hao et al. 2007; Hao et al. 2008; Yamamoto et al. 2010). I found that in strains expressing wildtype Ste11, as well as Ste11-3D and Ste11-3A, methylation accumulated at a higher rate in the osmotically stressed condition than in the unstressed condition (Fig. 2.14). In addition, the average methylation level was higher in the stressed samples than in the unstressed samples, for all three versions of Ste11 and at all three timepoints measured (Fig 2.15). This indicates that Ste11 interacts with Sho1 more during osmotic stress, and that this increase in interaction is independent of the activation state of Ste11.

2.3.2. The interaction of Ste11 with Msb2 and Opy2 increases during stress, and is independent of its activation state

As the previous result did not support the oligomerisation model, I then measured the interaction of the mutant Ste11 constructs to Msb2 and Opy2 to verify this finding (Fig. 2.16). In the experiment described in figure 2.16A, Msb2-FRB was expressed from an integrative plasmid under the control of its native promoter at the *LEU2* locus. In the case of both Msb2 and Opy2, both mutants showed more methylation in the osmotically stressed samples than in the unstressed samples. I therefore concluded that Ste11 comes into closer proximity to all three transmembrane proteins during osmotic stress, that this increased proximity is independent of the activation state of Ste11 and that localisation of Ste11 at the plasma membrane does not follow the Progression Model.

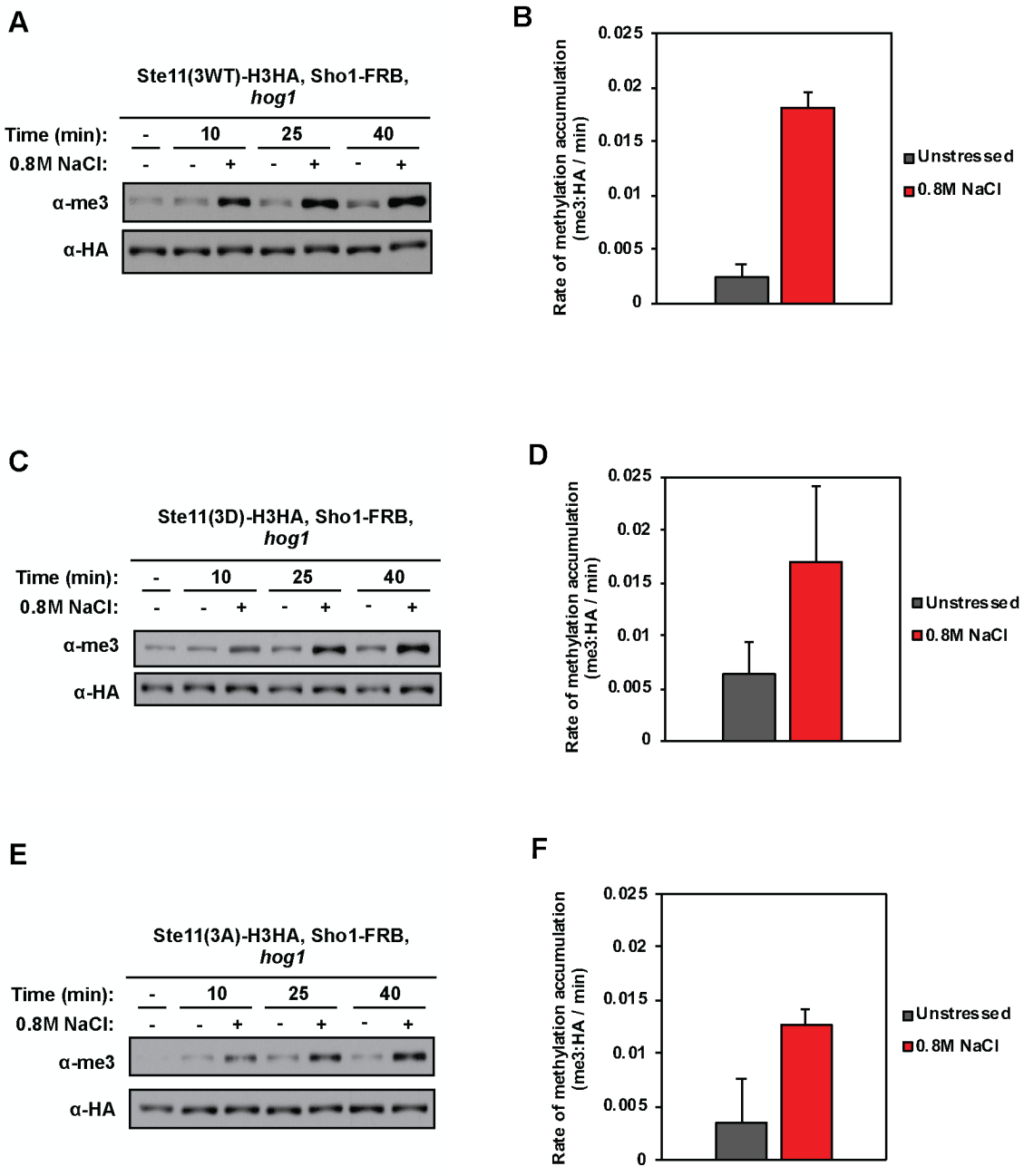

Figure 2.14

M-Track analysis of the Sho1 interaction with wildtype, 3D and 3A forms of Ste11

(A, C, E) Immunoblot of the M-Track assay using strains yJA323, yJA325 and yJA293 as described in the Materials and Methods section.

(B, D, F) Rates of methylation accumulation. Error bars represent SD (n=3).

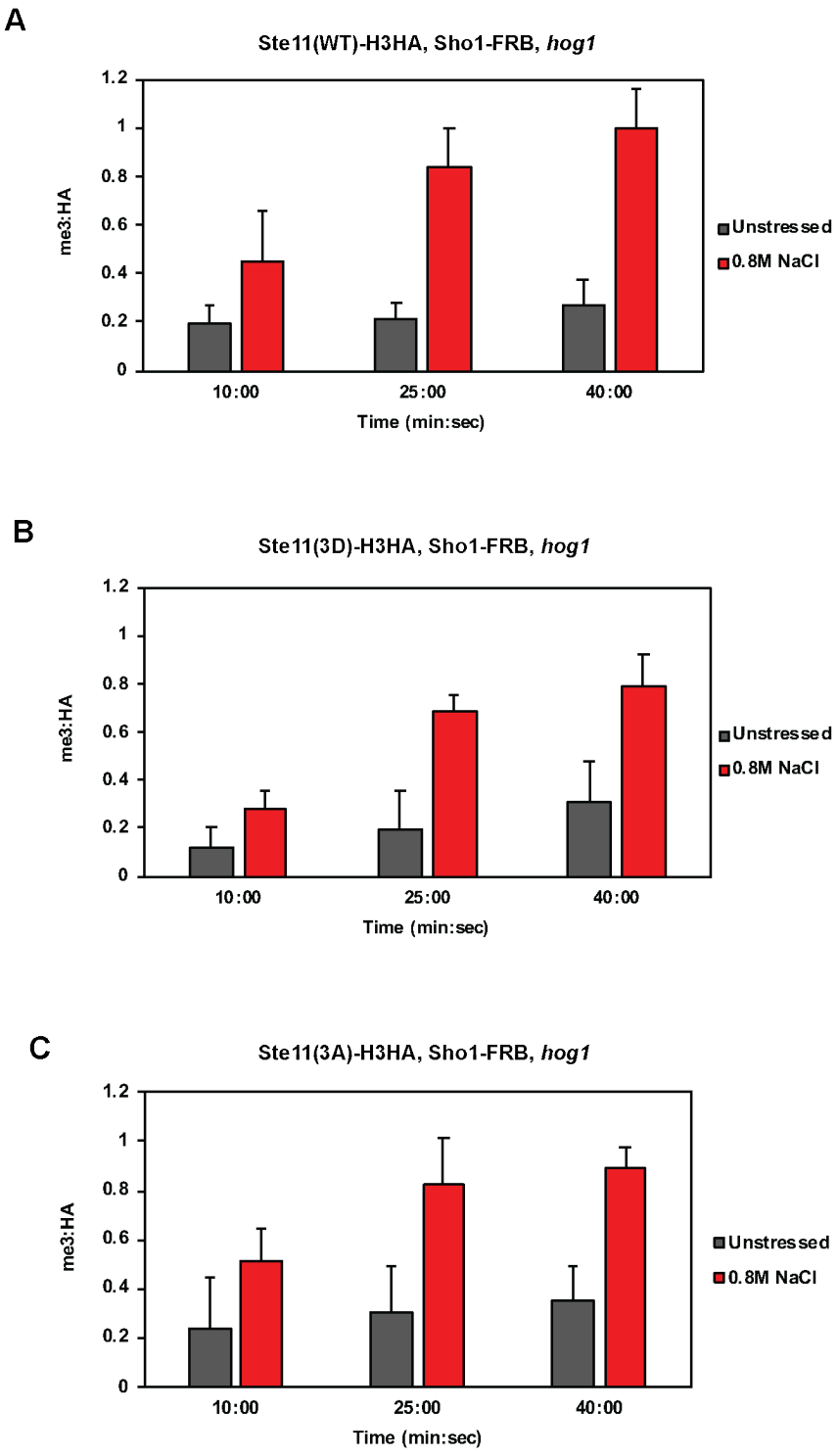

Figure 2.15

M-Track analysis of the Sho1 interaction with different forms of Ste11

(A-C) Mean of calculated me3:Cdc28 ratios. Error bars represent SD (n=3).

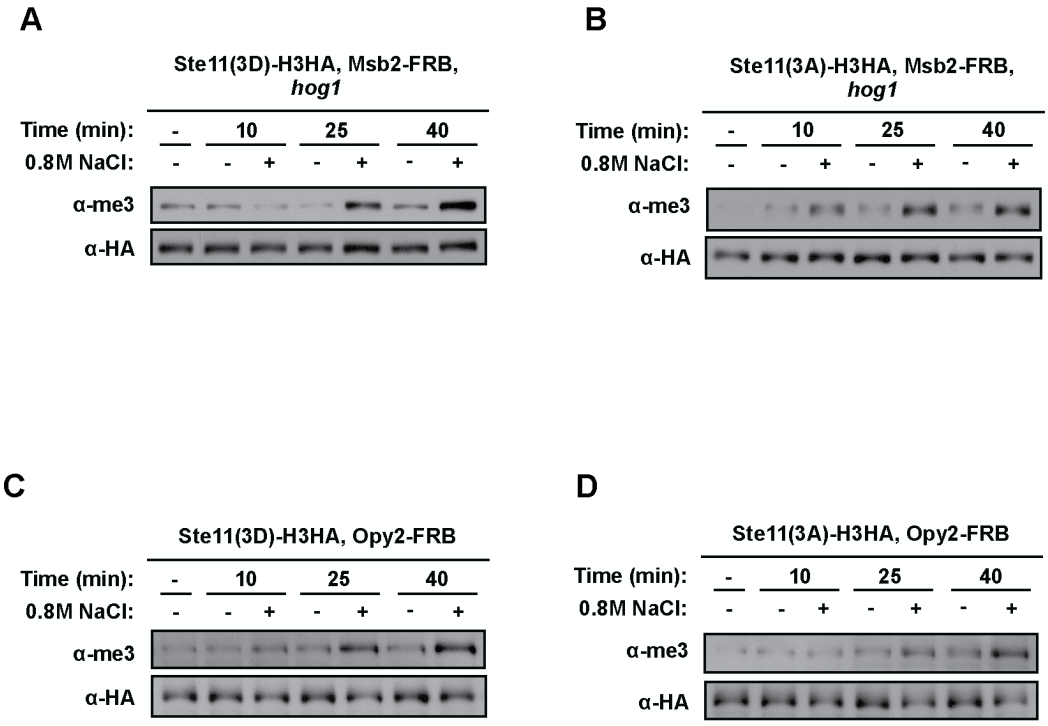

Figure 2.16

M-Track analysis of the interaction of mutant forms of Ste11 with Msb2 and Opy2

Immunoblot of the M-Track assay using strains (A) yJA340, (B) yJA288, (C) yJA261 and (D) yJA262 as described in the Materials and Methods section.

Further results from our group showed that the Ste11-Sho1 interaction required Msb2/Hkr1 and Opy2, and that Ste11-Msb2 interaction required Opy2 and Sho1 (Zuzuarregui et al. 2015). The co-dependent nature of these proximities, i.e. that Sho1 was needed for interaction with Msb2 and vice versa, led to the creation of a second model of Ste11 plasma membrane localisation, namely the Oligomerisation Model. In this model, Ste11 binds the transmembrane proteins weakly with low affinity and thus, in the absence of osmotic stress, it is not stably localised at the plasma membrane. Upon osmotic stress, clustering of the transmembrane proteins increases the local concentration of Ste11 at the membrane. One Ste11 molecule can then bind multiple transmembrane proteins simultaneously with high avidity, resulting in stable localisation at the plasma membrane. As I have already shown that the transmembrane proteins cluster upon osmotic stress, I am yet to find evidence contradicting this model.

2.3.3. Stress-induced Ste11/50-Opy2 proximity is reduced but not abolished in the absence of Sho1

As the interaction of Ste11 with Sho1 and Msb2 has already been studied in detail (Zuzuarregui et al. 2015), I decided to measure the Ste11-Opy2 interaction during osmotic stress, to test the validity of the Oligomerisation model. Based on the Oligomerisation model I hypothesised that deletion of Msb2/Hkr1 and Sho1 would lead to reduced localisation of Ste11 at the plasma membrane. Consistent with the results from interaction of the Ste11 mutants with Opy2 (Fig. 2.16), in wildtype cells, upon addition of rapamycin, methylation of wildtype Ste11-H3HA accumulated at a faster rate in the osmotically stressed condition than in the unstressed condition (Fig. 2.17). In the absence of Sho1, although stressed samples contained more methylation than unstressed samples, rate of accumulation was lower than in wildtype cells (Fig. 2.17A and B). Correspondingly, the average methylation levels of stressed samples from *Δsho1* cells were less than those from wildtype cells (Fig 2.17C). This result indicates that the Ste11-Opy2 interaction is reduced in the absence of Sho1 and that Sho1 is partially required to localise Ste11 at the plasma membrane. This supports the Oligomerisation model.

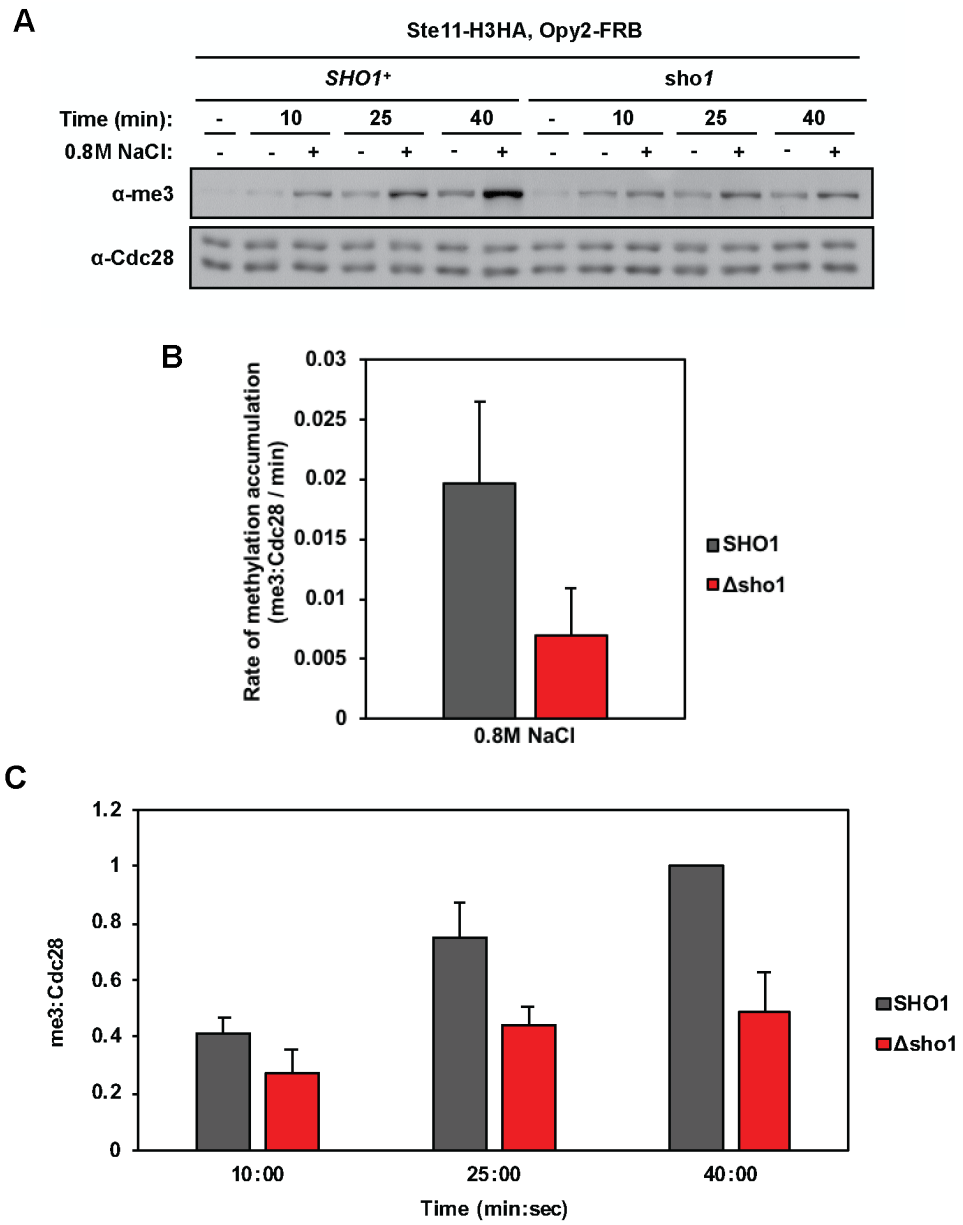

Figure 2.17

M-Track analysis of the Ste11-Opy2 interaction in *SHO1*$^{+}$ and *sho1* backgrounds

(A) Immunoblot of the M-Track assay using strains yJA281 and yJA399 as described in the Materials and Methods section. (B) Rate of methylation accumulation. Error bars represent SD (n=3). (C) Mean of calculated me3:Cdc28 ratios. Error bars represent SD (n=3). No methylation could be quantified in any of the unstressed samples. Therefore neither me3:Cdc28 ratios, nor rates of methylation accumulation could be calculated for these conditions.

As Ste11 localises to the plasma membrane by binding Ste50, I sought to determine whether Ste11 dynamically localised to the plasma membrane alone or whether this localisation was due to dynamic localisation of Ste50. To this aim, I measured the Ste50-Opy2 interaction in the presence and absence of Sho1. Upon addition of rapamycin, methylation only accumulated in osmotically stressed cells (Fig 2.18). In the absence of Sho1, methylation still

only accumulated in the stressed cells, but to a lesser extent than in wildtype cells. In addition, the average methylation levels of stressed samples from *Δsho1* cells were less than those from wildtype cells (Fig 2.18C). This result indicates that the Ste50-Opy2 interaction is reduced in the absence of Sho1 and that Sho1 is partially required to localise Ste50 at the plasma membrane. As the results of the Ste11-Opy2 and Ste50-Opy2 interactions are similar, this suggests that dynamic localisation of Ste11 at the plasma membrane is due to a dynamic interaction between Ste50 and Opy2, rather than between Ste11 and Ste50. Given this result and the reports of others that the Ste11-Ste50 interaction does not change upon osmotic stress (Francesc Posas et al. 1998; Wu et al. 1999), I will henceforth refer to these proteins together as Ste11/50.

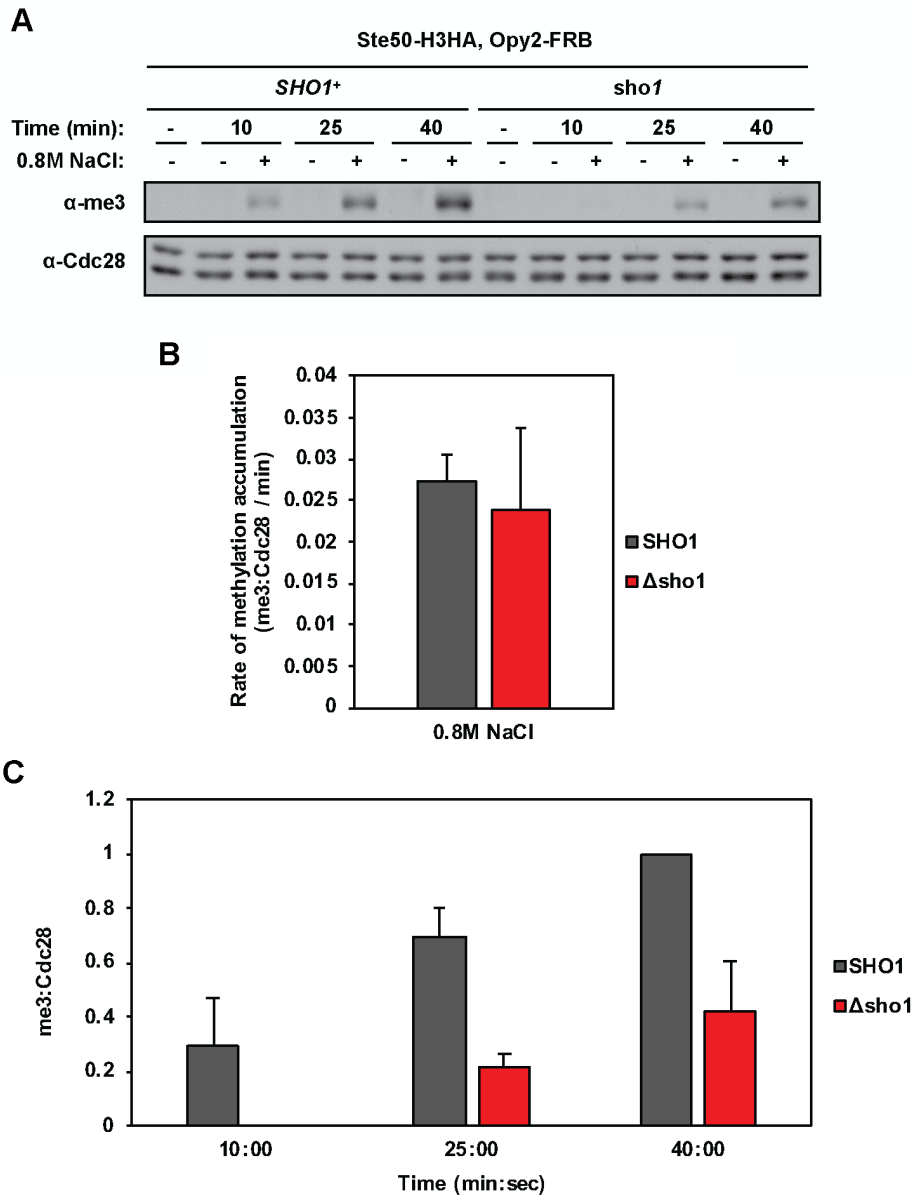

Figure 2.18

M-Track analysis of the Ste50-Opy2 interaction in *SHO1*$^{+}$ and *sho1* backgrounds

(A) Immunoblot of the M-Track assay using strains yJA425 and yJA434 as described in the Materials and Methods section. (B) Rate of methylation accumulation. Error bars represent SD (n=3). (C) Mean of calculated me3:Cdc28 ratios. Error bars represent SD (n=3). No methylation could be quantified in any of the unstressed samples. Therefore neither me3:Cdc28 ratios, nor rates of methylation accumulation could be calculated for these conditions.

2.3.4. Stress-induced Ste11/50-Opy2 proximity is reduced but not abolished in the absence of Msb2, Hkr1 and Sho1

As the oligomerisation model suggests that Ste11/50 localisation to the plasma membrane would be reduced in the absence of Msb2 and Hkr1, I measured the interaction of Ste11/50 with Opy2 in *Δmsb2/Δhkr1* cells. Upon addition of rapamycin, methylation accumulated faster in osmotically stressed cells than unstressed cells (Fig 2.19A and B). In the absence of Msb2/Hkr1, methylation accumulated to a lesser extent than in wildtype cells. Furthermore, the average methylation levels of stressed samples from *Δmsb2/Δhkr1* cells were less than those from wildtype cells (Fig 2.19C). This result indicates that Msb2/Hkr1 are partially required to localise Ste11 at the plasma membrane, and thus supports the Oligomerisation model.

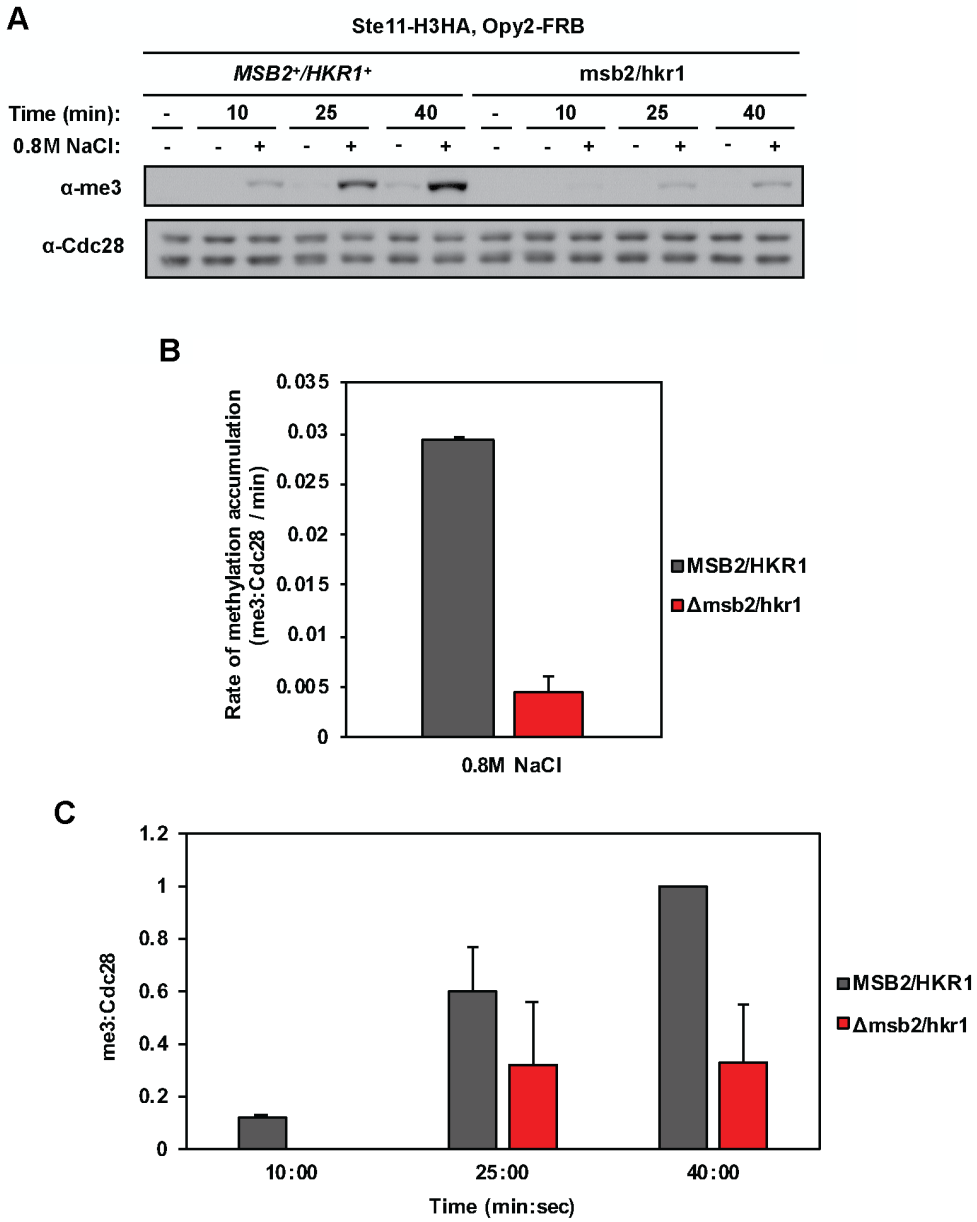

Figure 2.19

M-Track analysis of the Ste11-Opy2 interaction in *MSB2*$^{+}$*HKR1*$^{+}$ and msb2/*hkr1* backgrounds

(A) Immunoblot of the M-Track assay using strains yJA427 and yJA439 as described in the Materials and Methods section. (B) Rate of methylation accumulation. (C) Mean of calculated me3:Cdc28 ratios. Error bars represent SD (n=3). No methylation could be quantified in any of the unstressed samples. Therefore, rates of methylation accumulation could be calculated for these conditions.

Since in the absence of Sho1 and Msb2/Hkr1 individually, Ste11/50 still showed osmotic stress-induced localisation to the plasma membrane, I speculated that Msb2/Hkr1 and Sho1 might act in a redundant manner in the localisation of Ste11/50. According to the Oligomerisation model, the presence of Opy2 alone would not be sufficient to cause osmotic stress-induced relocalisation of Ste11/50 to the plasma membrane. I therefore repeated the

M-Track in *Δmsb2/Δhkr1Δsho1* cells and hypothesised that Ste11/50 plasma membrane recruitment would be abolished. Unexpectedly, I found that in the absence of all three transmembrane proteins, methylation still accumulated more in the stressed cells than in the unstressed cells (Fig 2.20A). Furthermore, the average levels of methylation in the stressed condition were similar in both the absence of Msb2/Hkr1 and in the absence of Msb2/Hkr1 and Sho1 (Fig. 2.20C). This result, together with previous findings from our group, indicate that Ste11/50 localisation to the plasma membrane is partially independent of all transmembrane proteins except Opy2.

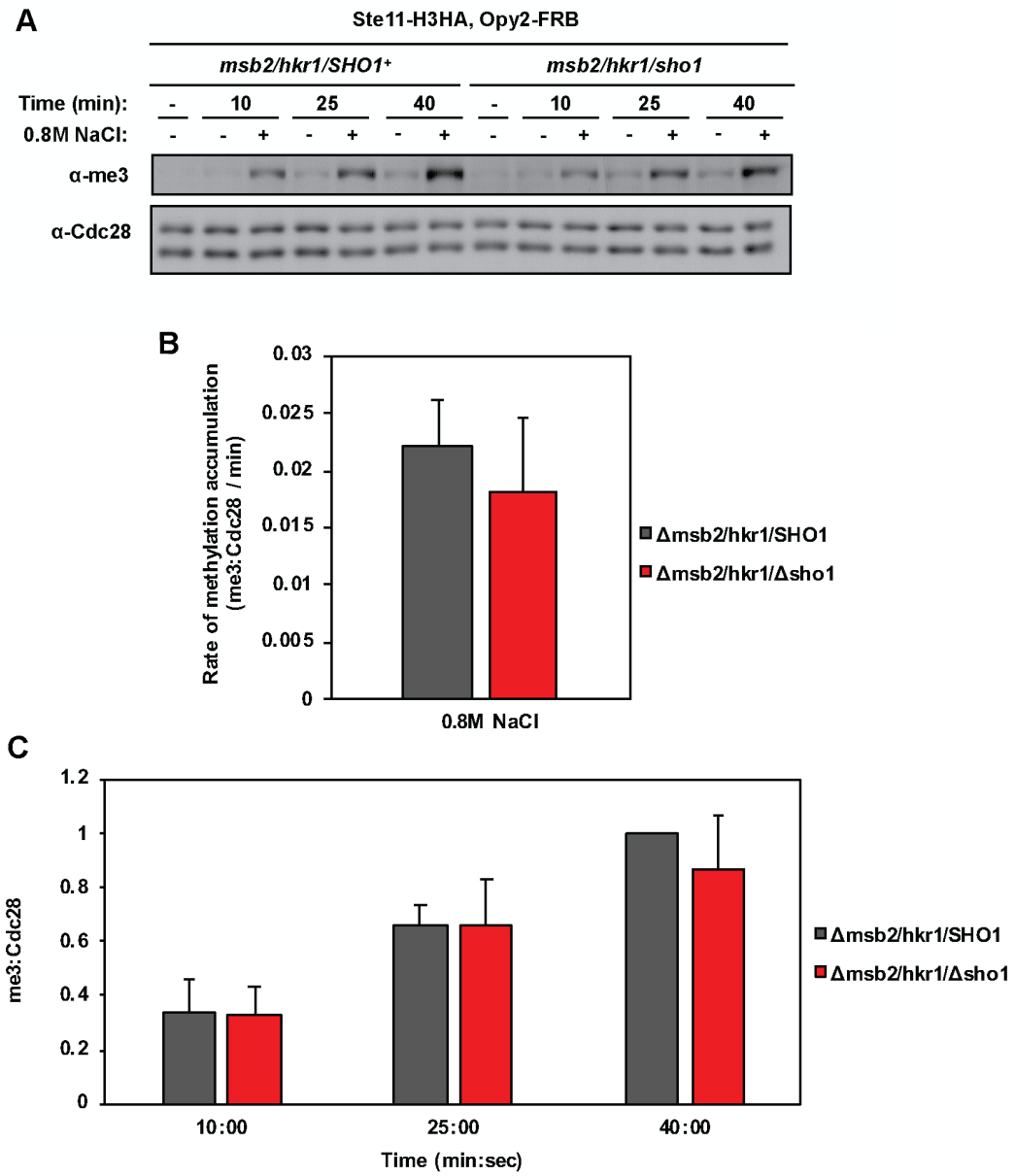

Figure 2.20

M-Track analysis of the Ste11-Opy2 interaction in *msb2/hkr1/SHO1*$^{+}$ and msb2/*hkr1/sho1* backgrounds

(A) Immunoblot of the M-Track assay using strains yJA461 and yJA459 as described in the Materials and Methods section. (B) Rate of methylation accumulation. (C) Mean of calculated me3:Cdc28 ratios. Error bars represent SD (n=3). No methylation could be quantified in any of the unstressed samples. Therefore neither me3:Cdc28 ratios, nor rates of methylation accumulation could be calculated for these conditions.

2.3.5. The stress-induced increase of the Ste11/50-Opy2 interaction occurs in the absence of Calcineurin activity

Given the previous result and the fact that HOG pathway activation is not the only signalling event that occurs upon exposure to hyperosmotic stress, I decided to investigate whether the residual localisation of Ste11/50 at the plasma membrane was regulated by a pathway other than the HOG pathway. Two signalling pathways that are affected by hyperosmotic stress are those of Ca^{2+}/Calmodulin signalling, and TORC2-Ypk1/2 signalling. In Ca^{2+}/Calmodulin signalling, exposure to hyperosmotic stress causes an increase in the intracellular Ca^{2+} concentration (Denis & Cyert 2002). Ca^{2+} then binds to and activates Calmodulin which then binds to Cnb1, the regulatory subunit of the protein phosphatase Calcineurin. Binding of Ca^{2+}/Calmodulin to Cnb1 results in Calcineurin activation. Activated Calcineurin can then dephosphorylate its protein targets which leads to protective events such as depolarisation of the actin cytoskeleton, delay in cell-cycle progression and transcriptional activation (Cyert 2001; Cyert 2003; Mulet et al. 2006). As a result, cells lacking Cnb1 are sensitive to high external NaCl concentrations (Mendoza et al. 1994).

Ypk1 and 2 are redundant protein kinases and the principle effector kinases responsible for TORC2 signalling (Roelants et al. 2011). Upon hyperosmotic stress, TORC2 signalling is switched off and Ypk1/2 are rapidly inactivated (Muir et al. 2015). Not only are Ca^{2+}/Calmodulin and TORC2-Ypk1/2 signalling activated under different cellular conditions, they have also been reported to antagonise each other in multiple ways. Calcineurin is hyperactive in the absence of TORC2 signalling, and TORC2-signalling activation events are enhanced in the absence of Calcineurin activity (Mulet et al. 2006). Furthermore, Ypk1 and Calcineurin have been known to phosphorylate and dephosphorylate the same residues of target proteins, respectively (Fig. 2.21).

Interestingly, these signalling events happen on a similar timescale to Hog1 activation and occur independently of the HOG pathway activation (Muir et al. 2015). I therefore hypothesised that Calcineurin activation or Ypk1/2 inactivation might be required for Ste11/50 to localise to the plasma membrane, and therefore for the HOG pathway to be activated. To test this, I first measured the Ste11/50-Opy2 interaction in *Δmsb2/Δhkr1Δsho1* strains in the absence of Cnb1, the essential positive regulatory subunit of Calcineurin. In both *CNB1*$^{+}$ and *Δcnb1* cells, methylation accumulated faster in the stressed condition than in the unstressed condition (2.22A and B). In addition, the average levels of methylation were higher for stressed

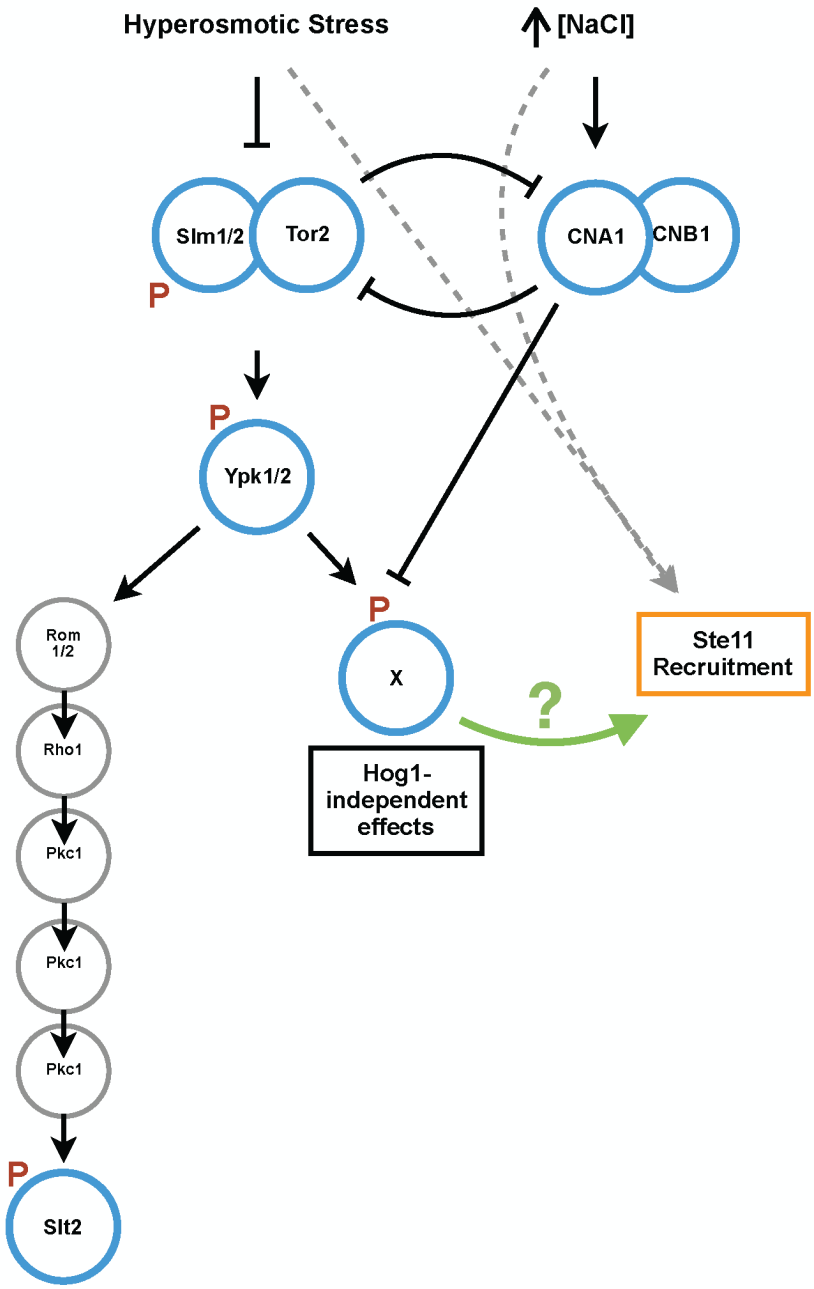

Figure 2.21

Proposed model of Ypk1 and Calcineurin (CN) Signalling during osmotic stress

Hyperosmotic stress inhibits Ypk1 phosphorylation and activation, and activates Calcineurin (CNA1 and CNB1) independent of Hog1. This leads to dephosphorylation of osmostress-responsive Hog1-independent targets. This dephosphorylation might lead to Ste11 recruitment. An additional effect of Ypk1 inactivation is Slt2 dephosphorylation.

samples than unstressed samples at all three timepoints measured (2.22C). At the 10-minute timepoint, the methylation level of the stressed *Δcnb1* cells was higher than that of the stressed *CNB1*$^{+}$ cells. As a result, the calculated rate of accumulation was lower in this

condition (see the text corresponding to figure 2.4 for a more detailed explanation). This result indicates that Calcineurin activity is not required for Ste11 plasma membrane localisation.

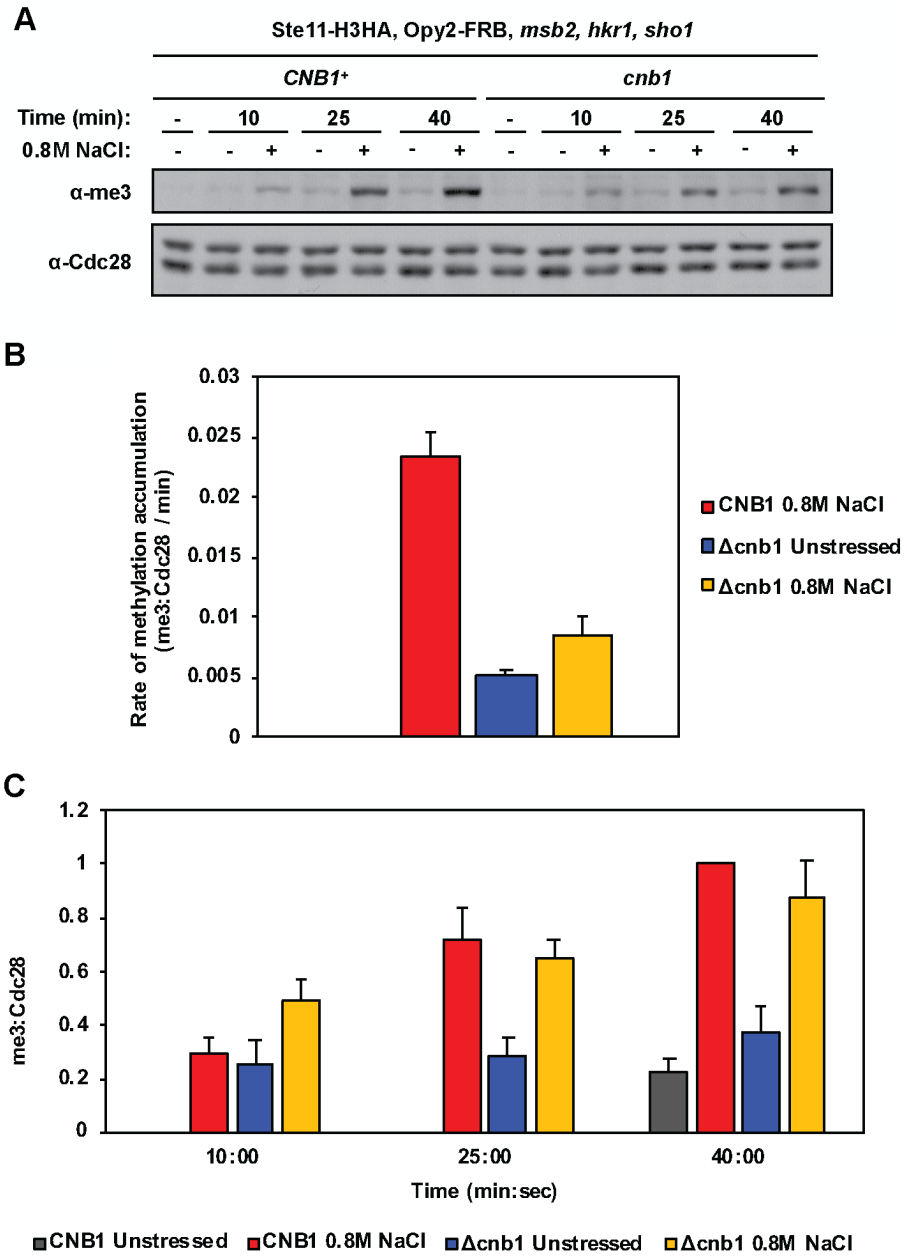

Figure 2.22

M-Track analysis of the Ste11-Opy2 interaction in *CNB1*⁺ and *cnb1* backgrounds

(A) Immunoblot of the M-Track assay using strains yJA527 and yJA565 as described in the Materials and Methods section. (B) Rate of methylation accumulation. Error bars represent SD (n=3). (C) Mean of calculated me3:Cdc28 ratios. Error bars represent SD (n=3). No methylation could be quantified for the 10 or 25-minute *CNB1*⁺ unstressed samples. Therefore neither me3:Cdc28 ratios, nor rates of methylation accumulation could be calculated for these conditions.

2.3.6. Inhibition of Ypk1/2 activity does not cause the Ste11/50-Opy2 interaction

To investigate the role of Ypk1/2 signalling in Ste11/50 localisation, I created strains in which *YPK2* had been deleted and *YPK1*$^{+}$ was replaced with an analogue-sensitive (*as*) allele (L424A) whose activity could be inhibited by the ATP analogue 3MB-PP1. As I hypothesised that inactivation of Ypk1/2 signalling might cause Ste11/50 localisation, I predicted that Ypk1 inhibition alone would be sufficient for localisation. I therefore measured the interaction of Ste11/50 with Opy2 in *Δmsb2/Δhkr1Δsho1Δypk2* strains in which Ypk1-as had been inhibited. No methylation could be observed in the unstressed inhibited samples suggesting that inhibition of Ypk1 alone was not sufficient to cause the Ste11/50-Opy2 interaction (Fig 2.23). Furthermore, in both the absence and presence of Ypk1 inhibition, methylation accumulated faster in stressed cells than in unstressed cells. To verify the effect of the inhibitor on the cells, I measured the levels of Slt2 phosphorylation in all samples because it has previously been suggested in the literature that Ypk1-as inhibition results in reduced Slt2 phosphorylation (Helliwell et al. 1998; Levin 2011; Schmidt et al. 1997) As expected, less Slt2 was less phosphorylated when Ypk1 was inhibited (Fig. 2.23). Taken together, these results suggest that Ypk1/2 signalling does not affect Ste11/50 plasma membrane localisation.

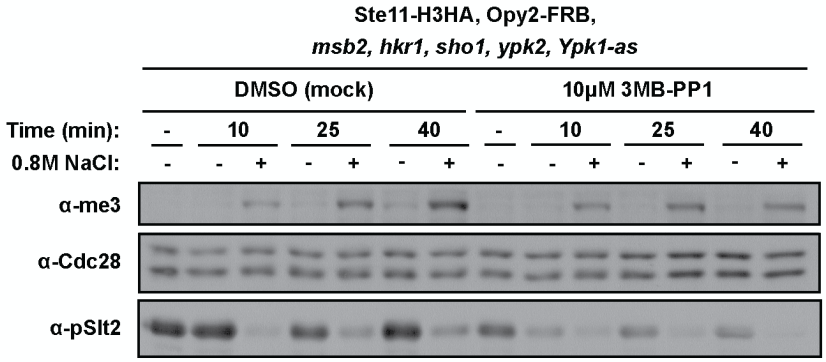

Figure 2.23

M-Track analysis of the Ste11-Opy2 interaction in an *msb2/hkr1/sho1/ypk2/YPK1-as* background following Ypk1 inhibition

(A) Immunoblot of the M-Track assay using strain yJA552. Cells were pre-treated either with 3MB-PP1 (final conc. 10μM) or an equivalent volume of mock (DMSO) for 60. At time = 0 min, rapamycin was added, and the assay was performed as described in the Materials and Methods section.

3. Discussion and Conclusion

The aims of my thesis were to 1) use the inducible M-Track system to describe the interactions between proteins of the SHO1-branch of the HOG pathway in the absence and presence of osmotic stress to create a model of the dynamic changes that occur during pathway activation and 2) characterise the interdependency these interactions. I will now discuss the interpretation and potential implications of my results to produce a final model of pathway activation.

3.1. Pbs2 Localisation

My M-Track analysis of the Pbs2-Sho1 interaction as a proxy for Pbs2 localisation to the plasma membrane showed that the interaction increased upon exposure to hyperosmotic conditions. This indicates that, in the absence of stress, rather than being permanently localised at the plasma membrane, Pbs2 is located in the cytoplasm. This is consistent with previous findings that locate Pbs2 in the cytoplasm both before and during osmotic stress (Ferrigno et al. 1998; Reiser et al. 2000; Tatebayashi et al. 2003). A previous study from our group found that Pbs2, inactivated either through point mutation or deletion of upstream kinases, could not delocalise from the plasma membrane once recruited by osmotic stress (Reiser et al. 2000). This suggests that in wildtype cells, inactive Pbs2 localises to the plasma membrane where it is phosphorylated and activated and then rapidly delocalises.

As the Pbs2-Sho1 interaction is therefore transient, one would expect it not to be detected using methods which require stable interactions such as co-IP. In fact, the only report of successful co-IP of Sho1 and Pbs2 was performed in cells expressing both Sho1 and Pbs2 under strong promoters (Posas & Saito 1997). I propose that the overexpression of the proteins that caused them to interact, and at wild-type levels the interaction would be too weak to be seen through co-IP.

Pbs2 does not appear to be completely delocalised from the plasma membrane in the absence of osmotic stress because my results also showed that the Pbs2-Sho1 interaction in unstressed cells can lead to saturation of the H3HA tag within 40 minutes. One possible explanation is that in the absence of stress, Pbs2 shuttles to and from the plasma membrane, allowing gradual accumulation of methylation, whereas in the presence of stress, Pbs2 localises to the plasma membrane for longer. However, given that during stress, inactive Pbs2 cannot delocalise from the plasma membrane, this suggests that inactive Pbs2 in the absence

of stress also cannot delocalise from the plasma membrane. An exception would be if stressed cells could somehow “trap” Pbs2 at the plasma membrane whereas unstressed cells could not. As it was shown that Cdc42, which is needed for pathway activation, is also needed to “trap” Pbs2 at the plasma membrane (Reiser et al. 2000), it seems plausible that the hyperosmotic stress-induced mechanism which allows Cdc42 to activate the pathway might also allow it to “trap” inactive Pbs2 molecules.

A benefit of such a mechanism is that, upon osmotic stress, it would allow the shuttling Pbs2 molecules which were currently localised at the plasma membrane to be stabilised there. In addition, they would remain localised until Ste11 was also localised and activated, and activated Pbs2. Activated Pbs2 would then dissociate, and inactive Pbs2 would take its place. This would allow many molecules of Pbs2 to be activated in quick succession. Furthermore, it is advantageous that Pbs2 is not permanently localised to Sho1 because this might lead to its sequestration away from its other activators, Ssk2/22. Therefore shuttling of Pbs2 might allow optimal activation of both pathways.

3.2. The Sho1-Sho1 Interaction

In my thesis I confirmed previous results suggesting that Sho1 forms oligomers and that Pbs2 localises to these oligomeric structures. Oligomerisation of Sho1 allows the concentration of Pbs2 molecules at the membrane. This means that, when also recruited to the plasma membrane, Ste11 is in close proximity to many molecules of Pbs2 at the same time, which it can activate. This is therefore a potential amplification step in pathway activation.

My results suggested an increase in the Sho1-Sho1 interaction during stress. Galactose-induced co-IP studies from the Saito group have previously suggested that the Sho1-Sho1 interaction neither increases nor decreases upon osmotic stress (Tatebayashi et al. 2015). However, crosslinking analysis in the same study suggested that in the absence of stress, the first transmembrane domain (TM1) of Sho1 molecules are more than 16Å apart and that upon hyperosmotic stress, the distance between TM1s reduces to less than 16Å. Therefore, it is possible that there is in fact a stress-induced increase in proximity but since Sho1 molecules also interact in the absence of stress, this stress-induced increase cannot be seen by less sensitive methods such as galactose-induced co-IP.

A separate study suggested a stress-induced decrease in oligomerisation (Hao et al. 2007). Hao and colleagues found that Sho1 is phosphorylated by Hog1 at Ser166 and that this

phosphorylation reduced Sho1 oligomerisation. They also found that a phosphomimicking mutant showed reduced pathway activation whereas a non-phosphorylatable mutant showed prolonged pathway activation. These results therefore suggest the following negative feedback mechanism: hyperosmotic stress leads to Hog1 activation, active Hog1 then phosphorylates Sho1 causing a reduction in its oligomerisation, non-oligomerised Sho1 cannot transduce the activation signal and therefore the pathway is switched off.

Although indications of both a stress-induced increase and decrease in interaction might seem contradictory, it is possible that hyperosmotic stress first causes an increased interaction which is then reduced due to the negative feedback mechanism. Moreover, the fact that a negative feedback mechanism exists in which the Sho1-Sho1 interaction decreases, suggests that it is counteracting a mechanism in which the interaction first increases.

My analysis of the Sho1-Sho1 interaction in the absence of Msb2/Hkr1 indicated that the osmosensors partially inhibit the Sho1-Sho1 interaction. One possible explanation for this finding could be that Msb2 and Hkr1 are arranged amongst and between Sho1 oligomers, thereby creating distance between individual Sho1 molecules. As a result, in the absence of Msb2 or Hkr1, Sho1 molecules might be able to come closer to each other. Conclusions from Tatebayashi and colleagues suggested such an arrangement between Sho1, Msb2 and Hkr1, thus supporting this interpretation. Although they did not measure the ability of Sho1 to co-immunoprecipitate with itself in *msb2/hkr1* cells, they did report that the stress-induced structural change was maintained in the double mutant (Tatebayashi et al. 2015). This finding is consistent with results which showed that the interaction was maintained in these cells. To gain further insight into the arrangement of Sho1 oligomers in *msb2/hkr1* cells, total internal reflection fluorescence (TIRF) microscopy could be used since this method has already successfully been used to visualise the arrangement of proteins at the plasma membrane in yeast (Berchtold et al. 2012).

In the absence of Opy2, the Sho1-Sho1 interaction was reduced. However, this is most probably due to the decreased expression of the FRB tagged Sho1 construct in this strain. As the H3HA-tagged construct, which was expressed from the native *SHO1* locus, was equally expressed in both the presence and absence of osmotic stress, it is unlikely that the presence of Opy2 is required for *SHO1* expression in wildtype cells. Therefore it is most probable that deletion of *OPY2* in this strain somehow led to modification of the *LEU2* locus where the *SHO1-FRB* construct was situated. Furthermore, hyperosmotic stress-induced structural changes in the Sho1-Sho1 interaction have been reported to not be affected by deletion of Opy2 (Tatebayashi et al. 2015).

3.3. The Msb2-Sho1 Interaction

Although it has been shown that Sho1 mutants with reduced binding to Msb2 also have a reduced ability to activate Hog1 (Tatebayashi et al. 2007), the effect of hyperosmotic stress on the Msb2-Sho1 interaction has not yet been reported. Msb2 and Sho1 are also known known to interact in the filamentous growth (FG) pathway and it is thought that their actions in the HOG and FG pathways are similar. Mutations in both Msb2 and Sho1 which hyperactivate the HOG pathway also hyperactivate the FG pathway (Cullen et al. 2004; Tatebayashi et al. 2007; Vadaie et al. 2008). In addition, these Msb2 mutants require the presence of Sho1 in order to hyperactivate both pathways. Since it has been reported that the interaction between Sho1 and Msb2 is increased in cells undergoing FG, one could speculate that their interaction might also increase during hyperosmotic stress.

My M-Track analysis of the Msb2-Sho1 interaction suggested that there is no hyperosmotic stress-induced change in interaction. However, this result could be due to the length of the time course used. My initial 40-minute time course did not show a stress-induced increase in the Sho1-Sho1 interaction, but my 10-minute time course did. It is therefore possible that, in the case of the Msb2-Sho1 interaction, rapid increases in proximity were missed. Analysis of a 10-minute time course of the Msb2-Sho1 interaction would provide clarity on this topic.

3.4. The Msb2-Opy2 Interaction

In my thesis I also measured the interaction of Msb2 with Opy2. My results suggested that there is a slight increase in the interaction upon hyperosmotic stress. This stress-induced difference is consistent with reports of a structural change in the Msb2-Opy2 interaction upon stress (Yamamoto et al. 2015). Yamamoto and colleagues were unable to detect a hyperosmotic stress-induced change in interaction through co-immunoprecipitation of galactose-induced constructs. As with their analysis of the Sho1-Sho1 interaction, it is possible that overexpression of the constructs prevented subtle changes in affinity or residence time from being detected. Therefore, it remains plausible that the interaction of Msb2 and Opy2 increases during hyperosmotic stress.

As Msb2 binds to Ste20 via Bem1 (Tanaka et al. 2014), an increase in interaction with Opy2 would allow the MAPKKKK and the MAPKKK to come into close proximity, resulting in activation of Ste11. Therefore, regulation of the Opy2-Msb2 interaction would play an

important role in regulating pathway activation. This is consistent with findings that cells in which Msb2 and Opy2 cannot interact, cannot activate the HOG pathway (in the absence of Hkr1 and Ssk2/22).

3.5. The Sho1-Opy2 Interaction and Dependence on Msb2/Hkr1

My M-Track analysis of the Sho1-Opy2 interaction indicates that it increases during hyperosmotic stress and that this increase is dependent on Msb2/Hkr1. Not only is the increase in interaction dependent on Msb2/Hkr1 but also the basal interaction level. Therefore, in cells without Msb2 or Hkr1, Ste11/50 cannot come into close proximity with Pbs2, Pbs2 cannot be activated and therefore Hog1 cannot be activated. Although it has previously been shown that Msb2 and Hkr1 are redundantly essential for pathway activation (Tatebayashi et al. 2007), the effect of their deletion on the physical arrangement of other HOG pathway proteins has, as of yet, only been assumed but not shown. Therefore, my finding is of great importance.

It has been suggested that Hkr1 functions through its ability to bind both Opy2 and Sho1 (Tatebayashi et al. 2015). Abolishing the Hkr1-Opy2 interaction, also abolished signalling in cells expressing wildtype Ste11. In cells expressing constitutively active Ste11, however, signalling was only reduced but not abolished. This suggested that one role of the Opy2-Hkr1 interaction, namely to bring Ste11 close enough to Ste20 to be activated, was bypassed by hyperactive Ste11 but that another role existed.

The second role of the Hkr1-Opy2 interaction was proposed to be stabilisation of a direct interaction between Sho1 and Opy2 because cells in which Hkr1 could bind neither Opy2 nor Sho1 (and therefore carry out its stabilising function) could not activate the HOG pathway (Tatebayashi et al. 2015). As my results suggest the roles of Msb2 and Hkr1 to be similar with regard to the Sho1-Opy2 interaction, the results of Tatebayashi and colleagues are consistent with my own. In my experiments, deletion of Msb2 meant that it could bind neither Opy2 nor Sho1 and in these cells the Sho1-Opy2 interaction was reduced, suggesting it could not be stabilised. In addition, the direct interaction between Sho1 and Opy2 might be responsible for the very minimal levels of methylation in *msb2/hkr1* cells. As this interaction is insufficient to activate the HOG pathway (Tatebayashi et al. 2007), these results indicate that the stabilised interaction of Sho1 and Opy2 is essential for pathway activation.

My attempt to bypass the function of Msb2 by artificially dimerising Sho1 and Opy2 was unsuccessful, indicating that bridging the interaction between Sho1 and Opy2 was not the sole function of Msb2. These results are consistent with the idea that Msb2 and Hkr1 also function to bring Ste20 into close proximity to Ste11 (as mentioned above).

3.6. Ste11/50 Localisation

In my thesis, I found that localisation of Ste11 to Opy2, Msb2 and Sho1 does not depend on its activation state. This result is consistent with findings from our group that showed that the Ste11-Sho1 interaction was neither abolished nor enhanced by deletion of *STE20* (Zuzuarregui et al. 2015). Therefore, although activation of Ste11 is essential for pathway activation, in contrast to Pbs2, its activation state does not affect its membrane localisation.

One of the most striking findings of my thesis was that the interaction of Ste11 with Opy2, Msb2 and Sho1 increases upon hyperosmotic stress. Previous work from our lab showed only slight increases in interaction, and other reports suggested decreased interaction during stress (Yamamoto et al. 2010; Zuzuarregui et al. 2015). Both of these previous reports proposed that Ste11 is localised at the plasma membrane in unstressed cells. Given that permanent localisation of hyperactive Ste11 results in hyperactivation of the pathway but localisation of wildtype Ste11 does not (Tatebayashi et al. 2006), it was thought that Ste11 was primarily activated through its movement along the membrane towards Ste20. My results however suggest that relocalisation of Ste11 from the cytoplasm to the plasma membrane during stress plays an important role in its activation.

My M-Track analyses also suggest that Ste11/50 localises to the membrane through both Opy2 and Sho1 because the interaction of Opy2 with both Ste11 and Ste50 was reduced in the absence of Sho1. This is consistent with reports that Ste50 can interact with Sho1 independently of its interaction with Opy2 (Tatebayashi et al. 2015). Ste50 binds the intracellular loop of Sho1. This region is not present in cells in which wildtype *SHO1* is deleted and a myristolated C-terminal region of Sho1 is localised to the plasma membrane (to recruit Pbs2). However these cells can still activate the HOG pathway. Therefore, the Ste50-Sho1 interaction is not essential for pathway activation. In contrast, deletion of *OPY2* results in complete abrogation of HOG pathway activation. Taken together, this suggests that the Ste50-Sho1 interaction is not as important as the Ste50-Opy2 interaction for Ste11 membrane localisation.

My hypothesis that Sho1 and Msb2/Hkr1 play redundant roles in Ste11/50 recruitment was disproven by my result showing that *msb2/hkr1/*sho1 cells were just as able to recruit Ste11/50 as msb2*/hkr1/SHO1* cells. Although this result was initially surprising, it can be explained by considering my Sho1-Opy2 analyses. In msb2*/hkr1/SHO1* cells, Sho1 is not in close proximity to Opy2 and so cannot stabilise the Ste11/50-Opy2 interaction. As a result, deletion of Sho1 in addition does not have any additional effect on Ste11/50 recruitment. Ste50 has also been reported to bind Cdc42 (Truckses et al. 2006). However this binding is independent of the activation state of Cdc42 and therefore is not thought to be a key regulation mechanism for recruiting Ste11/50 to the plasma membrane.

When I investigated the effect of Calcineurin signalling on Ste11/50 localisation I found that recruitment still occurred in the absence of the essential Calcineurin regulatory protein, Cnb1. Moreover, I found that localisation was enhanced in *cnb1* cells. *cnb1* cells are less resistant to osmotic stress than wildtype cells (Mendoza et al. 1994). If this lower resistance were caused by overactivation of the pathway, Ste11/50 might be more able to activate the pathway in these cells. This might explain the increased levels methylation seen in both unstressed and stressed samples at the 10-minute timepoint.

Inactivation of TOR2-Ypk1/2 signalling did not seem to have an effect on Ste11/50 membrane localisation. As *ypk1/ypk2* cells are inviable, I had to inhibit Ypk1 activity rather than delete the gene. It is possible that Ypk1 was not fully inhibited during the assay. If Ypk1 is expressed at higher levels than are needed for all its cellular functions, inhibition of only a proportion of Ypk1 molecules in the cell might not affect Ypk1-dependent processes. However, if it is expressed at a level much greater than those needed for some processes, but at an almost limiting level for other processes, it is possible that some processes were inhibited during the assay whereas others were not. In this case, if Ypk1 inhibition were needed for Ste11/50 recruitment, inhibition might be sufficient to reduce the levels of Slt2 phosphorylation without affecting the ability of Ypk1 to recruit Ste11/50 to the membrane. Moreover, if Ypk1 were only partially inhibited, Ste11/50 membrane localisation might have indeed been induced but at levels undetectable by the assay. An experiment to clarify the role of TOR2-Ypk1/2 signalling in Ste11/50 membrane localisation could theoretically involve the (over)expression of a hyperactive mutant which cannot be inactivated by hyperosmotic stress. In this experimental setup it would be hypothesised that Ste11 would be unable to localise to the plasma membrane.

Rather than trying to understand regulation of Ste11/50 membrane localisation by looking at stress-induced changes in general cellular processes, an alternative approach is to look at stress-induced changes of the Ste50 and Opy2 molecules themselves.

The cytoplasmic tail of Opy2 is unstructured and contains four conserved regions (CRs), CR-A, CR-B, CR-C and CR-D (Ekiel et al. 2009; Yamamoto et al. 2010). Extensive analysis of the Ste50-Opy2 interaction by the Saito group has shown that whereas CR-A, -B and -D are accessory to Ste50 binding, CR-C is inhibitory. Opy2 mutants lacking CR-C co-immunoprecipitate Ste50 more than wildtype Opy2. I speculate that this increased binding ability could be because Opy2 lacking CR-C is not able to regulate its binding to Ste50, resulting in its permanent association. When I performed initial experiments to measure the interaction of Ste11 with Opy2ΔCR-C, I found methylation in both unstressed and stressed samples. However, in these strains Opy2ΔCR-C was greatly overexpressed, so it is not clear if the unregulated association of Ste11 and Opy2 was due to increased binding affinity or overexpression. Further investigation of the Ste11-Opy2ΔCD-C interaction might reveal a possible regulation mechanism involving masking of the CR-C domain upon stress to allow Ste11/50 binding.

Since it is known that non-phosphorylatable Ste50 interacts with Opy2 more than wildtype Ste50, and also leads to prolonged Hog1 activation (Hao et al. 2007; Yamamoto et al. 2010), phosphorylation of Ste50 could be an important regulation step. It would be interesting to know if hyperosmotic stress-activated phosphatases other than Calcineurin rapidly dephosphorylate Ste50 upon osmotic stress, thus allowing it to localise to the plasma membrane.

3.7. The Inducible M-Track Method

The inducible M-Track method has been essential in elucidation of HOG pathway protein interactions. Discrepancies between my findings and those of others can be explained almost completely by the differences in methods used. The main advantage of the M-Track assay is that it is sensitive enough to detect protein-protein interactions that could not be detected using co-IP. It must be emphasised here that M-Track assay is an *in vivo* protein-proximity assay and therefore cannot distinguish between direct and indirect interactions. However, this is also a caveat of co-IP. In general, methods which take place *in vivo* under conditions in which the proteins would normally interact, are unable to distinguish between direct interactions, indirect interactions and close proximity. Methods used to determine direct interaction such as Yeast Two-Hybrid or *in vitro* have their own caveats such as the forced proximity of proteins that

would normally be found in different cellular compartments, or the lack of post-translational modifications which might be necessary for certain interactions.

Many interactions reported by the Saito group to be static were found to be dynamic during my analysis, namely those of Sho1 with Sho1, Opy2 and Sho1, Opy2 and Msb2, and Opy2 and Ste11/50. Although there was evidence that these proteins might interact more during osmotic stress, the use of co-IP in combination with expression of constructs from strong promoters often prevented these increases from being seen. In the cases of the Sho1-Sho1 and Opy2-Msb2 interactions, changes in cross-linking capabilities between the proteins were an indication of stress-induced changes in interaction (Tatebayashi et al. 2015; Yamamoto et al. 2015). Using the inducible M-Track method I was able to confirm these indications. In the cases of the Sho1-Opy2 and Ste11/50-Opy2 interactions, stress-induced interactions using co-IP have not been seen. The inducible M-Track, however, showed clear increases in interaction in both cases.

Several interactions that I studied using the inducible M-Track system were previously studied by our group using the non-inducible M-Track system (Dohnal 2005; Friedmann 2010; Zuzuarregui et al. 2015). The main difference between my results and those of previous analyses is due to the presaturation of the H3HA tag which can occur in the non-inducible assay. For example, if the interaction between two proteins increases during stress but the H3HA tags on all molecules are already (on average) 70% methylated before the start of the assay, then only a 42% increase in methylation can be seen (from 70% to 100%). If the tags are 100% methylated, i.e. completely saturated, before the assay then no increase in methylation can be seen. Concerning the Ste11 interaction with Sho1 and Msb2, slight increases were previously seen (Zuzuarregui et al. 2015), however restudying this interaction using the inducible assay prevented partial saturation of H3HA tag before rapamycin addition and therefore allowed greater increases in methylation to be seen. In the case of the Pbs2-Sho1 interaction, presaturation of the tag meant than no increase in methylation upon stress could be seen using the non-inducible assay (Dohnal 2005), contrastingly the inducible M-Track assay showed large increases in methylation upon stress.

A caveat of both forms of the M-Track assay is that they cannot distinguish between two proteins which are permanently in moderately close proximity, and two proteins which interact directly but with high on and off rates. In both cases, a moderate methylation signal would be measured, i.e. a signal which is stronger than those of non-interacting proteins but weaker than those of permanently directly interacting proteins. To distinguishing between these two options, it would be necessary to consider other evidence. For example, in the case of the

Pbs2-Sho1 interaction, moderate accumulation of methylation combined with the knowledge that Pbs2 is reported to be located in the cytoplasm strongly suggests that the Pbs2-Sho1 interaction is one with high on and off rates. In the case of the Sho1-Opy2 interaction, moderate accumulation of methylation combined with the knowledge that Msb2 interacts with both proteins in the absence of stress strongly suggests that Sho1 and Opy2 are permanently in moderately close proximity. As mentioned in the introduction, M-Track is not an indicator of affinity as this would require calculation of on and off rates. These rates could be calculated using a combination of methods such as TIRF and fluorescence recovery after photobleaching (FRAP). Determining the binding affinity of the interactions studied in this thesis would provide further insight into the dynamic nature of the system.

3.8. General Conclusions

Interactions of the SHO1-branch of the HOG pathway are more dynamic than previously thought. Both Ste11 and Pbs2 dynamically localise to the plasma membrane albeit in different ways. Ste11(and Ste50) are located in the cytoplasm in the absence of stress and relocalise to the plasma membrane upon stress. Pbs2, on the other hand, is thought to demonstrate dynamic shuttling between the cytoplasm and plasma membrane in unstressed cells. Upon osmotic stress its occupancy at the membrane increases. These two events are independent of each other as Pbs2 can localise to the plasma membrane in the absence of Ste11/50 (Dohnal 2005; Reiser et al. 2000), and I have shown that Ste11/50 can localise to the plasma membrane in the absence of Sho1 (and therefore Pbs2).

These two independent essential events are coordinated by Msb2/Hkr1. Msb2 (and Hkr1) enables clustering of Sho1 and Opy2 upon osmotic stress. This clustering has at least two purposes. Firstly, it stabilises Ste11 at the plasma membrane by allowing accessory binding of Sho1 to Ste50. Secondly, it enables Ste11/50 and Pbs2 to come into close proximity (via Opy2 and Sho1 respectively). Moreover, Msb2 (and Hkr1) and Opy2 grouping might coordinate the association of Ste20 and Ste11. These events are summarised in figure 3.1.

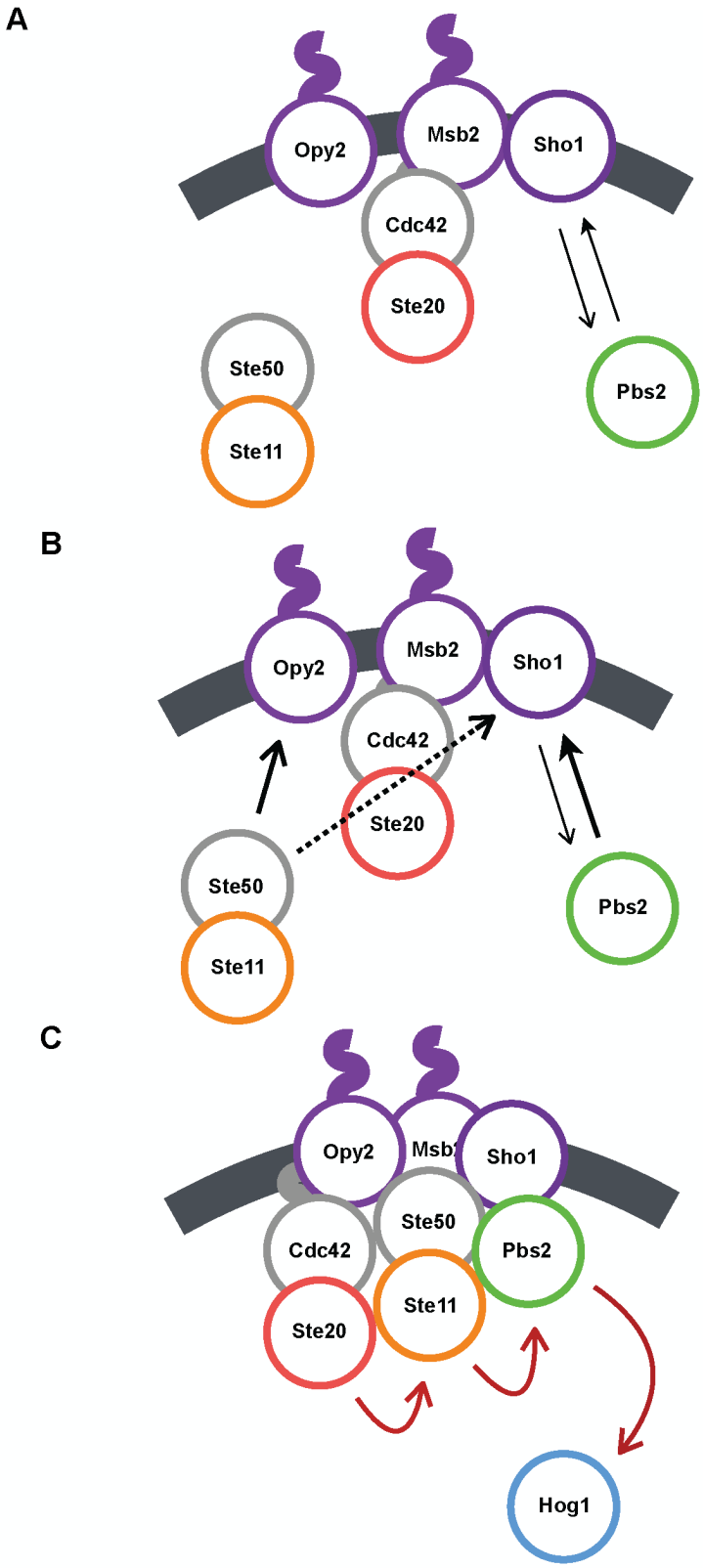
A
Opy2
Msb2
Sho1
Cdc42
Ste20
Ste50
Ste11
Pbs2
B
Opy2
Msb2
Sho1
Cdc42
Ste20
Ste50
Ste11
Pbs2
C
Opy2
Sho1
Ste50
Cdc42
Pbs2
Ste11
Ste20
Hog1

Figure 3.1

Final Model of HOG Pathway Activation

(A) Before hyperosmotic stress, Ste11/50 is not localised at the plasma membrane, whereas Pbs2 shuttles to and from Sho1. (B) Upon hyperosmotic stress, Ste11/50 localises to Opy2 and the interaction is stabilised by the interaction of Ste50 with Sho1 (dashed arrow). Opy2 moves into closer proximity to Msb2 and Sho1, bringing Ste11 to Ste20. Pbs2 also interacts with Sho1 more often. (C) During osmotic stress, clustering of proteins at the membrane allows efficient signal transfer from Ste20 to Pbs2.

4. Materials and Methods

4.1. Round The Horn (RTH) Mutagenesis

Using the wild-type Ste11 ORF as a template, DNA fragments were amplified using Kapa HiFi (Kapa Biosystems) according to the standard protocol. The wildtype ORF contained the sequence 841-AGCGAATTTATTTCTACC-858, corresponding to the amino acid sequence 281-SEFIST-286. Primers used replaced the wildtype sequence with that of GCCGAATTTATTGCTGCC for the 3A mutant corresponding to the amino acid sequence 281-AEFIAA-286, and GACGAATTTATTGATGAC for the 3D mutant corresponding to the amino acid sequence 281-DEFIDD-286. Changes in nucleotide and amino acid sequences are underlined.

1µL DpnI (NEB) was added to the PCR reaction and followed by incubation at 37°C for 1 hour. The PCR reaction mix was then cleaned using the Promega Wizard® SV Gel and PCR Clean-Up System according to the standard protocol and eluted in 30µL ddH_2O.

20 pmol 5' termini, 2µL Buffer A for T4 Polynucleotide Kinase (PNK) (Thermo Scientific), 2µL 10mM ATP and 1µL T4 PNK were combined and ddH_2O was added to a final volume of 20µL. The reaction mix was incubated at 37°C for 20 minutes before heat inactivation at 75°C for 10 minutes. The PCR reaction mix was then cleaned using the Promega Wizard® SV Gel and PCR Clean-Up System according to the standard protocol and eluted in 30µL ddH_2O.

The newly phosphorylated ends of the purified DNA were ligated together using the Roche Rapid DNA Ligation Kit according to the standard protocol. For transformation into *E. coli,* 10µL of reaction mix was added to 100µL of competent cells.

4.2. Transformation into *E. coli*

DNA was mixed with 100µL of competent DH5α cells and incubated on ice for 30 minutes. The cells/DNA mix was then heat shocked at 42°C for 45 seconds and then returned to the ice for 2 minutes. Cells were plated on agar plates containing 2xTY and 100mg/L ampicillin, and incubated overnight at 37°C.

4.3. PCR for Transformation into Yeast

DNA for transformation was amplified using a forward primer which, at the 3' end, contained the sequence tccggttctgctgctag which annealed to 20nt of the template DNA (either knockout

or tagging plasmid) and, at the 5' end contained 40-60nt of sequence homologous to the yeast genome. The reverse primer used contained the sequence cctcgaggccagaagac at the 3'end which annealed to 20nt of the template DNA, and at the 5' end contained 40-60nt of sequence homologous to the yeast genome.
PCR products were amplified using Kapa HiFi (Kapa Biosystems) according to the standard protocol. The PCR reaction was then run on a 1% agarose gel before amplified DNA was extracted and purified using the Promega Wizard® SV Gel and PCR Clean-Up System according to the standard protocol.

4.4. Annealing Oligonucleotides to create double-stranded DNA

5µL of 100mM oligonucleotides RmvURAFw and RmvURARe were combined and ddH_2O was added to a final volume of 50µL. The oligonucleotide mix was incubated at 95°C for 5 minutes before being left at room temperature for 2-3 hours to cool and for the strands to anneal to each other. This annealing step was also performed for the oligonucleotide pair tor1-1_mut_fw and tor1-1_mut_re.

4.5. Preparation of integrative plasmids for transformation

Approximately 2µg of plasmid DNA were linearised using a restriction enzyme (NEB) that cut at a single site in the region encoding the auxotrophic marker. The restriction enzyme was then heat inactivated at the temperature stated in the manufacturer's instructions for 15 minutes before being stored at 4°C.

4.6. Transformation Protocol

An overnight culture of cells grown in YEPD was shifted to OD_{600} 0.1-0.2 in a final volume of 50mL YEPD and grown to an OD_{600} of 1. Cells were centrifuged at 2000rpm for 2 minutes. The supernatant was removed, and cells were resuspended in 250µL 0.1M LiAc/1xTE.
The DNA to be transformed was combined with 480µL 50% PEG-3350, 60µL 1M LiAc, 60µL 10xTE, 10µL denatured salmon sperm DNA and 100µL of the above cell/LiAc/TE suspension. The mixture was vortexed before being incubated at 30°C and shaking at 650rpm for 30 minutes. 70µL DMSO were then added and the mixture was incubated at 42°C, without shaking, for a further 10 minutes. Cells were then pelleted by centrifugation at 2000rpm for 2 minutes before being resuspended in 1mL 1xTE. Cells were then repelleted at 2000rpm for 2 minutes before being resuspended in 200µL 1xTE. The cell suspension was then transferred

to an agar plate selective for the required marker and cells were distributed on the plate using glass beads. The plates were then incubated for 2-3 days at 30°C before being checked for successful transformants.

4.7. PCR for Checking

A PCR reaction mix using (for one colony) was prepared as follows:
2.5µL 10x DreamTaq Buffer (Thermo Scientific), 0.5µL 10mM dNTPs, 0.5µL forward checking primer, 0.5µL reverse checking primer, 0.5µL primer 'RevAnUp', 2.5U DreamTaq DNA Polymerase (Thermo Scientific) were combined and ddH_2O was added to a final volume of 25µL in a PCR tube. A small number of cells taken from a plate were added to the tube using a tip and were dispersed by wiping the tip on the inside of the tube.
The thermal cycling conditions used were as follows:
1) 95°C for 13 minutes, 2) 95°C for 1 minute, 3) 51°C for 1 minute, 4) 72°C for 1 minute, 5) Repeat steps 2-4 for 34 cycles, 6) 72°C for 1 minute.
The PCR reactions were run on a 1% agarose gel and visualised using a UV box.

4.8. M-Track Assay

4.8.1. Strain Preparation

Strains chosen for the M-Track assay were prepared by transforming them with pCK911 to introduce the FKBP-HKMT construct.

4.8.2. Growing Cultures

An 50mL overnight culture of cells grown in –His medium was centrifuged at 2000rpm for 2 minutes. The supernatant was removed, and the pellet was resuspended in 10mL YEPD by inversion. The OD_{600} was measured and cells were shifted to OD_{600} 0.1-0.2 in a final volume of 120mL YEPD and grown to an OD_{600} of approximately 1.

4.8.3. Inhibition of Ypk1-as

When cells had grown to an OD_{600} of approximately 0.7, cells were pre-treated either with 3MB-PP1 (Millipore # 529582, final conc. 10µM) or an equivalent volume of mock (DMSO) for 60 minutes.

4.8.4. Rapamycin Induction

Rapamycin was added to 90mL of logarithmically growing cells at a final concentration of 1µg/mL. The cell culture was then immediately split into two 45mL cultures, referred to as the "no stress" and "stress" cultures, and flasks were returned to the 30°C shaker.

4.8.5. Salt Stress

Five minutes after rapamycin addition, 9mL of 5M NaCl were added to the "stress" culture. At the indicated time points after NaCl addition, 12.5mL of culture were removed from the "no stress" flask, and 15mL were removed from the "stress" flask.

4.8.6. Harvesting

Cells were spun at 2000rpm for 2 minutes and all but 1mL of supernatant were removed. The cells were resuspended in the remaining media and transferred to an Eppendorf tube. Cells were then repelleted by centrifuging at 8000rpm for 20 seconds. The supernatant was removed, and the pellets were immediately frozen in liquid nitrogen. Cell pellets were stored at -80°C for 1-3 days before cell lysis.

4.8.7. Cell Breakage

Cell pellets were thawed on ice in 400-600µL Urea Lysis Buffer (50mM Tris/HCl pH 8, 50mM Sodium Phosphate buffer pH 8, 8M Urea, 0.3M NaCl, 0.5% Nonidet P-40) and transferred to 2mL screwcap tubes with equal amounts of glass beads. The tubes were then shaken in a homogenizer for 45 seconds at a speed of 6.0m/s, and then placed back on ice.

The bottoms of the tubes were then pierced to create a small hole, inserted into Eppendorf tubes, and spun at 3000rpm for 2 minutes at 4°C to transfer the cell lysate from the screwcap tube into the Eppendorf tube. The Eppendorf tubes were then spun again in a microcentrifuge at 13,000rpm and 4°C for 10 minutes. 100µL of supernatant were then transferred into a fresh Eppendorf.

The relative protein concentrations of the cleared cell lysates were determined by measuring the A_{280} using a NanoDrop spectrophotometer. Protein concentrations of the different lysates were equalised by diluting the most highly concentrated lysates in an appropriate amount of

Urea Lysis Buffer. The absolute protein concentration of one lysate was then measured using the Bradford Protein Assay (BioRad) and compared to a BSA standard.
Cleared lysates were then mixed in a 1:1 ratio with 2x Urea Loading Buffer (40mM Tris/HCl pH6.8, 8M Urea, 5% SDS, 0.1µM EDTA, 1% β-mercaptoethanol, bromophenol blue) before being incubated at 95°C for 5 minutes and stored at -20°C.

4.9. Western Blot Analysis

4.9.1. SDS PAGE and Protein Transfer

Solutions used during SDS-PAGE and protein transfer were as follows:

- 4x Resolving Buffer (375mM Tris, 0.4% (w/v) SDS, pH8.8)
- 2x Stacking Buffer (62.5mM Tris, 0.2% (w/v) SDS, pH6.8)
- 40% Acrylamide:N,N′-Methylenebisacrylamide 29:1 solution (Sigma)
- 20% (w/v) APS in ddH_2O (BioRad)
- TEMED (BioRad)
- 1x Running Buffer (25mM Tris, 192mM Glycine, 0.1% (w/v) SDS, pH 8.3)
- 1x Transfer Buffer (25mM Tris, 192mM Glycine, 20% (v/v) methanol, pH 8.0)
- PBST (137mM NaCl, 2.68mM KCl, 10.2mM Na_2HPO_4, 1.76mM KH_2PO_4, 0.05% Tween-20)
- TBST: 25mM Tris/HCl pH 8.0, 150mM NaCl, 0.1% Tween-20)

One 8 and 10% SDS polyacrylamide gel had the following composition:

	Resolving Gel			Stacking Gel
	8%	10%		5%
ddH_2O	4.4 mL	4 mL	ddH_2O	1.5 mL
4x Resolving Buffer	2 mL	2 mL	2x Stacking Buffer	2 mL
40% Acrylamide	1.6mL	2 mL	40% Acrylamide	0.5 mL
20% APS	40 µL	40 µL	20% APS	20 µL
TEMED	3.2 µL	3.2 µL	TEMED	4 µL

Gels were run at 50mA per gel for 1 hour. Proteins were transferred onto 0.2µm nitrocellulose membrane (Amersham Protran) at 250mA per tank for 2.5 hours in Transfer Buffer.

Membranes were washed for 5 minutes in ddH_2O and then were stained for total protein by incubating with PonceauS (Sigma) for 2-3 minutes. Excess PonceauS was removed from the membranes and membranes were washed 2-3 times in ddH_2O to remove unbound Ponceau solution. After the membranes were checked for visual differences in transfer efficiency across the membrane, and for regions of no transfer due to air bubbles, membranes were destained by washing in PBST.

4.9.2. Antibody Incubation Conditions

α-me3 (Novus Biologicals (6F12-H4)):
Membranes were blocked overnight using 2% skimmed milk in PBST. They were incubated with α-me3 (1:2000 in 10% yeast extract/PBST) for 1 hour at 4°C. α-me3 was removed and membranes were incubated with Peroxidase-conjugated goat anti-mouse IgG (Jackson ImmunoResearch, 1:5000 in 10% yeast extract/PBST) for 1 hour at 4°C. Finally, membranes were washed three times for 5 minutes in PBST.

α-HA (Gift from Ogris Lab (12CA5)):
Membranes were blocked overnight using 5% skimmed milk in PBST. They were incubated with α-HA (1:2000 in PBST) for 1 hour at room temperature. α-HA was removed, and membranes were washed three times for 5 minutes in PBST. Membranes were incubated with Peroxidase-conjugated goat anti-mouse IgG (Jackson ImmunoResearch, 1:5000 in PBST) for 1 hour at room temperature before being washed three times for 5 minutes in PBST.

α-V5 (abcam (ab27671)):
Membranes were blocked overnight using 5% skimmed milk in PBST. They were incubated with α-V5 (1:1250 in PBST) for 1 hour at room temperature. α-V5 was removed, and membranes were washed three times for 5 minutes in PBST. Membranes were incubated with Peroxidase-conjugated goat anti-mouse IgG (Jackson ImmunoResearch, 1:5000 in PBST) for 1 hour at room temperature before being washed three times for 5 minutes in PBST.

α-myc (Gift from Ogris Lab (4A6)):
Membranes were blocked overnight using 5% skimmed milk in PBST. They were incubated with α-myc (1:2000 in PBST) for 1 hour at room temperature. α-myc was removed, and membranes were washed three times for 5 minutes in PBST. Membranes were incubated with Peroxidase-conjugated goat anti-mouse IgG (Jackson ImmunoResearch, 1:5000 in PBST) for 1 hour at room temperature before being washed three times for 5 minutes in PBST.

α-pHog1 (Cell Signalling (phospho-p38 (3D7) #9217)):
(In the case of being the first antibody incubation on the blot, membranes were blocked for 1 hour using 5% skimmed milk in TBST). Membranes were incubated with α-pHog1 (1:3000 in 5% milk/TBST) overnight at 4°C. α-pHog1 was removed, and membranes were washed three times for 5 minutes in TBST. Membranes were incubated with Peroxidase-conjugated goat anti-rabbit (Jackson ImmunoResearch, 1:5000 in TBST) for 1 hour at room temperature before being washed three times for 5 minutes in PBST.

α-Cdc28 (Sigma (P7962)):
Membranes were incubated with α-Cdc28 (1:10,000 in 5% BSA/TBST) for 1 hour at room temperature. α-Cdc28 was removed, and membranes were washed three times for 5 minutes in TBST. Membranes were then incubated with Peroxidase-conjugated goat anti-mouse IgG (Jackson ImmunoResearch, 1:5000 in TBST) for 1 hour at room temperature before being washed three times for 5 minutes in TBST.

α-pSlt2 (Cell Signalling (phospho-p42/44 (D13.14.4E) #4370)):
(In the case of being the first antibody incubation on the blot, membranes were blocked for overnight using 5% skimmed milk in TBST). Membranes were incubated with α-Slt2 (1:4000 in 0.5% milk/TBST) for 1 hour at room temperature. α-pSlt2 was removed, and membranes were washed three times for 5 minutes in TBST. Membranes were incubated with Peroxidase-conjugated goat anti-rabbit (Jackson ImmunoResearch, 1:5000 in TBST) for 1 hour at room temperature before being washed three times for 5 minutes in PBST.

4.9.3. Detection of Proteins

Proteins were detected using SuperSignal™ West Chemiluminescent Substrate (Thermo Scientific) according to the standard protocol, and using X-ray films.

4.9.4. Quantification of Blots

Films were scanned at a resolution of 600dpi in greyscale and saved in .tiff format and images were opened in ImageJ. Rectangles encompassing individual bands of interest were created and the density of black pixels within the rectangle was measured. The density measurements of the bands were then used to calculate me3:HA and me3:Cdc28 ratios. The rate of

methylation accumulation was determined by plotting the me:HA or me:Cdc28 ratio against time after rapamycin addition, and calculating the slope the data points.

4.10. Droplet Tests

An overnight culture of cells grown in YEPD was shifted to OD_{600} 0.1-0.2 in a final volume of 5mL YEPD and grown to an OD_{600} of 1. 2mL of cells were centrifuged at 2000rpm for 2 minutes before being resuspended in 2mL 1xTE. Cells were diluted 1:9 in 1xTE to create the starting cell concentration. Three serial dilutions of cells were then created by mixing 100µL of cells with 400µL 1xTE. The calculated cell densities were: 0.1, 0.02, 0.004 and 0.0008. 4µL of each dilution were then dropped onto the indicated plate. Plates were incubated for 2-3 days at 30°C.

4.11. List of yeast strains used

Strain	Genotype	Source
W303-1A	MATa leu2-3,112 trp1-1 his3-11,15 ura3-1 can1-100 ade2-1	Lab collection
yJA227	W303-1A; tor1-1 fpr1::NatMX4	This study
yJA261	W303-1A; tor1-1 fpr1::NatMX4 ste11::KanMX6 Opy2-TEV-FRB-V5::LEU2 ura3-1::YIplac211-Ste11(3A)-2xHA-TEV-2xProteinA-4xH3-3xHA	This study
yJA262	W303-1A; tor1-1 fpr1::NatMX4 ste11::KanMX6 Opy2-TEV-FRB-V5::LEU2 ura3-1::YIplac211-Ste11(3D)-2xHA-TEV-2xProteinA-4xH3-3xHA	This study
yJA281	W303-1A; tor1-1 fpr1::NatMX4 ste11::KanMX6 Opy2-TEV-FRB-V5::LEU2 ura3-1::YIplac211-Ste11(WT)-2xHA-TEV-2xProteinA-4xH3-3xHA	This study
yJA288	W303-1A; tor1-1 fpr1::NatMX4 ste11::KanMX6 msb2::HphMX6 hog1::klTRP1 ura3-1::YIplac211-Ste11(3D)-2xHA-TEV-2xProteinA-4xH3-3xHA leu2-3,112::YIplac128-Msb2-TEV-FRB-V5	This study
yJA293	W303-1A; tor1-1 fpr1::NatMX4 ste11::KanMX6 hog1::klTRP1 Sho1-TEV-FRB-V5::LEU2 ura3-1::YIplac211-Ste11(3A)-2xHA-TEV-2xProteinA-4xH3-3xHA	This study
yJA323	W303-1A; tor1-1 fpr1::NatMX4 ste11::KanMX6 hog1::klTRP1 Sho1-TEV-FRB-V5::LEU2 ura3-1::YIplac211-Ste11(WT)-2xHA-TEV-2xProteinA-4xH3-3xHA	This study
yJA325	W303-1A; tor1-1 fpr1::NatMX4 ste11::KanMX6 hog1::klTRP1 Sho1-TEV-FRB-V5::LEU2 ura3-1::YIplac211-Ste11(3D)-2xHA-TEV-2xProteinA-4xH3-3xHA	This study

yJA340	W303-1A; tor1-1 fpr1::NatMX4 ste11::KanMX6 msb2::HphMX6 hog1::klTRP1 ura3-1::YIplac211-Ste11(3A)-2xHA-TEV-2xProteinA-4xH3-3xHA leu2-3,112::YIplac128-Msb2-TEV-FRB-V5	This study
yJA355	W303-1A; tor1-1 fpr1::NatMX4 Sho1-2xHA-TEV-2xProteinA-4xH3-3xHA::URA3 Msb2-TEV-FRB-V5::LEU2	This study
yJA359	W303-1A; tor1-1 fpr1::NatMX4 Sho1-2xHA-TEV-2xProteinA-4xH3-3xHA::URA3 Opy2-TEV-FRB-V5::LEU2	This study
yJA362	W303-1A; tor1-1 fpr1::NatMX4 Pbs2-4xH3-3xHA::URA3 leu2-3,112::YIplac128-Sho1ΔSH3-TEV-FRB-V5	This study
yJA370	W303-1A; tor1-1 fpr1::NatMX4 Pbs2-4xH3-3xHA::URA3 leu2-3,112::YIplac128-Sho1-TEV-FRB-V5	This study
yJA372	W303-1A; tor1-1 fpr1::NatMX4 Sho1-2xHA-TEV-2xProteinA-4xH3-3xHA::URA3 leu2-3,112::YIplac128-Sho1-TEV-FRB-V5	This study
yJA374	W303-1A; tor1-1 fpr1::NatMX4 Sho1-2xHA-TEV-2xProteinA-4xH3-3xHA::URA3 leu2-3,112::YIplac128-Sho1ΔSH3-TEV-FRB-V5	This study
yJA388	W303-1A; tor1-1 fpr1::NatMX4 sho1::KanMX6 Pbs2-4xH3-3xHA::URA3 leu2-3,112::YIplac128-Sho1ΔSH3-TEV-FRB-V5	This study
yJA390	W303-1A; tor1-1 fpr1::NatMX4 sho1::KanMX6 Pbs2-4xH3-3xHA::URA3 leu2-3,112::YIplac128-Sho1-TEV-FRB-V5	This study
yJA396	W303-1A; tor1-1 fpr1::NatMX4 msb2::HphMX6 Sho1-2xHA-TEV-2xProteinA-4xH3-3xHA::URA3 Opy2-TEV-FRB-V5::LEU2	This study
yJA399	W303-1A; tor1-1 fpr1::NatMX4 ste11::KanMX6 sho1::HphMX6 Opy2-TEV-FRB-V5::LEU2 ura3-1::YIplac211-Ste11(WT)-2xHA-TEV-2xProteinA-4xH3-3xHA	This study

yJA401	W303-1A; tor1-1 fpr1::NatMX4 msb2:HphMX6 Sho1-2xHA-TEV-2xProteinA-4xH3-3xHA::URA3 leu2-3,112::YIplac128-Sho1-TEV-FRB-V5	This study
yJA408	W303-1A; tor1-1 fpr1::NatMX4 msb2::HphMX6 hkr1::KanMX6 Sho1-2xHA-TEV-2xProteinA-4xH3-3xHA::URA3 Opy2-TEV-FRB-V5::LEU2	This study
yJA411	W303-1A; tor1-1 fpr1::NatMX4 msb2::HphMX6 hkr1::KanMX6 Sho1-2xHA-TEV-2xProteinA-4xH3-3xHA::URA3 leu2-3,112::YIplac128-Sho1-TEV-FRB-V5	This study
yJA414	W303-1A; tor1-1 fpr1::NatMX4 hkr1::KanMX6 Sho1-2xHA-TEV-2xProteinA-4xH3-3xHA::URA3 Opy2-TEV-FRB-V5::LEU2	This study
yJA425	W303-1A; tor1-1 fpr1::NatMX4 Ste50-4xH3-3xHA::URA3 Opy2-TEV-FRB-V5::LEU2	This study
yJA427	W303-1A; tor1-1 fpr1::NatMX4 Ste11-4xH3-3xHA::URA3 Opy2-TEV-FRB-V5::LEU2	This study
yJA434	W303-1A; tor1-1 fpr1::NatMX4 sho1::HpHMX6 Ste50-4xH3-3xHA::URA3 Opy2-TEV-FRB-V5::LEU2	This study
yJA439	W303-1A; tor1-1 fpr1::NatMX4 msb2::KanMX6 hkr1::HphMX6 Ste11-4xH3-3xHA::URA3 Opy2-TEV-FRB-V5::LEU2	This study
yJA459	W303-1A; tor1-1 fpr1::NatMX4 msb2::KanMX6 hkr1::HphMX6 sho1::klTRP1 Ste11-4xH3-3xHA::URA3 Opy2-TEV-FRB-V5::LEU2	This study
yJA461	W303-1A; tor1-1 fpr1::NatMX4 msb2::KanMX6 hkr1::HphMX6 Ste11-4xH3-3xHA::URA3 Opy2-TEV-FRB-V5::LEU2 trp1-1::YIplac204(empty)	This study
yJA467	W303-1A; tor1-1 fpr1::NatMX4 Opy2-4xH3-3xHA::URA3 Msb2-TEV-FRB-V5::LEU2	This study
yJA482	W303-1A; tor1-1 fpr1::NatMX4 ste20::HphMX6 Ste11-4xH3-3xHA::URA3 Opy2-TEV-FRB-V5::LEU2	This study
yJA492	W303-1A; tor1-1 fpr1::NatMX4 ste50::HphMX6 Ste11-4xH3-3xHA::URA3 Opy2-TEV-FRB-V5::LEU2	This study

yJA516	W303-1A; ssk2::NatMX4 ssk22::NatMX4 tor1-1 fpr1::HphMX6 hkr1::klTRP1	This study
yJA527	W303-1A; tor1-1 fpr1::NatMX4 msb2::KanMX6 hkr1::HphMX6 sho1 Ste11-4xH3-3xHA:: Opy2-TEV-FRB-V5::LEU2	This study
yJA532	W303-1A; ssk2::NatMX4 ssk22::NatMX4 tor1-1 fpr1::HphMX6 hkr1::klTRP1 Sho1-9xmyc-FKBP::HIS3MX6 Opy2-TEV-FRB-V5::LEU2	This study
yJA543	W303-1A; ssk2::NatMX4 ssk22::NatMX4 tor1-1 fpr1::HphMX6 hkr1::klTRP1 msb2::URA3	This study
yJA552	W303-1A; tor1-1 fpr1::NatMX4 msb2::KanMX6 hkr1::HphMX6 sho1 ypk2::URA3 Ypk1-as(L424A) Ste11-4xH3-3xHA:: Opy2-TEV-FRB-V5::LEU2	This study
yJA565	W303-1A; tor1-1 fpr1::NatMX4 msb2::KanMX6 hkr1::HphMX6 sho1 cnb1::URA3 Ste11-4xH3-3xHA:: Opy2-TEV-FRB-V5::LEU2	This study
yJA582	W303-1A; ssk2::NatMX4 ssk22::NatMX4 tor1-1 fpr1::HphMX6 hkr1::klTRP1 msb2::URA3 Sho1-9xmyc-FKBP::HIS3MX6 Opy2-TEV-FRB-V5::LEU2	This study
yJA613	W303-1A; tor1-1 fpr1::NatMX4 opy2::HphMX6 Sho1-2xHA-TEV-2xProteinA-4xH3-3xHA::URA3 leu2-3,112::YIplac128-Sho1-TEV-FRB-V5	This study

4.12. List of plasmids used

Plasmid	Description	Source
pJA48	PCR template for inserting C-terminal H3HA tag at native locus; GAfw-2xHA-TEV-2xProteinA-4xH3-3xHA::URA3-GAre	This study
pJA97	PCR template for inserting C-terminal H3HA tag at native locus; GAfw-4xH3-3xHA::URA3-GAre	This study
pJA36	PCR template for inserting C-terminal FRB tag at native locus; GAfw-TEV-FRB-V5::LEU2-GAre	This study
pJA103	YIplac128-P_{SHO1}-Sho1ΔSH3-TEV-FRB-V5 (LEU2, integrative plasmid)	This study
pJA104	YIplac128-P_{SHO1}-Sho1-TEV-FRB-V5 (LEU2, integrative plasmid)	This study
pCK911	pRS413-P_{ADH1}-FKBP-mycHKMT (HIS3, CEN)	Brezovich *et al.* (2015)
pAX50	PCR template for replacing Ypk1 knockout cassette with analogue-sensitive ORF BG1805 Ypk1-as(L424A)	Muir *et al.* (2014)
pJA92	YIplac211-P_{STE11}-Ste11-2xHA-TEV-2xProteinA-4xH3-3xHA (URA3, integrative plasmid)	This study
pJA82	YIplac211-P_{STE11}-Ste11(S281D,S285D,S286D)-2xHA-TEV-2xProteinA-4xH3-3xHA (URA3, integrative plasmid)	This study
pJA80	YIplac211-P_{STE11}-Ste11(S281A,S285A,S286A)-2xHA-TEV-2xProteinA-4xH3-3xHA (URA3, integrative plasmid)	This study
pJA91	YIplac128-P_{MSB2}-Msb2-TEV-FRB-V5 (LEU2, integrative plasmid)	This study
pGA2259	PCR template for replacing ORFs with G418 resistance marker;	Lab collection

	GAfw-KanMX6-GAre	
pJA46	PCR template for replacing ORFs with Hygromycin resistance marker; GAfw-HphMX6-GAre	This study
pGA2264	PCR template for replacing ORFs with Kluyveromyces lactis tryptophan auxotrophic marker; GAfw-klTrp1-GAre	Lab collection
pJA41	PCR template for replacing ORFs with nourseothricin resistance marker; GAfw-NatMX4-GAre	This study
pJA143	PCR template for replacing ORFs with uracil auxotrophic marker, including 50nt up- and downstream homology to *Sho1* locus; $50ntP_{SHO1}$-GAfw-URA3-GAre-$50ntT_{SHO1}$	This study
pJA140	PCR template for inserting C-terminal FKBP tag at native locus; GAfw-9xMyc-FKBP::HIS3MX6-GAre	This study
YIplac204	Empty Integrative Vector *(TRP1)*	Lab collection
pJA110	PCR template for replacing Sho1 ORF with Hygromycin resistance marker, cut with AccI and BsrGI prior to transformation; $736ntP_{SHO1}$-GAfw-HphMX6-GAre-$595ntT_{SHO1}$	This study

4.13. List of primers used

Name	**5'-3' Sequence**	
RmvURAFw	ttcaattcatcatttttttttattctttttttgatttcggttt/tcaatttaattatatcagttattaccctatgcggtgtgaaatacc	
RmvURARe	ggtatttcacaccgcatagggtaataactgatataattaaattga/aaaccgaaatcaaaaaaaagaataaaaaaaaaatgatgaattgaa	
tor1-1_mut_fw	TCTATGGCACGAATTATGGTATGAAGGACTGGAAGATGCGCGCCGCCAATTTTTCGTTGAACATAACATAGAAAAAATGTT	
tor1-1_mut_re	AACATTTTTTCTATGTTATGTTCAACGAAAAATTGGCGGCGCGCATCTTCCAGTCCTTCATACCATAATTCGTGCCATAGA	
tor1-1 seq fw	TCCTACGGTGAGTAATTCCC	
tor1-1 seq re	GGGGAGAAACATGCTGTAAG	
For amplification of tagging cassettes		
Ste50-ctag-fw	GATGAACGGAAGTGACAATGTCACCCCCGGTGGAAGACTCtccggttctgctgctag	
Ste50-ctag/ko-re	CGTGTAAGTTTAGTATGATGATGTGCATGACAACTGCACAcctcgaggccagaagac	
Ste11-ctag-fw	TGAATTGCTGCAGCATCCATGGCTGGATGCACACATAATTtccggttctgctgctag	
Ste11-ctag/ko-re	CACTTTAGTGCCATAAAAAGAATTAATAAGTAGCCCTTTTcctcgaggccagaagac	
Pbs2-ctag-fw	GTGAGAATGGTTTATCTAAAAATGTACCGGCATTACATATGGGTGGTTTAtccggttctgctgctag	
Pbs2-ctag/ko-re	TATATTCACGTGCCTGTTTGCTTTTATTTGGATATTAACGcctcgaggccagaagac	

Sho1-ctag60-fw	ACAGGTATTATTCCAAGCAATTATGTTCAACTAATCGATGGTCCAGAAGAAATGCATC GT/tccggttctgctgctag	
Sho1-ctag/ko60-re	GATAGGTTTCTTTATTTTTTTCCTTTGACTCGAGAATCCATGCTATAAGATTGTTAATCA /cctcgaggccagaagac	
Msb2-ctag60-fw	TCCATACCAAAAATTTCAAGACCAATTGCTAGCCAAAACTCCCTGGGTTGGAACGAAG TTtccggttctgctgctag	
Msb2-ctag/ko60-re	AGGTATCGTTATAAGTTTATAAGGTTATGCAAGCGGAGAAAGTCTCTGCAGACATTGC TAcctcgaggccagaagac	
Opy2-ctag-fw	GAGCCCGTTTGAGGACAAGTTCGAAATACACGATGAACGAtccggttctgctgctag	
Opy2-ctag/ko-re	TATTTTCCCCGGGATTGCAGAATACTGACACGCCTTTTATcctcgaggccagaagac	
For verification of successful C-terminal tagging		
RevAnUp	ctagcagcagaaccgga	
cSte50-fw	CAACAGCGAACACACCGGGGCCATC	
cSte50-re	GGCCAAGCCAATTTCAAATATAG	
cSte11-fw	GGTTCCGTATTCTGGATGTCACCAG	
cSte11-re	TATTCATGTGAATGAAACTCTATGG	
cPbs2-fw	CGCTCAATTGAGAGAAAATGTTGTC	
cPbs2-re	TCAGACAATTCCAGAGCATTTTTTC	
cSho1-fw	CTACGATGGGAGACACTTTGGGTCTG	
cSho1-re	GGTGTCATCGCTAATCCTAAGGGTG	
cMsb2-fw	GCTTTCAAGTATATCATAAGAAGGCGG	
cMsb2-re	CATGAAAGGCCTGCAGTCTAAC	

cOpy2-fw	CCAGGTACTCAATAAGGACGCAGACG	
cOpy2-re	GCAAGTTTGCTGTATTTTAGTCCCG	
For amplification of knockout cassettes		
Ste50-ko-fw	CGAAAAGACAGAGGTCGTACTAGCAGAGATAGCAAATCAGtccggttctgctgctag	
Ste50-ctag/ko-re	see above	
Ste20-ko-fw	CATCCTAAATATCCCACAAGATCCTCGACTAATACAAGAAtccggttctgctgctag	
Ste20-ctag/ko-re	TATACTTTGTCGATAATAAGGTGTACCCTGCTTGCTACGTcctcgaggccagaagac	
Ste11-ko-fw	TAAAGCTAGTATGATAAGATCACCGGTAGACGAAATATACtccggttctgctgctag	
Ste11-ctag/ko-re	see above	
Fpr1-GAko-fw	CTTTCACCTAAACTCGAGTATAAGCAAAAAATCAATCAAAACAAGTAATAtccggttctgctgctag	
Fpr1-GAko-re	TAAACATAAATAAAAAGCAGAAAGGCGGCTCAATTGATAGTACTTTGCTTCcctcgaggccagaagac	
Sho1-ko-fw	GCCATCTTTTCAGAAACACCAAAAATCACGTTTTCAAAATtccggttctgctgctag	
Sho1-ctag/ko-re	see above	
Msb2-ko-fw	TTTATTGACTTTTCATTAGGCTTCCTAATTATACCCATCTtccggttctgctgctag	
Msb2-ctag/ko60-re	see above	
Hkr1-ko-fw	ACTGACGCAGTCAACAGTCAGAAACAGAGAATGTATAAAGtccggttctgctgctag	
Hkr1-ko-re	TTCCAGCAGCGTTTATTGCACAGTCAATAATCATTTTTCGcctcgaggccagaagac	
Opy2-ko-fw	AACAGCGGTGGTATGTTCCG	
Opy2-ctag/ko-re	see above	
Ssk2-ko-fw	AAGAGAAGCCTTTGCGTAAACTATTTGACAGGCACAAATAtccggttctgctgctag	

Ssk2-ko-re	TTTGATTTTACATATAATACAACAAACCTTCTCAACTTAAcctcgaggccagaagac	
Ssk22-ko-fw	ACTTAGGGTGGCTATAAAAGGTAGTTCCTTGTAGGTGAAAtccggttctgctgctag	
Ssk22-ko-re	TATATATCGTAGTATATCATATTTTTAGACGTTGACCACTcctcgaggccagaagac	
Hog1-ko-fw	AAAGGGAAAACAGGGAAAACTACAACTATCGTATATAATA/tccggttctgctgctag	
Hog1-ko-re	GAAGTAAGAATGAGTGGTTAGGGACATTAAAAAAACACGT/cctcgaggccagaagac	
Ypk1-ko-ins-fw	cacataaggagattagtaaagaagtagatgctttaattgcacaactgtcc/tccggttctgctgctag	
Ypk1-ko-ins-re	atgtccaccaatctactgcctttgtatagcctaaacctagcaatagttct/cctcgaggccagaagac	
Gib.Ypk1.ORFins-fw	ggaagaacagcagaataatcaagc	
Gib.Ypk1.ORFins-re	ctaatgcttctaccttgcacc	
Ypk2-ko-fw	CTAAACCAGAATTGTTCAACTGGGTCAAATTATCGCGTATACAAATATACATATAGTAA Ctccggttctgctgctag	
Ypk2-ko-re	CCTCTTGCGGCTATAGCTATAAATTCCGTCCGGCTCGGCTCGGCTTGCTTCGGCTTG CTTcctcgaggccagaagac	
Cnb1-ko-fw	AGCTAAAACTTGGTAACTCAATGGTGATCAGAATCCATAGAAGCATTTTTATTTCTTAA Atccggttctgctgctag	
Cnb1-ko-re	ATTATTCTTCTTTTCTTAAAAATATTGGCATACCATAAATGAATGAAGTGTCCCCTAGTC cctcgaggccagaagac	
For verification of successful gene deletion		
RevAnUp	see above	
Trp1RevAnUp	ggaggagtagagactgatggtatc	

cSte50-ko-fw	GCAACTGTTTCCAGCCTTCAC	
cSte50-ko-re	AGCCTTGTGTACTGCGATTG	
cSte20-ko-fw	ACTACGAACACTGTGGCAGG	
cSte20-ko-re	CAGAGGAGGAAGATACTCGGG	
cSte11-ko-fw	ACGGTGCTGGTCTTCGATAC	
cSte11-ko-re	AGCAGTGGATAGAGAGCTTAC	
cFpr1-ko-fw	AGAGTACGGTGCAGATGAAC	
cFpr1-ko-re2	CGCGATAATAAACGCTCATCC	
cSho1-ko-fw	CTCCATTGAGAGGCAAGAGC	
cSho1-ko-re	TTGGGACCATCCGCATACAC	
cMsb2-ko-fw	GCTACGTGGACGAACTGGTG	
cMsb2-ko-re	TGGGAAGTGGAGCTCGCATC	
cHkr1-fw	GCCGAGTGGTTAAGGCGAAAG	
cHkr1-ko-re	GGGTGGGTACAATGCTACTAC	
cOpy2-ko-fw	AACAGCGGTGGTATGTTCCG	
cOpy2-ko-re	GATGCCTCTTCCAATTTCAAAGC	
cSsk2-ko-fw	CTGTGACAGGGGTCTGAATG	
cSsk2-ko-re	TGACCTTGAGGTATACCCGG	
cSsk22-ko-fw	CCCCACCGTACATCGTCTCG	
cSsk22-ko-re	TGAGTTTTATGCCCCTCGTG	
cHog1-ko-fw	TGCACTGCTGTCTTCACTTC	
cHog1-ko-re	CTGTTCCTTGTAATTCCGTGAC	
cYpk1-ko-ins-fw	cgatgcatcctcatcgacc	

cYpk1-ko-ins-re	ctttctttctgacttgcatcac	
cYpk2-ko-fw	CACAGATTTGGACGGTTCTG	
cYpk2-ko-re	TCAGTAGACGACTGACTAGC	
cCnb1-ko-fw	ACGCCATTGATGAAATCGAG	
cCnb1-ko-re	CTCTTGAAAATCCACGTCCC	

5. References

Albertyn, J. et al., 1994. GPD1, which encodes glycerol-3-phosphate dehydrogenase, is essential for growth under osmotic stress in Saccharomyces cerevisiae, and its expression is regulated by the high-osmolarity glycerol response pathway. *Molecular and Cellular Biology*, 14(6), pp.4135–4144. Available at: http://mcb.asm.org/lookup/doi/10.1128/MCB.14.6.4135.

Bacia, K., Kim, S.A. & Schwille, P., 2006. Fluorescence cross-correlation spectroscopy in living cells. *Nature Methods*, 3(2), pp.83–89.

Balleza, E., Kim, J.M. & Cluzel, P., 2018. Systematic characterization of maturation time of fluorescent proteins in living cells. *Nature Methods*, 15(1), pp.47–51.

Berchtold, D. et al., 2012. Plasma membrane stress induces relocalization of Slm proteins and activation of TORC2 to promote sphingolipid synthesis. *Nature Cell Biology*, 14(5), pp.542–547. Available at: http://www.nature.com/doifinder/10.1038/ncb2480.

Bose, I. et al., 2001. Assembly of scaffold-mediated complexes containing Cdc42p, the exchange factor Cdc24p, and the effector Cla4p required for cell cycle-regulated phosphorylation of Cdc24p. *The Journal of biological chemistry*, 276(10), pp.7176–86. Available at: http://www.ncbi.nlm.nih.gov/pubmed/11113154 [Accessed December 2, 2014].

Brewster, J.L. et al., 1993. An osmosensing signal transduction pathway in yeast. *Science (New York, N.Y.)*, 259(5102), pp.1760–1763.

Brewster, J.L. & Gustin, M.C., 2014. Hog1: 20 years of discovery and impact. *Science Signaling*, 7(343), pp.re7-re7. Available at: http://stke.sciencemag.org/cgi/doi/10.1126/scisignal.2005458 [Accessed September 17, 2014].

Brezovich, A. et al., 2015. An in vivo detection system for transient and low abundant protein interactions and their kinetics in budding yeast. *Yeast*, 32, pp.355–365.

Chen, R.E. & Thorner, J., 2007. Function and regulation in MAPK signaling pathways: Lessons learned from the yeast Saccharomyces cerevisiae. *Biochimica et Biophysica Acta (BBA) - Molecular Cell Research*, 1773(8), pp.1311–1340. Available at: http://linkinghub.elsevier.com/retrieve/pii/S0167488907001218 [Accessed August 14, 2014].

Choi, J. et al., 1996. Structure of the FKBP12-Rapamycin Complex Interacting with Binding Domain of Human FRAP. *Science*, 273(5272), pp.239–242. Available at: http://www.sciencemag.org/cgi/doi/10.1126/science.273.5272.239 [Accessed July 9, 2014].

Cuadrado, A. & Nebreda, A.R., 2010. Mechanisms and functions of p38 MAPK signalling. *Biochemical Journal*, 429(3), pp.403–417. Available at: http://biochemj.org/lookup/doi/10.1042/BJ20100323.

Cullen, P.J. et al., 2004. A signaling mucin at the head of the Cdc42- and MAPK-dependent filamentous growth pathway in yeast. *Genes & development*, 18(14), pp.1695–708. Available

at:
http://www.pubmedcentral.nih.gov/articlerender.fcgi?artid=478191&tool=pmcentrez&rendertype=abstract [Accessed July 30, 2014].

Cyert, M.S., 2003. Calcineurin signaling in Saccharomyces cerevisiae: how yeast go crazy in response to stress. *Biochemical and Biophysical Research Communications*, 311(4), pp.1143–1150. Available at: http://linkinghub.elsevier.com/retrieve/pii/S0006291X03015523 [Accessed October 20, 2014].

Cyert, M.S., 2001. Genetic analysis of calmodulin and its targets in Saccharomyces cerevisiae. *Annual review of genetics*, 35, pp.647–72. Available at: http://www.ncbi.nlm.nih.gov/pubmed/11700296.

Denis, V. & Cyert, M.S., 2002. Internal Ca2+ release in yeast is triggered by hypertonic shock and mediated by a TRP channel homologue. *Journal of Cell Biology*, 156(1), pp.29–34.

Dohnal, I., 2005. Characterization of signal-transducing protein complexes in Saccharomyces cerevisiae.

van Drogen, F. et al., 2000. Phosphorylation of the MEKK Ste11p by the PAK-like kinase Ste20p is required for MAP kinase signaling in vivo. *Current biology : CB*, 10(11), pp.630–9. Available at: http://www.ncbi.nlm.nih.gov/pubmed/10837245.

Ekiel, I. et al., 2009. Binding the atypical RA domain of Ste50p to the unfolded Opy2p cytoplasmic tail is essential for the high-osmolarity glycerol pathway. *Molecular biology of the cell*, 20(24), pp.5117–26. Available at: http://www.pubmedcentral.nih.gov/articlerender.fcgi?artid=2793289&tool=pmcentrez&rendertype=abstract.

Ferrigno, P. et al., 1998. Regulated nucleo/cytoplasmic exchange of HOG1 MAPK requires the importin ?? homologs NMD5 and XPO1. *EMBO Journal*, 17(19), pp.5606–5614.

Friedmann, C., 2010. Signalling in space and time: Catching dynamic interactions using a novel enzymatic tagging approach in the S. cerevisiae HOG pathway.

Hao, N. et al., 2007. A systems-biology analysis of feedback inhibition in the Sho1 osmotic-stress-response pathway. *Current biology : CB*, 17(8), pp.659–67. Available at: http://www.ncbi.nlm.nih.gov/pubmed/17363249 [Accessed June 11, 2014].

Hao, N. et al., 2008. Control of MAPK specificity by feedback phosphorylation of shared adaptor protein Ste50. *The Journal of biological chemistry*, 283(49), pp.33798–33802. Available at: http://www.pubmedcentral.nih.gov/articlerender.fcgi?artid=2662209&tool=pmcentrez&rendertype=abstract [Accessed May 22, 2014].

Helliwell, S.B. et al., 1998. The Rho1 effector Pkc1, but not Bni1, mediates signalling from Tor2 to the actin cytoskeleton. *Current Biology*, 8(22), pp.1211-S2. Available at: http://www.sciencedirect.com/science/article/pii/S0960982207005118.

Hersen, P. et al., 2008. Signal processing by the HOG MAP kinase pathway. , 105(20).

Hu, C.-D. & Kerppola, T.K., 2003. Simultaneous visualization of multiple protein interactions in living cells using multicolor fluorescence complementation analysis. *Nature Biotechnology*, 21(5), pp.539–545. Available at: https://www.nature.com/articles/nbt816.

Johnsson, N. & Varshavsky, A., 1994. Split ubiquitin as a sensor of protein interactions in vivo. *Proceedings of the National Academy of Sciences*, 91(22), pp.10340–10344. Available at: http://www.pnas.org/cgi/doi/10.1073/pnas.91.22.10340.

Kim, D.I. et al., 2016. An improved smaller biotin ligase for BioID proximity labeling. *Molecular Biology of the Cell*, 27(8), pp.1188–1196.

Lamson, R.E. et al., 2006. Dual role for membrane localization in yeast MAP kinase cascade activation and its contribution to signaling fidelity. *Current biology : CB*, 16(6), pp.618–23. Available at: http://www.ncbi.nlm.nih.gov/pubmed/16546088 [Accessed June 25, 2014].

Lamson, R.E., Winters, M.J. & Pryciak, P.M., 2002. Cdc42 Regulation of Kinase Activity and Signaling by the Yeast p21-Activated Kinase Ste20. *Molecular and Cellular Biology*, 22(9), pp.2939–2951. Available at: http://mcb.asm.org/cgi/doi/10.1128/MCB.22.9.2939-2951.2002 [Accessed January 12, 2015].

Leberer, E. et al., 1997. Functional characterization of the Cdc42p binding domain of yeast Ste20p protein kinase. *The EMBO journal*, 16(1), pp.83–97. Available at: http://www.pubmedcentral.nih.gov/articlerender.fcgi?artid=1169616&tool=pmcentrez&rendertype=abstract [Accessed January 13, 2015].

Levin, D.E., 2011. Regulation of cell wall biogenesis in Saccharomyces cerevisiae: The cell wall integrity signaling pathway. *Genetics*, 189(4), pp.1145–1175.

Macia, J. et al., 2009. Dynamic signaling in the Hog1 MAPK pathway relies on high basal signal transduction. *Science signaling*, 2(63), p.ra13. Available at: http://www.ncbi.nlm.nih.gov/pubmed/19318625 [Accessed November 5, 2014].

Maeda, T., Takekawa, M. & Saito, H., 1995. Activation of yeast PBS2 MAPKK by MAPKKKs or by binding of an SH3-containing osmosensor. *Science (New York, N.Y.)*, 269(5223), pp.554–8. Available at: http://www.ncbi.nlm.nih.gov/pubmed/7624781 [Accessed October 31, 2014].

Maeda, T., Tsai, a Y. & Saito, H., 1993. Mutations in a protein tyrosine phosphatase gene (PTP2) and a protein serine/threonine phosphatase gene (PTC1) cause a synthetic growth defect in Saccharomyces cerevisiae. *Molecular and cellular biology*, 13(9), pp.5408–5417.

Maeda, T., Wurgler-Murphy, S.M. & Saito, H., 1994. A two-component system that regulates an osmosensing MAP kinase cascade in yeast. *Nature*, 369, pp.242–245.

Maeder, C.I. et al., 2007. Spatial regulation of Fus3 MAP kinase activity through a reaction-diffusion mechanism in yeast pheromone signalling. *Nature cell biology*, 9(11), pp.1319–1326.

Magliery, T.J. et al., 2005. Detecting protein-protein interactions with a green fluorescent protein fragment reassembly trap: Scope and mechanism. *Journal of the American Chemical Society*, 127(1), pp.146–157.

Marles, J. a. et al., 2004. Protein-protein interaction affinity plays a crucial role in controlling the Sho1p-mediated signal transduction pathway in yeast. *Molecular Cell*, 14(6), pp.813–823.

Martínez-Montañés, F., Pascual-Ahuir, A. & Proft, M., 2010. Toward a Genomic View of the Gene Expression Program Regulated by Osmostress in Yeast. *Omics : a journal of integrative biology*, 14(6), pp.619–627.

Mendoza, I. et al., 1994. The protein phosphatase calcineurin is essential for NaCl tolerance of Saccharomyces cerevisiae. *The Journal of biological chemistry*, 269(12), pp.8792–6. Available at: http://www.ncbi.nlm.nih.gov/pubmed/8132612 [Accessed October 21, 2014].

Muir, A. et al., 2015. Down-regulation of TORC2-Ypk1 signaling promotes MAPK-independent survival under hyperosmotic stress. *eLife*, 4(AUGUST2015), pp.1–13.

Mulet, J.M. et al., 2006. Mutual antagonism of target of rapamycin and calcineurin signaling. *Journal of Biological Chemistry*, 281(44), pp.33000–33007.

de Nadal, E., Alepuz, P.M. & Posas, F., 2002. Dealing with osmostress through MAP kinase activation. *EMBO reports*, 3(8), pp.735–40. Available at: http://www.pubmedcentral.nih.gov/articlerender.fcgi?artid=1084212&tool=pmcentrez&rendertype=abstract.

de Nadal, E., Ammerer, G. & Posas, F., 2011. Controlling gene expression in response to stress. *Nature Publishing Group*, 12(12), pp.833–845. Available at: http://dx.doi.org/10.1038/nrg3055.

de Nadal, E., Real, F.X. & Posas, F., 2007. Mucins, osmosensors in eukaryotic cells? *Trends in Cell Biology*, 17(12), pp.571–574.

Phizicky, E.M. & Fields, S., 1995. Protein-protein interactions: methods for detection and analysis. *Microbiological reviews*, 59(1), pp.94–123. Available at: http://www.pubmedcentral.nih.gov/articlerender.fcgi?artid=239356&tool=pmcentrez&rendertype=abstract.

Posas, F. et al., 1996. Yeast HOG1 MAP kinase cascade is regulated by a multistep phosphorelay mechanism in the SLN1-YPD1-SSK1 “two-component” osmosensor. *Cell*, 86, pp.865–875.

Posas, F. & Saito, H., 1997. Osmotic Activation of the HOG MAPK Pathway via Ste11p MAPKKK: Scaffold Role of Pbs2p MAPKK. *Science*, 276(5319), pp.1702–1705. Available at: http://www.sciencemag.org/cgi/doi/10.1126/science.276.5319.1702 [Accessed January 8, 2015].

Posas, F., Takekawa, M. & Saito, H., 1998. Signal transduction by MAP kinase cascades in budding yeast. *Current opinion in microbiology*, 1(2), pp.175–182.

Posas, F., Witten, E.A. & Saito, H., 1998. Requirement of STE50 for Osmostress-Induced Activation of the STE11 Mitogen-Activated Protein Kinase Kinase Kinase in the High-Osmolarity Glycerol Response Pathway Requirement of STE50 for Osmostress-Induced Activation of the STE11 Mitogen-Activated Prote. , pp.1–10.

Raitt, D.C., Posas, F. & Saito, H., 2000. Yeast Cdc42 GTPase and Ste20 PAK-like kinase regulate

Sho1-dependent activation of the Hog1 MAPK pathway. , 19(17), pp.4623–4631.

Reiser, V., Salah, S.M. & Ammerer, G., 2000. Polarized localization of yeast Pbs2 depends on osmostress, the membrane protein Sho1 and Cdc42. *Nature cell biology*, 2(9), pp.620–7. Available at: http://www.ncbi.nlm.nih.gov/pubmed/10980703.

Roelants, F.M. et al., 2011. Protein kinase Ypk1 phosphorylates regulatory proteins Orm1 and Orm2 to control sphingolipid homeostasis in Saccharomyces cerevisiae. *Proceedings of the National Academy of Sciences*, 108(48), pp.19222–19227. Available at: http://www.pnas.org/cgi/doi/10.1073/pnas.1116948108.

Roux, K.J., Kim, D.I. & Burke, B., 2013. BioID : A Screen for Protein-Protein Interactions. *Current Protocols in Protein Science*, 74(1), p.19.23.1-19.23.14.

Saito, H. & Posas, F., 2012. Response to hyperosmotic stress. *Genetics*, 192(2), pp.289–318. Available at: http://www.pubmedcentral.nih.gov/articlerender.fcgi?artid=3454867&tool=pmcentrez&rendertype=abstract [Accessed May 26, 2014].

Schmidt, A. et al., 1997. The yeast phosphatidylinositol kinase homolog TOR2 activates RHO1 and RHO2 via the exchange factor ROM2. *Cell*, 88(4), pp.531–542.

Slaughter, B.D., Schwartz, J.W. & Li, R., 2007. Mapping dynamic protein interactions in MAP kinase signaling using live-cell fluorescence fluctuation spectroscopy and imaging. *Proceedings of the National Academy of Sciences of the United States of America*, 104(51), pp.20320–20325. Available at: http://www.pubmedcentral.nih.gov/articlerender.fcgi?artid=2154429%7B%7B%7D%7B&%7D%7B%7D%7Dtool=pmcentrez%7B%7B%7D%7B&%7D%7B%7D%7Drendertype=abstract%5Cnhttp://www.pubmedcentral.nih.gov/articlerender.fcgi?artid=2154429%7B&%7Dtool=pmcentrez%7B&%7Drendertype.

Stagljar, I. et al., 1998. A genetic system based on split-ubiquitin for the analysis of interactions between membrane proteins in vivo. *Proceedings of the National Academy of Sciences of the United States of America*, 95(9), pp.5187–92. Available at: http://www.ncbi.nlm.nih.gov/pubmed/9560251.

Tanaka, K. et al., 2014. Yeast osmosensors hkr1 and msb2 activate the hog1 MAPK cascade by different mechanisms. *Science signaling*, 7, p.ra21. Available at: http://www.ncbi.nlm.nih.gov/pubmed/24570489.

Tatebayashi, K. et al., 2006. Adaptor functions of Cdc42, Ste50, and Sho1 in the yeast osmoregulatory HOG MAPK pathway. *The EMBO journal*, 25(13), pp.3033–44. Available at: http://www.pubmedcentral.nih.gov/articlerender.fcgi?artid=1500976&tool=pmcentrez&rendertype=abstract [Accessed May 30, 2014].

Tatebayashi, K. et al., 2015. Osmosensing and scaffolding functions of the oligomeric four-transmembrane domain osmosensor Sho1. *Nature Communications*, 6, p.6975. Available at:

http://www.nature.com/doifinder/10.1038/ncomms7975.

Tatebayashi, K. et al., 2007. Transmembrane mucins Hkr1 and Msb2 are putative osmosensors in the SHO1 branch of yeast HOG pathway. *The EMBO journal*, 26(15), pp.3521–3533. Available at: http://www.pubmedcentral.nih.gov/articlerender.fcgi?artid=1949007&tool=pmcentrez&rendertype=abstract [Accessed May 21, 2014].

Tatebayashi, K., Takekawa, M. & Saito, H., 2003. A docking site determining specificity of Pbs2 MAPKK for Ssk2/Ssk22 MAPKKKs in the yeast HOG pathway. *The EMBO journal*, 22(14), pp.3624–34. Available at: http://www.pubmedcentral.nih.gov/articlerender.fcgi?artid=165623&tool=pmcentrez&rendertype=abstract [Accessed October 29, 2014].

Torggler, R. et al., 2016. Two Independent Pathways within Selective Autophagy Converge to Activate Atg1 Kinase at the Vacuole. *Molecular Cell*, 64(2), pp.221–235.

Truckses, D.M., Bloomekatz, J.E. & Thorner, J., 2006. The RA Domain of Ste50 Adaptor Protein Is Required for Delivery of Ste11 to the Plasma Membrane in the Filamentous Growth Signaling Pathway of the Yeast Saccharomyces cerevisiae The RA Domain of Ste50 Adaptor Protein Is Required for Delivery of Ste11 to t.

Vadaie, N. et al., 2008. Cleavage of the signaling mucin Msb2 by the aspartyl protease Yps1 is required for MAPK activation in yeast. *Journal of Cell Biology*, 181(7), pp.1073–1081.

Wagner, E.F. & Nebreda, Á.R., 2009. Signal integration by JNK and p38 MAPK pathways in cancer development. *Nature Reviews Cancer*, 9(8), pp.537–549. Available at: http://dx.doi.org/10.1038/nrc2694.

Warmka, J. et al., 2001. Ptc1, a type 2C Ser/Thr phosphatase, inactivates the HOG pathway by dephosphorylating the mitogen-activated protein kinase Hog1. *Molecular and cellular biology*, 21(1), pp.51–60.

Wu, C. et al., 2006. Adaptor protein Ste50p links the Ste11p MEKK to the HOG pathway through plasma membrane association. *Genes & development*, 20(6), pp.734–46. Available at: http://www.pubmedcentral.nih.gov/articlerender.fcgi?artid=1413288&tool=pmcentrez&rendertype=abstract [Accessed November 5, 2014].

Wu, C. et al., 1999. Functional characterization of the interaction of Ste50p with Ste11p MAPKKK in Saccharomyces cerevisiae. *Molecular biology of the cell*, 10(7), pp.2425–40. Available at: http://www.pubmedcentral.nih.gov/articlerender.fcgi?artid=25464&tool=pmcentrez&rendertype=abstract [Accessed December 1, 2014].

Wu, C. et al., 1995. Molecular Characterization of Ste20p, a Potential Mitogen-activated Protein or Extracellular Signal-regulated Kinase Kinase (MEK) Kinase Kinase from Saccharomyces cerevisiae. *Journal of Biological Chemistry*, 270(27), pp.15984–15992. Available at: http://www.jbc.org/cgi/doi/10.1074/jbc.270.27.15984 [Accessed January 9, 2015].

Wurgler-Murphy, S.M. et al., 1997. Regulation of the Saccharomyces cerevisiae HOG1 mitogen-activated protein kinase by the PTP2 and PTP3 protein tyrosine phosphatases. *Molecular and cellular biology*, 17(3), pp.1289–1297.

Yakovlev, A.A., 2009. Crosslinkers and their utilization for studies of intermolecular interactions. *Neurochemical Journal*, 3(2), pp.139–144. Available at: http://link.springer.com/10.1134/S181971240902010X.

Yamamoto, K. et al., 2010. Dynamic control of yeast MAP kinase network by induced association and dissociation between the Ste50 scaffold and the Opy2 membrane anchor. *Molecular cell*, 40(1), pp.87–98. Available at: http://www.ncbi.nlm.nih.gov/pubmed/20932477 [Accessed May 28, 2014].

Yamamoto, K., Tatebayashi, K. & Saito, H., 2015. Binding of the extracellular eight-cysteine motif of Opy2 to the putative osmosensor Msb2 is essential for activation of the yeast High Osmolarity Glycerol (HOG) pathway. *Molecular and Cellular Biology*, 36(3), pp.475–487. Available at: http://mcb.asm.org/lookup/doi/10.1128/MCB.00853-15.

Zarubin, T. & Han, J., 2005. Activation and signaling of the p38 MAP kinase pathway. *Cell Research*, 15(1), pp.11–18.

Zhang, W., Liu, H.T. & Tu LIU, H., 2002. MAPK signal pathways in the regulation of cell proliferation in mammalian cells. *Cell Research*, 12(1), pp.9–18. Available at: http://www.cell-research.com.

Zuzuarregui, A. et al., 2012. M-Track: detecting short-lived protein-protein interactions in vivo. *Nature Methods*, 9(6), pp.594–596. Available at: http://www.nature.com/doifinder/10.1038/nmeth.2017 [Accessed May 29, 2014].

Zuzuarregui, A. et al., 2015. Msb2 is a Ste11 membrane concentrator required for full activation of the HOG pathway. *Biochimica et Biophysica Acta (BBA) - Gene Regulatory Mechanisms*, pp.1–9. Available at: http://linkinghub.elsevier.com/retrieve/pii/S1874939915000498.